Microbial Degradation of Polyfluorinated Chemicals and Detection of Fluoride via a Colorimetric Assay

---

A THESIS SUBMITTED TO THE FACULTY OF THE UNIVERSITY OF MINNESOTA BY

Madison D Bygd

IN PARTIAL FULFILLMENT OF THE REQUIREMENTS FOR THE DEGREE OF MASTER OF SCIENCE

Dr. Lawrence P. Wackett, Advisor

May 2022

Acknowledgement

I want to thank my advisor, Dr. Larry Wackett, for providing the opportunity to work and learn in his lab. I've gained many skills while working on this project and I'm very thankful for the opportunity and education. Huge thank you to Dr. Kelly Aukema for all her help with day-to-day project operations, suggestions and always having open ears for lab related (and unrelated) things. Much thanks to Jack Richman for assistance with NMR and teaching me a thing or two about organic chemistry and to Tony Dodge for helping me find equipment and answer questions.

Thank you also to Lawrence Wackett, Kelly Aukema, and Jack Richman as co-authors on the published material found in Chapter's 2 and 3.

Additional thank you to my friends and family for your support. A particularly special thanks to Madison Kalb for being a wonderful grad school buddy, a listening ear, and for always willing to take a coffee break.

Thank you to Exxon Mobil, MnDrive Environment and the College of Biological Sciences for funding and administrative support.

Madison Bygd

May 2022

Abstract

Polyfluorinated compounds have become a popular topic in recent years for their widespread use and prominence as a pollutant in our environment. Their use in thousands of commercial products and chemicals has raised concern due to their resistance to degradation, coining them the “forever chemicals.” To better understand how these compounds are degraded and find microorganisms capable of remediation, biological degradative mechanisms were investigated. It was shown that 2,2-difluoro-1,3-benzodioxole, a common fluorinated moiety found in agricultural chemicals and pharmaceuticals, can be degraded and defluorinated by *Pseudomonas putida* F1. To better detect and screen for additional microbial related defluorination mechanisms, a color screen using alizarin and lanthanum was developed for use in biological contexts. Compatible with various media and solvents, this assay uncovered an additional 23 defluorination reactions initiated by *P. putida* F1. Further screening was continued with the *E. coli* ASKA library in which an additional novel defluorination reaction was found to be catalyzed by the enzyme PgpB. The color screen proved to be a highly effective and efficient method for detecting fluoride release by biological means in a high-throughput manner. The data presented in this thesis show many previously undocumented defluorination reactions and outline an efficient and effective method for detecting microbial based bioremediation of polyfluorinated chemicals.

Table of Contents

Acknowledgements i

Abstract ii

List of Figures iv

List of Tables v

1. **General Introduction**
   - 1.1 History of Perfluorinated Chemicals ..……..……..……1
   - 1.2 Applications and Purpose of Polyfluorinated chemicals…..……..…....2
   - 1.3 Health Consequences ..……..……4
   - 1.4 Elimination of PFCs …….……...5
   - 1.5 Why bioremediation ……..……..…8
   - 1.6 Known fluorinated chemical degradation…….……..……..9
   - 1.7 Rationale for Research …….…11
2. **Unexpected Mechanism of Biodegradation and Defluorination of 2,2-difluoro-1,3-benzodioxole by *Pseudomonas putida* F1**
   - 2.1 Introduction ……...……12
   - 2.2 Results and Discussion…… .15
   - 2.3 Materials and Methods …..…….……..30
3. **Microwell Fluoride Screen for Chemical, Enzymatic, and Cellular Reactions Reveals Latent Microbial Defluorination Capacity for -CF_3 Groups**
   - 3.1 Introduction ……..…36
   - 3.2 Results ……..…39
   - 3.3 Discussion…….……54
   - 3.4 Materials and Methods …….……56
4. **Mircowell Fluoride Screen of *E. coli* ASKA Library Reveals Undocumented Defluorination of Sodium Fluorophosphate**
   - 4.1 Introduction ……..64
   - 4.2 Results ……..65
   - 4.3 Discussion ……68
   - 4.4 Materials and Methods ……70
5. **Conclusion**

References

Appendix A: Chapter 2 supplement

Appendix B: Chapter 3 supplement

List of Figures

1.1 Examples of perfluorinated chemicals (PFCs)……..……..... 2
1.2 Ways in which humans are exposed to PFCs ……..…….... 5
1.3 Examples of known defluorination reactions ..……..….10
2.1 Examples of commercially relevant perfluorinated compounds ……..…. 13
2.2 Fluoride release and color change in DFBD incubation with *P. putida* F1 ……..…..16
2.3 Toluene dioxygenase oxidation of DFBD to a cis-dihydrodiol ……..17
2.4 Comparison of dihydodiol dehydration products from *E. coli* pDTG601a compared to standards …….……..20
2.5 Extracted product from *E. coli* pDTG602 incubated with DFBD ……...…..…..21
2.6 Evidence for the defluorinated aromatic product, pyrogallol…….…… 25
2.7 Scheme showing DFBD oxidation by toluene dioxygenase to 4,5-DD-DFBD …….26
3.1 UV spectra of the lanthanum-alizarin complex bound to phosphate, water, and fluoride …….40
3.2 Ratio of lambda max of fluoride bound complex over the lambda max of the unbound complex …….……..……..… 41
3.3 Chemical and enzymatic defluorination of fluoroatrazine catalyzed by base of TrzN ……..44
3.4 Gas-chromatogram and spectra showing the initial fluorinated products from the oxidation of 4-fluorobenzotrifluoride by *P. putida* F1…..……. 49
3.5 Schematic showing the oxygenation and defluorination of 4-fluorobenzotrifluoride……...……. 52
4.1 Positive hit of sodium fluorophosphate defluorination after incubation with *E. coli* ASKA…….……..68

List of Tables

2.1 Homologs of the toluene dioxygenase alpha-subunit with high sequence identity over the majority of the sequence length ……..……... 28

2.2 Bacterial strains used, growth conditions selected, and known enzymes expressed under conditions specified ……. 31

3.1 Interfering and non-interfering buffers and growth media components for color assay…… 43

3.2 Types and number of fluorinated compounds tested with corresponding positive hits of fluoride release after incubation with *P. putida* F1 ….……. 46

3.3 Summarized assay and probe results after 2 mM fluorinated chemical incubation with *P. putida* F1……..48

4.1 Compounds screened for defluorination with the ASKA library….…….. 67

4.2 Incubation time and temperature of chemicals screening with ASKA library ……...72

CHAPTER 1

General Introduction

1.1 History of polyfluorinated chemicals

Polyfluorinated chemicals (PFCs) have become of particular interest in recent years. Having been used in many industrial applications since the 1940s, the accumulation of PFCs in our water and soil are of growing concern for ecological and human health.

By the mid-1900's, heavily fluorinated compounds were found in many industrial applications and commercial products (Ross, 2019, Mueller and Yingling, 2020). As polychlorinated compounds were being phased out for their overwhelming concern for human and ecological safety (Liu and Mullin, 2019), polyfluorinated compounds (PFCs) were on the way to taking their place in household products, agricultural chemicals, and drugs. The first uses of PFCs took place in waterproof coatings and non-stick cookware (Mueller and Yingling, 2020). Eventually the flexibility, strength and versatility of these compounds expanded their presence to firefighting foams, food packaging materials, carpet, stain prevention sprays, and thousands of other household and industrial products.

Many of these products most notably contain(ed) perfluoroalkyl substances (PFAS), which comprise a category of chemicals with long carbon chains, saturated with fluorine and capped with a carboxylic acid or a sulfonate group (**Figure 1.1**) (ATSDR, 2017). These PFAS compounds, in particular, have become buzz words in the scientific realm and general public alike. Concern over the thousands of variations of these PFAS compounds has warranted investigations into their effects on human health and prominence in our environment. However, many other forms of polyfluorinated chemicals have made their way into household products, drugs, and chemicals, emphasizing the importance of studying all variations of polyfluorinated chemicals. For the purpose of this thesis and the included research, all forms of polyfluorinated chemicals (PFCs) will be considered.

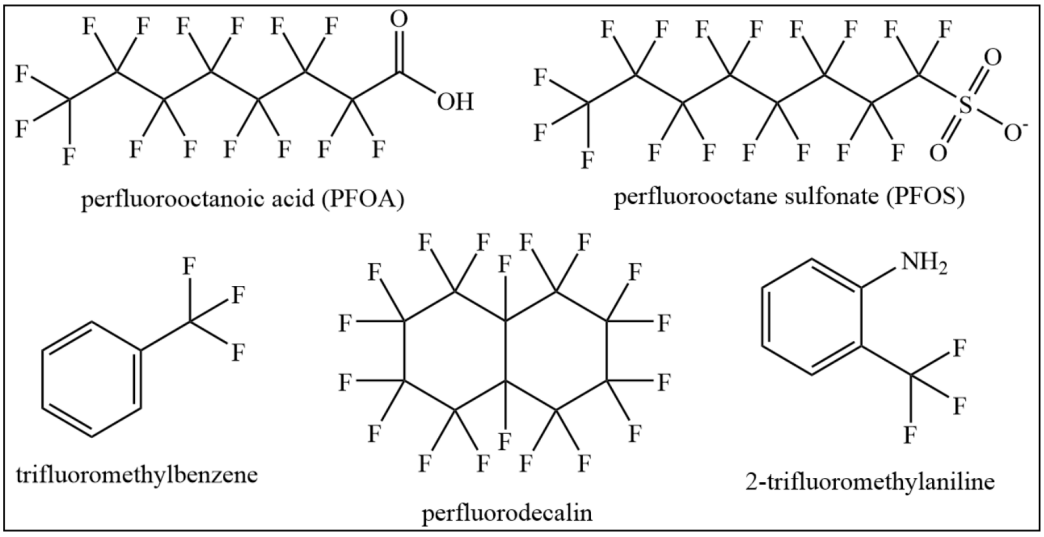

Figure 1.1 Examples of fluorinated chemicals. Perfluorooctanoic acid (PFOA) and Perfluorooctane sulfonate (PFOS) are highly stable and found in many commercial products (Lindstrom, et al., 2011, Huang and Jaffé, 2019, Mueller and Yingling, 2020). Other fluorine containing molecules can be cyclic and/or aromatic with varying moieties.

1.2 Applications and Purpose of Polyfluorinated Chemicals

As mentioned above, there are many forms and applications of PFCs. The most recent number suggests over 9000 PFAS compounds specifically, and likely tens of thousands of other (i.e, aromatic) polyfluorinated chemicals have been synthesized for use (Hogue, 2021). The ability of PFCs to be applied for many uses, including firefighting foams, aerosols, waterproof coatings on outdoor gear and non-stick pans, has allowed for their abundance in products and thus, the environment (Mueller and Yingling, 2020). There are many contributing factors to this abundance of use. Namely, PFCs are flexible, strong, resistant to both water and oil, as well as resistant to degradation (Mueller and Yingling, 2020, Wackett, 2021). To better understand this, we must dissect the chemical properties of the carbon fluorine bond, and its relevance to nature.

Fluorine itself is the most electronegative atom, making its bonding to carbon very strong in many cases. Bond strengths can range from highly reactive to some of the strongest known, such as in hexafluorobenzene (154 kcal/mol) (Edelbach and Jones, 1997). The more reactive compounds are usually monofluorinated and are not as relevant to industrial applications and pollution.

In addition to the C-F bond strength in PFC's, fluorine is a very small atom, similar in size to hydrogen. This makes it an advantageous substitute for hydrogen in applications where the

hydrogen containing compound could easily be degraded. In other words, the fluorine substitution can lead to lower reactivity. Although similar in size, the chemical properties of fluorine prevent the enzyme from acting on it (i.e, cleaving the carbon fluorine bond) (Wackett, 2021). This is of particular interest for companies making drugs or agricultural chemicals. Current examples include fludioxonil, a fungicide containing two fluorine atoms on a diether carbon, as well as the anticancer agent AS-604850 (Müller, et al., 2007, Thomas and Hand, 2012, Alexandrino, et al., 2020). The long half-life of these compounds and resistance to degradation allows them to act longer in their respective environments.

An additional factor to PFC degradation is the extent of their solubility. Long fluorocarbon chains and many highly fluorinated compounds are highly insoluble in water (Dalvi and Rossky, 2010). This feature allows for the use of these compounds in hydrophobic or wicking materials, which again affects the ability of these compounds to be degraded by biological systems. However, this concept cannot be applied to all fluorinated chemicals, as many partially fluorinated compounds can be very polar. Overall there is high variability within the general classification of PFCs in regards to reactivity, solubility and bond strength (Wackett, 2021).

One thing PFCs have in common is the fluorine atom(s). Fluorine is the 13th most abundant element on earth, but much of it is bound up in the Earth's crust as fluorite and fluorapatite, and has low relevance in biological systems (Aigueperse, et al., 2000, Wackett, 2021). This unfamiliarity of natural systems to organofluoride compounds amplifies its difficulty to be degraded. The lack of fluorine in natural products compared to other halogens like chlorine and iodine has prevented evolutionary processes to be selected for. This contrasts with several other elements of similar properties. Chlorine, for example is also highly abundant but it appears in many areas of the earth and natural organic compounds, unlike fluorine. In the ocean alone, chlorine outnumbers fluorine >7600 to 1 (Greenhalgh and Riley, 1961). Because of this, chlorine, bromine, and iodine are found more often in natural products. This includes marine natural products, hormones and toxins (Wackett, 2021). The significance is that microorganisms are at an evolutionary disadvantage for degrading fluorinated products. They have not been exposed to or evolved alongside polyfluorinated chemicals as they have for other halogenated chemicals.

As described above, many of the properties of fluorine combine to make fluorinated compounds advantageous for commercial uses. However, the stability of fluorinated organics also makes resistant to degradation, while accumulating in the environment and threatening our health and safety. Natural processes that have taken care of previous pollutants of concern, such as polychlorinated biphenyls, BTEX compounds or other hydrocarbons, are at an evolutionary disadvantage when it comes to fluorinated chemicals. PFCs are not produced naturally, so nature has not had time to evolve degradative pathways, and they are therefore much harder to eliminate through evolved processes. However, this thesis and the reported research has sought to explore and expand our knowledge on biodegradation and bioremediation of PFCs, testing the potential of microbes to biodegrade what some consider to be non-biodegradable.

1.3 Health Consequences

Generally, PFCs are of concern due to their bio accumulative nature. Consistent exposure to PFCs through food, water, and commercial products pose potential health consequences. Because of their resistance to degradation, they persist in the environment, ending up in food and water to accumulate in our bodies. In addition, the number of commercial products in which you can find PFCs is quite high, for example, the carpet in your living room, or your to-go pizza box (Müller, et al., 2007, Sunderland, et al., 2019, Mueller and Yingling, 2020, Wu, et al., 2020). These two factors, in combination, create a bombardment of PFCs in many aspects of our lives.

Studies thus far have shown significant amounts of PFAS compound in human blood and breast milk (Pan, et al., 2010, Göckener, et al., 2020, Zheng, et al., 2021). In breast milk, PFOA was found at a median concentration of 0.0139 ppb and PFOS at 0.0304 ppb (Zheng, et al., 2021), which can be concerning for parents, as studies have shown that breastfeeding can contribute up to 94% of PFAS intake for infants of 6 months (Huag, et al., 2011). A 2010 study found nine different PFCs in 233 blood samples from residents in 12 different cities in China (Pan, et al., 2010) and in another study, perfluorooctanoic acid (PFOA) and perfluorooctane sulfonic acid (PFOS) were found in 100 blood samples from 100 different people between 2009-2019 (Göckener, et al., 2020). This is problematic because the presence of PFCs in the blood at concentrations in the range of 100 ppm is thought to lead to effects such as hormone, immune, and reproductive disruption Use of, Crawford, et al., 2017). Additional consequences include a rise in cholesterol levels, lowered liver enzyme levels and reduced birth weights in infants, as

well as accelerated puberty in children (Panieri, et al., 2022). When certain PFCs were exposed to rats and monkeys it decreased body weight and, in pregnant mice, administered PFAS compounds led to neonatal mortality and decreased birth weight in surviving pups. Tumors, found in the liver, pancreas and testicles, were also seen in rodents exposed to 300 ppm PFOS (Biegel, et al., 2001, Lindstrom, et al., 2011). Although these levels would be abnormally high for human exposure, it is important to understand the health consequences if these compounds are allowed to proliferate. Currently, the Environmental Protection Agency has set a health advisory for lifetime consumption of PFOA and PFOS in drinking water to be 70 ng/L (approximately 0.07 ppb) (EPA, 2016.1, EPA, 2016.2) . It is evident that without remediation these compounds could leave a detrimental wake for humans and animals alike.

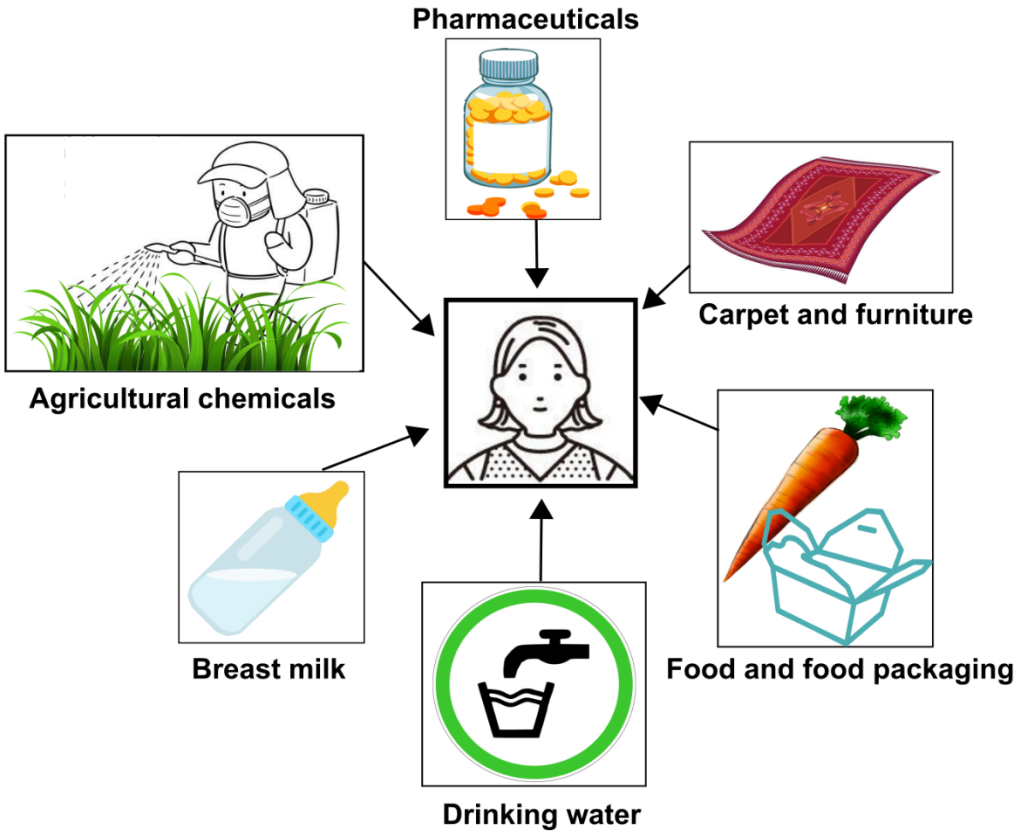

Figure 1.2 Various ways in which humans are exposed to polyfluorinated chemicals. PFCs are found in many aspects of our environments, from the food and water we consume to the furniture we sit on.

1.4 Eliminating PFAS compounds

To prevent human and ecological repercussions of PFC accumulation, measures are being taken to remediate and eliminate these compounds before they are life threatening. Some technologies have been implemented for soil or solid waste and others for liquid and water remediation.

Common treatment for solid PFC sources include capping, excavation and disposal, sorption, stabilization, and thermal decomposition. Capping technology places a cover over contaminated material such as landfill waste, contaminated soil, or sediments. This prevents the contact of the contaminated area with non-contaminated soil and water with the hope of preventing further spread of pollutants. Excavation and disposal involve removing the contaminated soil and hauling it to a permitted landfill or incineration facility. Sorption and stabilization include adding amendments to the soil to reduce or remove the potential for PFAS to mobilize from the soil to groundwater. Thermal treatment is the use of heat applied to the PFAS contaminated soil, typically at an incinerator, to vaporize or destroy the compounds (Mueller and Yingling, 2018).

Much of the current remediation has been focused on water because of high exposures in drinking water near concentrated PFC exposure sites. Not all areas of the globe have the same levels of PFCs, however sites where levels will be higher include groundwater and streams near industries that produce PFAS compounds, or near airports where PFAS containing firefighting foams have been used (EPA, 2022). PFC levels found in drinking water of these described areas have raised concern for humans since the concentration can be in the range of, or over 70 ng/L (0.07 ppb), which is the EPA's health advisory limit for lifetime consumption. Although not all water sources contain such high levels, many major cities in the United States are reported to contain levels of PFCs, namely Brunswick county, North Carolina and Quad Cities, Iowa, La Crosse, Wisconsin, and New York City, New York (Andrews and Naidenko, 2020, Evans, et al., 2020). In such cities, residents are often restricted to drinking and cooking with bottled water (Herken, 2021, Storlie, 2021). Additional studies have even shown low, but detectable concentrations of PFCs in remote areas across the globe far from PFC sources (Brusseau, et al., 2020).

Water treatments involve different types of technology, but with similar goals of treating solid waste. This includes treating groundwater, drinking water, industrial wastewater, as well as other water sources. Sorption involves two techniques of passing water through a granular media. The

use of activated carbon adsorbs the contaminated material as the water passes. Granulated activated carbon (GAC) is a common technique used in water treatment systems and is currently the most commonly used PFAS remediation technique. Biochar is a second form of sorption technology. It uses both biomass and charcoal as a carbon rich, porous material to filter water and adsorb contaminants. Ion exchange (IX) technology is the use of synthetic, polymeric media to remove PFAS from water. This can be used similarly to and in conjunction with activated carbon technology by using a cation to attract the negatively charged carboxylic acid and sulfonic acid heads of perfluoroalkyl acids. GAC and IX technologies have been implemented in large scale settings and are very effective in removing long chain PFAS (McCleaf, et al., 2017, Belkouteb, et al., 2020, Burkhardt, et al., 2022). In full scale applications, GAC has mostly been used in higher priority private and public water supply chains. IX is not quite as popular but there are full scale operations in Australia and one in the United States (Mueller and Yingling, 2018).

Other remediation methods are in early research stages but are being investigated for additional treatment applications. Precipitation/coagulation technology is early in development at the bench-scale but could be used as a pre-treatment approach for wastewater treatment. Similarly in the development stage, coagulants can be added to water to assist in forming solids, which can then be separated from the water and disposed of. Redox manipulation, the process of changing the oxidation-reduction potential of the water by adding reducing amendments, is still in bench scale investigation as well. This changes the PFAS compound by displacing atoms from it and slowly breaks it down. There are concerns with this method that there would be incomplete destruction of the compounds, which could mobilize other toxic products, such as shorter chain PFAS. Lastly, membrane filtration is another version of PFAS treatment, including reverse osmosis and nanofiltration. Both require the use of low pressure to move water across a membrane to take out the contaminants. These are partially developed technology, as further testing needs to be done for large scale applications (Mueller and Yingling, 2018).

As with all remediation techniques, there are pros and cons to these technologies. The advantage to using activated carbon or other adsorption filtration systems is the low cost and familiarity of this technology with water treatment centers. However, a disadvantage is the retention of the physical PFAS product. Activated carbon can “collect” the compounds from the water but it doesn’t destroy or degrade it. This is a large disadvantage to many remediation techniques that are cost effective- they often don’t eliminate the compound of interest, only transfer it from one

environment to another. This leaves a need to still destroy the chemical before it reenters the environment through landfills, for example. Other disadvantages to certain technologies may include the lack of specificity of the treatment method, as in thermal, photoelectric techniques, or redox. These are not specific to PFC's and can often eliminate many other compounds and nutrients or produce a product that is potentially more toxic. Overall, finding a method that not only degrades the specific contaminant from the environment, in our case PFCs, but is also cost efficient, safe, and effective is the goal. Bioremediation may be this solution. History has shown that bioremediation is an effective strategy and operates with the goal of complete elimination of the compound of interest.

1.5 Why Bioremediation

Bioremediation is an effective and non-disruptive technique that can often be implemented to fully eliminate a contaminant from the environment. In most cases it leaves non-hazardous by-products, or complete degradation of the compound of interest. This could take place in plants, bacteria, fungi, or even insects. For the purpose of this research, we will be focusing on bacterial biodegradation and remediation.

In the case of PFCs, bacteria may be able to use some of these compounds for food or as a carbon source, although it is not as commonly anticipated due to the complete oxidation of carbon in some compounds such as PFOA and PFOS. If the bacteria can take in the compounds for degradation, many have fluoride transporters in which they can export the otherwise toxic fluoride anion outside the cell. Outside of the cell the fluoride anion does not pose a threat at the typical concentrations that PFAS are found in the environment (a median level of PFAS found in soil is 2.7 ug/kg, or 2.7 ppb, from more than 30,000 samples from 2,500 sites throughout the world (Brusseau, et al., 2020)).

Additional advantages of bioremediation include the ability to work *in situ*, or at the site of contamination rather than *ex situ*, or away from the contamination. This can save energy and equipment costs to haul out contaminated soil, for example. Removing the contamination to work *ex situ* can also lead to the disruption of eco-systems and cause other environmental effects (i.e, deforestation, infrastructure destruction, emissions from equipment). Using bioremediation *in situ* can be minimally intrusive and reduce turnaround time for using the previously contaminated soil

or water. This is especially important when contamination occurs in drinking water, leaving residents to depend on bottled water until the compound(s) is eliminated.

One question that rises from a better understanding of PFCs and the need to degrade them is what organisms to use and the likelihood of natural degradation. History has shown that microbes left to evolve in the presence of anthropogenic products develop ways of degrading these products or using them for food. Examples include the degradation of BTEX compounds (biphenyl, toluene, ethyl benzene and xylene) from oil spills and polychlorinated chemicals (PCCs) (Mondello, 1989, Furukawa K, et al., 1993, Weelink, et al., 2010, Wackett and Robinson, 2020). Both examples, BTEX and PCCs are likely degraded easier due to their natural occurrence in the environment, or similarity to compounds that are degraded naturally (Wackett and Robinson, 2020, Wackett, 2021). BTEX compounds, found in oil, come from an originally biological source, in which many bacteria and fungi have evolved along with. In the case of polychlorinated compounds, chlorine is a very common compound found in nature as a part of natural products, specifically in marine environments. This similar exposure has allowed many organisms to develop ways or modify existing methods of degrading these compounds. In contrast, fluorinated natural products are rare and due to lack of exposure, microorganisms are at an evolutionary disadvantage for eliminating anthropogenic fluorinated products.

That being said, there are many opportunities in which microbes have shown broad specificity for certain chemicals. In some cases, one enzyme has been shown to initiate the degradation over 200 different substrates (i.e, toluene dioxygenase, naphthalene dioxygenase, cytochrome P450 (Bui, et al., 2001, Escalante, et al., 2017, Wang and Liu, 2020). The promiscuity of these enzymes provides reason to believe that, in conjunction with evolution, many of these PFCs could be degraded. Starting with microbes that have broad specificity for degrading many different compounds could be a useful place to look for a PFC degrader.

1.6 Known Defluorination Reactions

In an earlier section it was mentioned that not all fluorinated compounds are highly stable. Some monofluorinated compounds are more reactive and have known defluorination reactions.
The first, and likely most well-known degradation mechanism for a fluorinated (natural) product is the defluorination of fluoroacetate by fluoroacetate dehalogenase (Goldman, 1965) (**Figure**

1.3). Fluoroacetate is a natural product made by plants. However, this compound is toxic, resulting in consequences for animals, such as disruption of the TCA cycle. This results in citrate accumulation in tissues and plasma, causing energy deprivation and death (Leong, et al., 2017). Since fluoroacetate is a natural product many bacteria have evolved to degrade this compound, using an enzyme to cleave the carbon fluorine bond, which is one of the few cases in which direct cleavage of the C-F bond is shown in nature. A gene coding for an enzyme with similar function has been found in the stomach of ruminant animals to protect them from deadly consequences of fluoroacetate ingestion (Leong, et al., 2017).

The second example of a defluorination reaction is the highly reactive compound, Sanger's reagent, or 1-fluoro-2,4-dinitrobenzene (**Figure 1.3**) (Sanger, 1945). This compound has been used as a chemical and colorimetric indicator of proteins in reactions. The reagent spontaneously goes through nucleophilic aromatic substitution with an N-terminal amino group, resulting in an N-terminal chemical tag (Hassner and Namboothiri, 2012). This reaction can then be identified through colorimetric analysis because when defluorinated the compound reflects light around 580 nm, appearing yellow.

Lastly, fluorobenzene (**Figure 1.3**) serves as an additional example for known defluorination reaction for an aromatic fluorinated organic. This documented defluorination reaction is done by a series of enzymes, not directly defluorinating the benzene ring, but rather dioxygenating the ring and promoting downstream reactions. The reaction can result in two different defluorinated products, cis-dienelactone, or maleylacetate (Seong, et al., 2019).

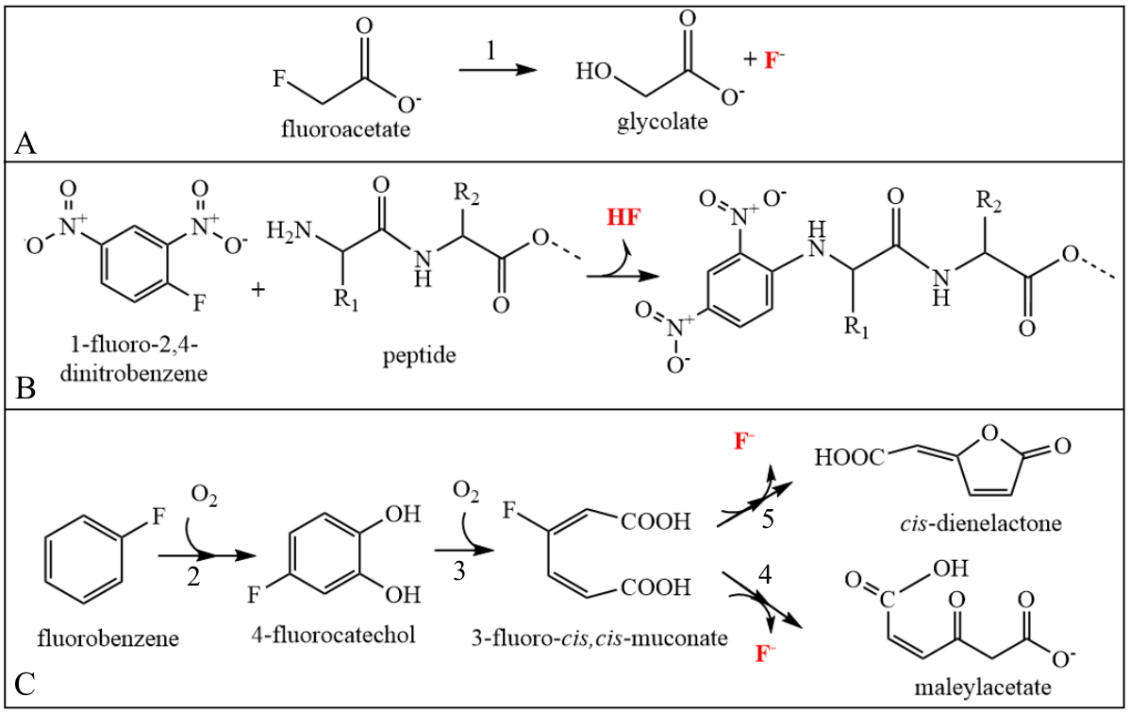

Figure 1.3. Three known defluorination reactions. A) Fluoroacetate is degraded in the presence of fluoroacetate dehalogenase (1) to release fluoride and leave glycolate as the product (Goldman, 1965, Goldman and Milne, 1966, Miranda-Rojas, et al., 2018). B) 1-fluoro-2,4-dinitrobenzene reacts with the N-terminus of a peptide to release hydrogen fluoride (Sanger, 1945, Hassner and Namboothiri, 2012). C) Fluorobenzene is not directly defluorinated, but rather is dioxygenated in the presence of fluorobenzene dioxygenase, oxygen, and NADH (2) to create a dihydrodiol. The dihydrodiol dehydrogenase (2) converts the dihydrodiol to 4-fluorocatechol, which is moved down the pathway via ring-cleavage by fluorocatechol 1,2-dioxygenase. From here, 3-fluoro-*cis,cis*-muconate can be converted to maleylacetate via trans-dienelactone hydrolase or to *cis*-dienelactone via fluoromuconate cycloisomerase, both of which reactions will release fluoride.

These examples of mono-fluorinated compounds are chemically more reactive than the polyfluorinated counterparts. Although they are not directly comparable to PFC degradation, the information we have on these defluorination mechanisms provides a starting point for understanding the degradation of polyfluorinated compounds possessing lower reactivity.

1.7 Rationale for research

While polyfluorinated compounds are useful in industrial and chemical manufacturing, they have become abundant in our products, such as textiles, food packaging, outdoor gear, and cookware. The prevalence of PFCs in products can lead to an accumulation of these chemicals in the environment at levels above the recommended lifetime limit of exposure (70 ng/L). Ingestion and

consistent exposure to PFCs above the recommended limit can directly impact our health and wellness and pose many risks that outweigh the benefits of their widespread use. Current techniques to reduce polyfluorinated chemical levels in our water have many downfalls, including high capital investment and incomplete elimination of the contaminant. Studying the ability of environmental microorganisms to degrade these problematic compounds could lead to a better understanding of potential remediation techniques, including how it's done, and through what mechanisms. Biodegradation often leads to non-toxic byproducts and/or complete degradation of the pollutant. Upscaling these processes for larger implementations could be crucial to preserving our water, soil, and health.

In the next chapters, I will describe:

1. A novel defluorination reaction of a difluorinated moiety commonly used in pharmaceuticals and agricultural chemicals, initiated by a soil bacterium;
2. The development of a colorimetric assay for fluoride detection in microbiological sources;
3. The implementation of the high-throughput fluoride screen with a bacterial library to uncover new defluorination reactions.

CHAPTER 2

Unexpected Mechanism of Biodegradation and Defluorination of 2,2-difluoro-1,3-benzodioxole by *Pseudomonas putida* F1

Authors: Madison D. Bygd, Kelly G. Aukema, Jack E. Richman, Lawrence P. Wackett

2.1 Introduction

Fluorinated organic compounds are considered to be one of the major foci of biodegradation currently because of their prevalence, emerging concerns about health effects, and their prolonged lifetime in the environment (Sunderland, et al., 2019). Naturally occurring compounds with carbon-fluorine bonds are relatively rare, and most contain a single fluorine substituent (Harper and O'Hagan, 1994, Key, et al., 1997, Murphy, et al., 2003). Synthetic, commercially important fluorinated compounds typically contain multiple fluorine atoms, and that makes them less reactive to defluorination, both chemically and biologically (Smart, 2001, O'Hagan, 2008). In light of that, there have been a limited number of studies demonstrating biodegradation of multiply fluorinated compounds. Recently, perfluorinated compounds have been shown to be biodegradable (Huang and Jaffé, 2019, Liu, et al., 2021) but the genes and enzymes involved in their defluorination are not yet known.

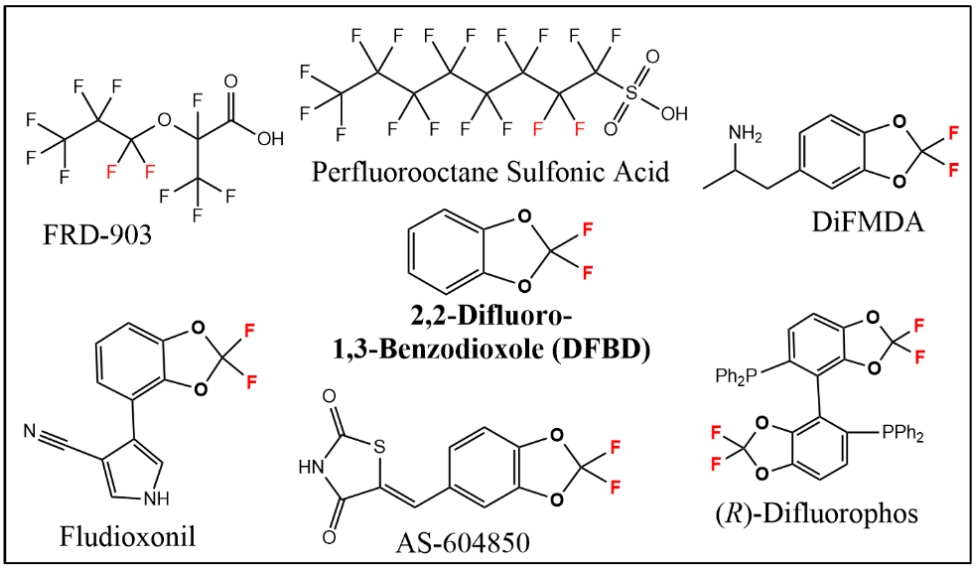

Figure 2.1. Examples of commercially relevant polyfluorinated compounds. The center compound in bold is 2,2-difluro-1,3-benzodioxole (DFBD). Compounds containing the DFBD moiety shown are the: experimental drug DiFMDA (difluoromethylenedioxyamphetamine), fungicide fludioxonil, the anti-cancer agent AS-604850, and the reagent for enantioselective synthesis (*R*)-difluorophos.

Difluorinated ethers are common in industrial chemicals, particularly in pharmaceutical and pesticidal compounds. They are of particular interest currently with the introduction of 2,3,3,3-tetrafluoro-2-(heptafluoropropoxy)propanoic acid, commonly known as FRD 903, as a substitute for other perfluorinated alkyl substances (PFAS) such as perfluorooctane sulfonic acid (Fig. 1). A common and emerging class of difluoro ether compounds contains the 2,2-difluoro-1,3-benzodioxole (DFBD) group (Müller, et al., 2007, Murphy, 2016). Commercial DFBD-containing compounds include the fungicide fludioxonil, the anticancer therapeutic AS-604850, the synthetic reagent (R)-difluorophos, and the experimental drug difluoromethylenedioxyamphetamine (DiFMDA) (Fig. 1). Many other DFBD-based difluoroethers are in commercial use currently (Newton, et al., 2020). The difluoromethylene group is designed into ring structures because it prolongs the lifetime of the compounds in both the human body and the environment. DFBD-containing pesticides are considered to be moderately recalcitrant, with several studies using enrichments from soil and water showing their disappearance in days to weeks (Thomas and Hand, 2012, Alexandrino, et al., 2020).

However, those studies did not identify the genes or enzymes responsible for the metabolism.

The defluorination of difluoromethylene carbons in ether linkages is not well studied, and DFBD provides an excellent model for developing understanding. It remains to be established if the fluorines would be displaceable via hydrolytic, reductive, or other mechanisms. The difluorinated carbon atom in DFBD is also bonded to two oxygen atoms. As such, it is completely oxidized and unlikely to undergo oxidative defluorination directly. Defluorination by oxidizing enzymes such as oxygenases is known (Wang and Liu, 2020, Yu, et al., 2020), typically with a carbon atom bonded to a single fluorine atom, unlike in DFBD (Renganathan, 1989, Bondar, et al., 1998, Ferreira, et al., 2009, Xie, et al., 2020). Perfluoroethylene is biodegraded to defluorinated products by soluble methane monooxygenase from Methylosinus trichosporium Ob3B (Fox, et al., 1990). Recently, an elimination mechanism has been proposed to initiate the biodegradation of 3,3,3-trifluoropropionic acid (Che, et al., 2021), but this mechanism would not apply to the DFBD difluorodiether group.

For more insights into DFBD defluorination, we chose to examine model *Pseudomonas* strains for which genomes are available and enzymes have been purified and characterized. The first defluorinating enzyme studied, fluoroacetate defluorinase, was purified and characterized from a Pseudomonas strain (Goldman, 1965). In one recent study, fluoroacetate was shown to undergo defluorination by multiple bacterial strains, but difluoro- and trifluoroacetates were uniformly recalcitrant (Alexandrino, et al., 2018). However, *Pseudomonas* strains are known to contain organochlorine dehalogenases that react with dichloro- and trichloro- substrates (Strotmann, et al., 1990, Nagata, et al., 1993). Moreover, Pseudomonas genomes are known to encode 25% proteins of unknown function, suggesting novel defluorinating activities may yet be discovered (Winsor, et al., 2009, Winsor, et al., 2016). After initially screening several Pseudomonas strains against a small library of fluorinated compounds, we observed significant levels of fluoride anion in the medium with strain *Pseudomonas putida* F1 and DFBD. This model strain has had its genome sequenced and multiple enzymes characterized in detail (Zylstra, et al., 1988, Reardon, et al., 2000). The most well-studied

enzymes are involved in the metabolism of aromatic hydrocarbons (Kasahara, et al., 2012), and DFBD contains an aromatic ring. Moreover, the DFBD moiety is known to be quite stable, underlying its incorporation into numerous commercial products (Fig. 1).

The present study focused on DFBD transformation by *P. putida* F1 and the mechanism by which free fluoride was released into the medium. Using the combined tools of nuclear magnetic resonance (NMR) spectroscopy, gas chromatography (GC), and mass spectrometry (MS), we propose here a novel mechanism underlying fluoride dis placement from the DFBD group. It was demonstrated that the only enzyme required for defluorination of DFBD is toluene dioxygenase, and the mechanism elucidated here has, to our knowledge, never been shown previously. Moreover, many environmental bacteria express toluene dioxygenase homologs, suggesting that the mechanism revealed here may be operative with DFBD compounds found in soil and water.

2.2 Results and Discussion

Metabolic studies with wild-type Pseudomonas putida F1. Wild-type cells of *P. putida* F1 were grown to mid-exponential phase on toluene vapors to induce toluene dioxygenase and related enzymes. The toluene vapor was removed and replaced with 2,2-difluoro-1,3-benzodioxole (DFBD) vapor, and free fluoride ion was detected immediately. Over time, color change of the medium was also observed (see Fig. S1 in

the supplemental material). The release of free fluoride ion was measured using a fluoride electrode, which showed a rapid accumulation of fluoride in the first 4 h (Fig. 2A). After this, fluoride in the medium plateaued at ;1 mM, which was followed by a darkening of the medium (Fig. 2B). Cells grown on L-arginine as a carbon source that were not induced with toluene produced minimal levels of fluoride (0.1 mM over 24 h). Additionally, DFBD was stable in medium in the absence of cells. No fluoride was

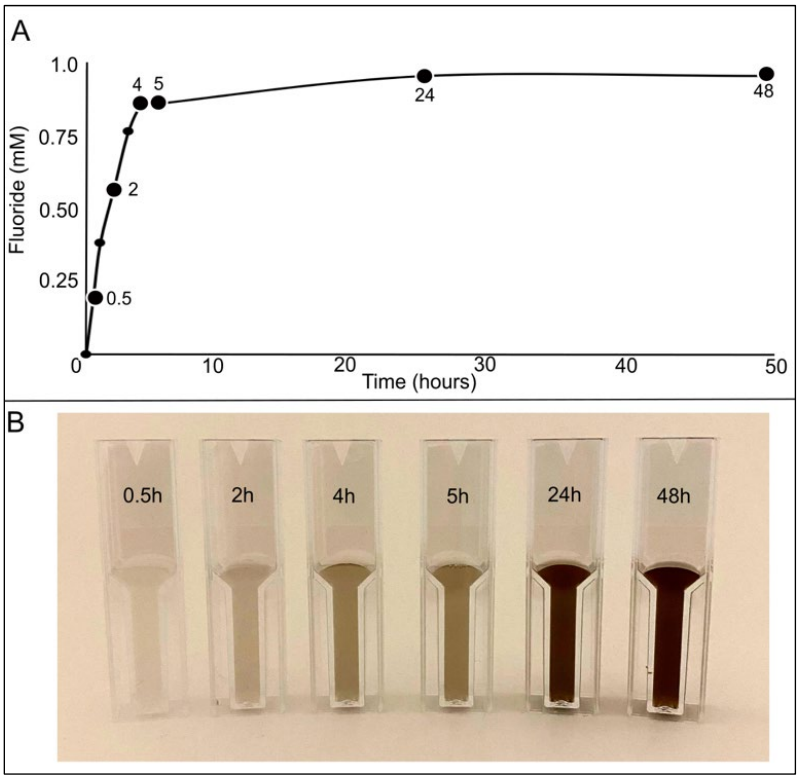

Figure 2.2. Fluoride release (A) and color change (B) in media of a culture of *Pseudomonas putida* F1 incubated with DFBD with shaking over 48 hours. *P. putida* F1 was grown with toluene as the carbon source, which induces the toluene catabolic pathway, and then the culture was switched to DFBD. For fluoride measurements, cells were removed, and the supernatant liquid analyzed for fluoride, using an ion specific electrode, as shown in (A). Aliquots of the culture were taken at the times indicated, stored frozen and then all were directly photographed, as shown in (B).

released, and there was no darkening of medium. When sodium fluoride was added to medium, no color change was observed. In multiple experiments, color change was always linked to fluoride release but lagged behind temporally as shown in Fig. 2.

The initial rate of fluoride ion release was 2,100 nmol/h per mg of cell protein. By way of comparison, the rates of initial enzymatic attack on toluene by different *Pseudomonas* strains are reported to range from 720 to 10,800 nmol/h per mg protein (Leahy and Olsen, 2006). Defluorination of difluoromethylene carbon atoms by microorganisms has rarely been reported, and when it has, it is typically orders of magnitude slower and

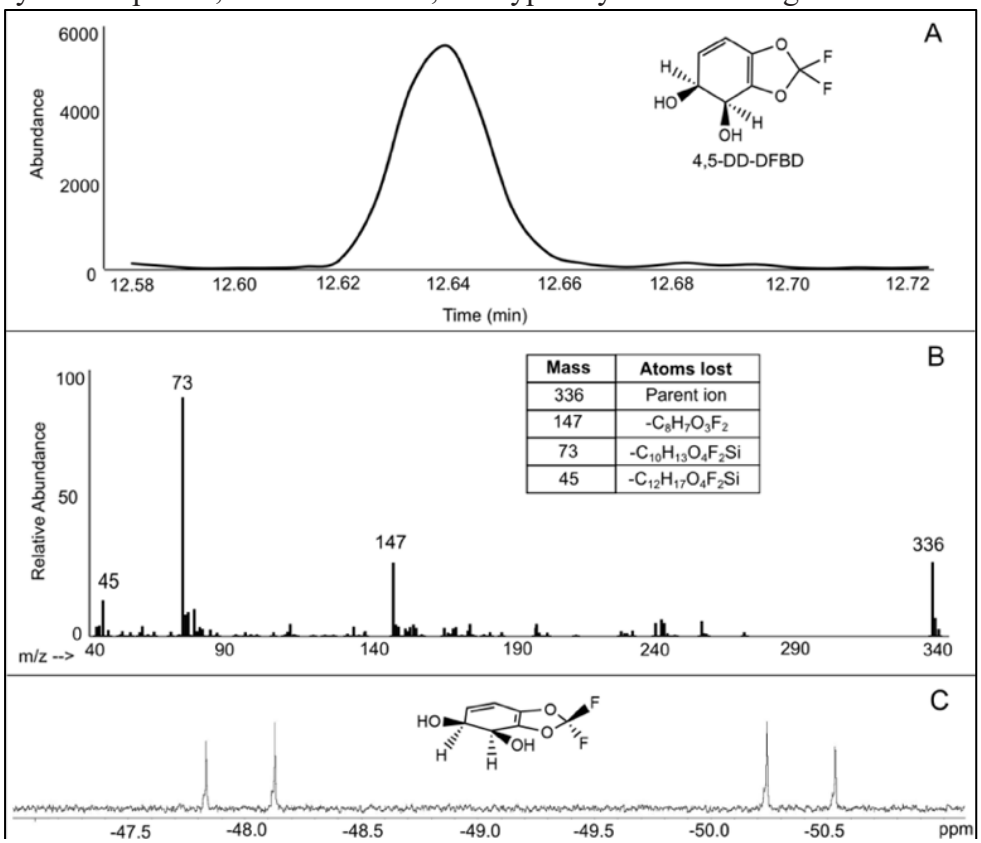

Figure 2.3. Toluene dioxygenase oxidation of DFBD to a *cis*-dihyrodiol. Analytical demonstration of 4,5-*cis*-dihydroxy-dihydro-2,2-difluoro-1,3-benzodioxole (4,5-DD-DFBD) by GC, MS and NMR. The structure of the compound is shown in the upper right of panel A. The material analyzed by GC and MS was derivatized as detailed in the Methods. While the data are consistent with a *cis*-dihydrodiol, the absolute stereochemistry has not been determined and that shown is consistent with dihydrodiols produced by toluene dioxygenase. (A) Gas chromatograph of the extracted product derivatized with trimethylsilane. B) Mass spectrum of the compound represented by the 12.64 min peak. The parent compound has a m/z = 336 and the m/z = 337,338 envelope is consistent with 1.1% natural abundance of ^{13}C and a compound containing thirteen carbon atoms. The disilyl fragment with a m/z = 147 is characteristic of compounds with two adjacent derivatized hydroxyl groups. (C) ^{19}F-NMR spectrum at 400 mHz of 4,5-DD-DFBD. The two coupled doublets are consistent with two fluorines on differentiated faces, in this case arising from the *cis*-configuration of the hydroxyl groups. The 3-dimensional depiction of 4,5-DD-DFBD illustrates the asymmetry imposed by the *cis*-dihydroxylation of DFBD.

measured over weeks or months (Huang and Jaffé, 2019, Liu, et al., 2021). The rapid plateau reached after 4 h suggests that some factor becomes limiting. This argues against a hydrolytic defluorination since that would require only water that would not become limiting. The observations are more consistent with a redox reaction, since NADH or other sources of electrons could conceivably become depleted. The observation that growth on toluene is required suggests a role for one or more components of the toluene metabolic pathway.

Metabolic studies with mutant P. putida F39/D and Escherichia coli (pDTG601a) expressing toluene dioxygenase. The observations with wild-type P. putida F1 suggested that one or more components of the toluene degradation pathway were involved in DFBD defluorination and the darkening of the medium. Since the pathway is initiated by toluene dioxygenase (TDO), we first aimed to examine that enzyme's reaction with DFBD in isolation. Toluene dioxygenase consists of three components that are highly unstable and separate upon cell lysis and purification. They are a flavoprotein reductase (TodA), a ferredoxin (TodB), and the Rieske dioxygenase protein ($TodC_1C_2$) (Finette and Gibson, 1988). So, an in vivo approach was pursued with P. putida F39/D, a derivative of P. putida F1 that lacks a functional second enzyme in the toluene catabolic pathway (Williams, et al., 1990), and the recombinant strain E. coli (pDTG601a), which contains the todC1C2BA genes encoding the complete TDO system but no other enzymes of the toluene pathway (Zylstra, et al., 1988). It is plausible that these two systems could give different results. For example, the TodE catechol oxygenase in *P. putida* F39/D could hypothetically catalyze ring cleavage leading to defluorination and *E. coli* DTG601a does not contain that enzyme.

P. putida F39/D was grown on L-arginine and induced with toluene vapor before incubation with DFBD. E. coli (pDTG60) was induced with isopropyl-b-D-hiogalactopyr anoside (IPTG) and subsequently incubated with DFBD. In both cases, the media were extracted with ethyl acetate, concentrated using a rotary evaporator, and analyzed by GC-MS and NMR as described in Materials and Methods. The GC-MS and ^{19}F-NMR

analyses were both consistent with the formation of a 4,5-dihydro-2,2-difluoro-1,3-benzo-dioxole-4,5-diol (4,5-DD-DFBD) (Fig. 3). Similar results were obtained with the *P. putida* F39/D and *E. coli* (pDTG601a) extracts. Because dihydrodiols are subject to decomposition in high temperatures of the GC inlet, extracted medium was derivatized prior to GC-MS analysis. Both the GC retention time and the mass spectrum of the prominent peak at 12.64 min are consistent with its identification as a derivatized dihydrodiol (Fig. 3A and B). Further structural information was gained from ^{19}F-NMR that showed that both fluorine atoms were retained in the product (Fig. 3C). The fluorine resonance splitting demonstrated that the plane of the benzene ring was asymmetric, consistent with a cis-dihydrodiol. The oxidation of bicyclic fused ring compounds, such as indan (Wackett, et al., 1988), by toluene dioxygenase has not been observed to produce bridgehead diols, and the enzyme consistently produces cis-dihydrodiols. Therefore, it was predicted that the cis-dihydrodiol being formed was most likely a 4,5-cis-dihydrodiol.

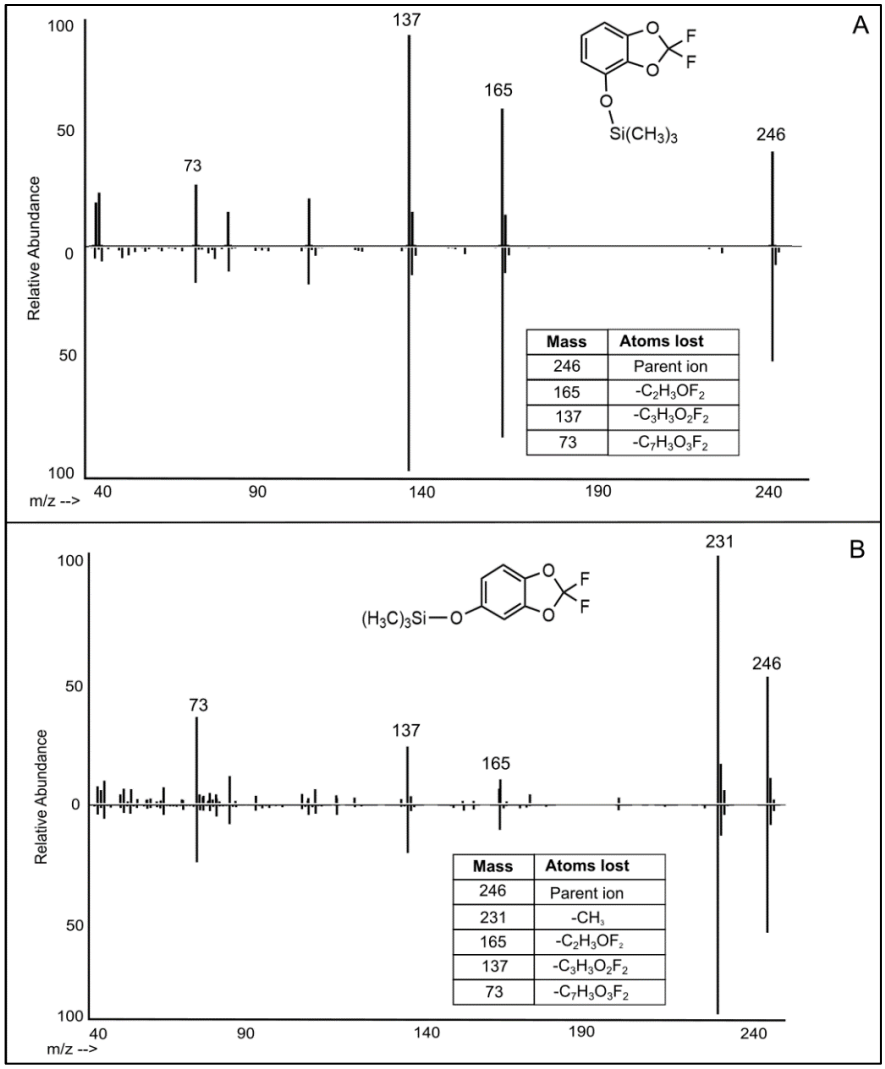

Figure 2.4. Comparison of dihydrodiol dehydration products from *E. coli* pDTG601a compared to synthetic standards following derivitization and mass spectrometry. A) Mass spectra of TMS-derivatized metabolite from cell cultures incubated with DFBD (top) and standard DFBD-4-ol (bottom). B) Mass spectra of TMS-derivatized metabolite from cell cultures incubated with DFBD (top) and standard DFBD-5-ol (bottom).

Dehydration of the cis-dihydrodiol-DFBD. It was decided that following the fate of 4,5-DD-DFBD would lead to insights into darkening of medium and the defluorination mechanism. Dihydrodiols are known to readily undergo dehydration to yield phenols. The dehydration reaction with substituted benzenes often produces a mixture of two phenols (Williams, et al., 1990). The initial evidence that the DFBD dihydrodiol is

unstable came from its low yield and subsequent NMR analysis, initially described in the previous section. When it was dried and taken up in $CDCl_3$, a solvent known to be slightly acidic, the ^{19}F-NMR spectrum showed a collapse of the fluorine doublet into a single resonance, consistent with a rearomatization of the benzene ring that would occur with dehydration, producing a monohydroxylated aromatic ring (Fig. S6, Appendix A). With rearomatization, the environments of the two fluorine substituents become

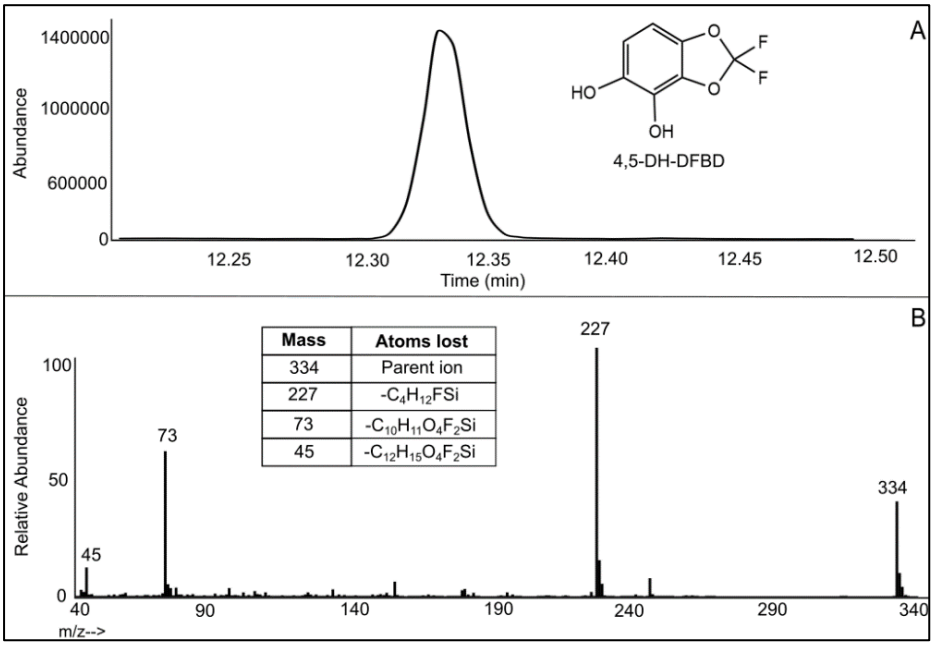

Figure 2.5. Extracted product derived from *E. coli* pDTG602 expressing toluene dioxygenase and toluene dihydrodiol dehydrogenase. A) Gas chromatogram of the compound identified as TMS-derivatized 4,5-dihydroxy-DFBD. B) Mass spectrum of TMS-derivatized 4,5-dihydroxy-DFBD. The parent compound shows a m/z of 334.

identical. From the NMR spectrum, it could not be discerned whether DFBD-4-ol, DFBD-5-ol, or both are formed.

Direct evidence was obtained that both DFBD-4-ol and DFBD-5-ol form in growth medium. This was determined by GC-MS, following derivatization to make both trimethylsilyl derivatives, and in comparison to authentic standards of each (Fig. 4). Together, they are not major products and account for ,20% of total products. Moreover, addition of DFBD-4-ol and DFBD-5-ol to P. putida F1 growth medium did not lead to formation of fluoride; both compounds are stable in medium. In addition, no evidence for

the metabolism of standard DFBD-4-ol and DFBD-5-ol by P. putida F39/D or E. coli (pDTG601a) in minimal salts basal (MSB) medium was observed. Based on these observations, additional metabolic studies were needed to uncover the mechanism of fluoride displacement.

***E. coli* (pDTG602) expressing toluene dioxygenase and diol dehydrogenase.** *P. putida* F1 is known to oxidize cis-dihydrodiols to catechols that can oxidize to form products that darken growth medium (Zylstra, et al., 1988). In that context, we sought to accumulate the catechol from DFBD and determine if that could help explain medium darkening and fluoride release. The experiment used E. coli (pDTG602), which contains genes encoding toluene dioxygenase and dihydrodiol dehydrogenase and is known to accumulate catechols (Zylstra, et al., 1988). This study produced a metabolite consistent with 4,5-dihydroxy DFBD (4,5-DH-DFBD), as demonstrated by ^{1}H-NMR (Fig. S7), ^{19}F-NMR (Fig. S8), and GC-MS after derivatization (Fig. 5). However, this intermediate also maintained the two fluorine substituents on the intact 1,3-dioxolane ring. This was confirmed via GC-MS (Fig. 5) and ^{19}F-NMR (Fig. S8, Appendix A). Moreover, similar to the presence of DFBD-4-ol and DFBD-5-ol in *E. coli* (pDTG601a) cultures, 4,5-dihydroxy-DFBD was formed in only low yield. More importantly, we observed that medium from E. coli pDTG602 incubated with DFBD did darken but not as quickly or to the same extent with as with P. putida F39/D and E. coli (pDTG601a). This suggested that the DFBD-4,5-dihydrodiol is undergoing some other reaction to give a colored product(s) and fluoride.

Identification of pyrogallol, a defluorinated product that explained medium darkening. The volatility of DFBD prevented our determining the stoichiometry of DFBD oxidized to the amount of fluoride released. The initial rate of fluoride release (Fig. 2) was high, and the yields of DFBD-4-ol, DFBD-5-ol, and 4,5-DH-DFBD were low, suggesting that the DFBD-cis-4,5-dihydrodiol undergoes another reaction leading to defluorination. In this context, another organic product was sought in cultures of *E. coli* (pDTG601a) and *P. putida* F39/D. GC-MS revealed the transient

formation of a nonfluorinated product, 1,2,3-benzenetriol, also known as pyrogallol (Fig. 6A). 1,2,3-Benzenetriol is known to undergo spontaneous oxidation in air (Abrash, et al., 1989, Ramasarma, et al., 2015), and our cultures are vigorously shaken to provide a continuous supply of oxygen for the dioxygenase reaction. These oxidation products absorb at varying wavelengths, which leads to dark-colored microbiological medium (Yoshida and Yamada, 1985, Osawa and Walsh, 1995).

To follow pyrogallol formation and decomposition, we used UV-visible (UV-vis) spectroscopy of biological material in comparison to standard pyrogallol and purpurogallin (Fig. 6B and C; see also Fig. S9 and S10, Appendix A). Pyrogallol, prior to oxidation, absorbs only below 300 nm, which is difficult to analyze because DFBD absorbs in the 250- to 300-nm region. So, we analyzed at wavelengths above 300 nm. When added to sterile growth medium, pyrogallol quickly oxidized to a species that adsorbs at 320 nm, purportedly purpurogallin (Fig. S10). Over time, this decayed with the appearance of absorbance at 420 to 440 nm, indicating the formation of purpurogallin-quinone (Abrash, et al., 1989). Over time, other absorbing species led to the previously described brown to black coloration of pyrogallol medium that was observed here with DFBD in medium in the presence of toluene dioxygenase (Fig. 6B) and standard pyrogallol in medium (Fig. 6C).

Mechanism of defluorination. A satisfactory explanation for DFBD defluorination had to align several key data. First, fluoride release was immediate and rapid and required toluene-grown cells, and medium darkening lagged temporally. All bacterial strains expressing toluene dioxygenase, even singly, released fluoride and darkened medium. However, known further transformation products of the toluene dioxygenase, which are 4,5-DD-DFBD and the phenols and catechols characterized here, did not undergo defluorination. Indeed, the presence of the enzyme dihydrodiol dehydrogenase, which transformed at least some 4,5-DD-DFBD to the corresponding catechol, diminished fluoride release and color formation. Those observations, together with the immediate fluoride release, indicated that 4,5-DD-DFBD was undergoing another reaction, and that reaction was fast enough to compete with the dehydrogenase

kinetically. This previously undescribed reaction pathway had to explain rapid fluoride release, pyrogallol appearance in the medium, and a lag in darkening of the medium.

It was not possible to isolate and store 4,5-DD-DFBD due to its extreme instability compared to other bicyclic dihydrodiols (Wackett, et al., 1988). Its instability was presumably linked to the highly electron-withdrawing $–OCF_2-$ moiety adjacent to the dihydrodiol group, precisely the atoms that are lost (Fig. 7). The carbon atom linking the

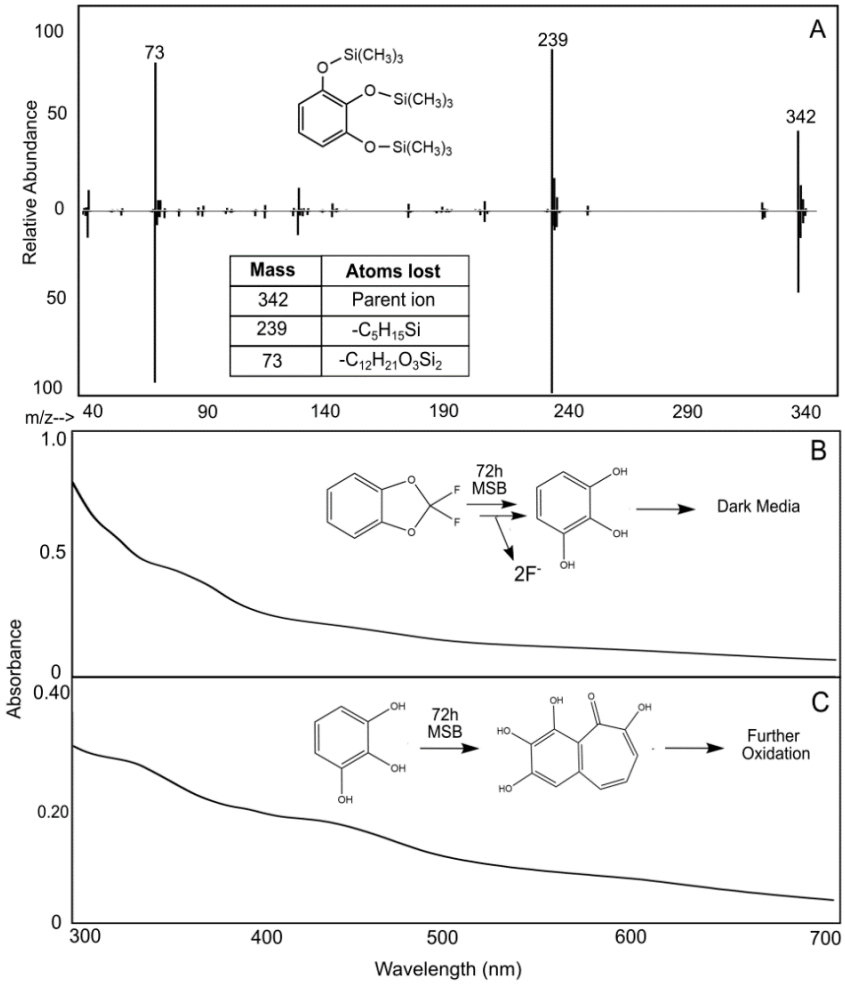

Figure 2.6. Evidence for the defluorinated aromatic product, pyrogallol, or 1,2,3-benzene triol. A) Mass spectrometry fragmentation pattern of derivatized 1,2,3-benzenetriol found in cell cultures from *E. coli* pDTG601a (top) compared to standard derivatized 1,2,3-benzenetriol (bottom). B) UV-vis spectrum of *E. coli* pDTG601a cell culture supernatant after incubation with DFBD for 72 h. C) UV-vis spectrum of standard 1,2,3-benzenetriol in MSB media after 72 h. Time course data is shown in Figure 11S.

two groups referred to above is a bridgehead carbon. This bridgehead carbon would be highly susceptible to nucleophilic attack by a hydroxide anion in solution. The resultant trihydroxy compound (middle left, Fig**. 7**) is expected to decompose with C-O breakage, rearomatization, and opening of the five-membered 1,3-dioxole ring. We propose here that these are spontaneous reactions, driven by the electrophilicity of the bridgehead carbon atom and the stabilization energy inherent in rearomatization that occurs with C-O bond cleavage. However, we cannot rule out the possibility of a cell component

assisting in hydroxide attack on the bridgehead carbon. Once the C-O bind cleaves, the resultant –OCF_2O- moiety is highly unstable, to undergo very rapid hydrolysis to produce carbon dioxide and the two fluorine atoms as fluoride. Pyrogallol, the other product, is not colored but over time will oxidize to a range of colored products that darken the medium (Fig**. 7**).

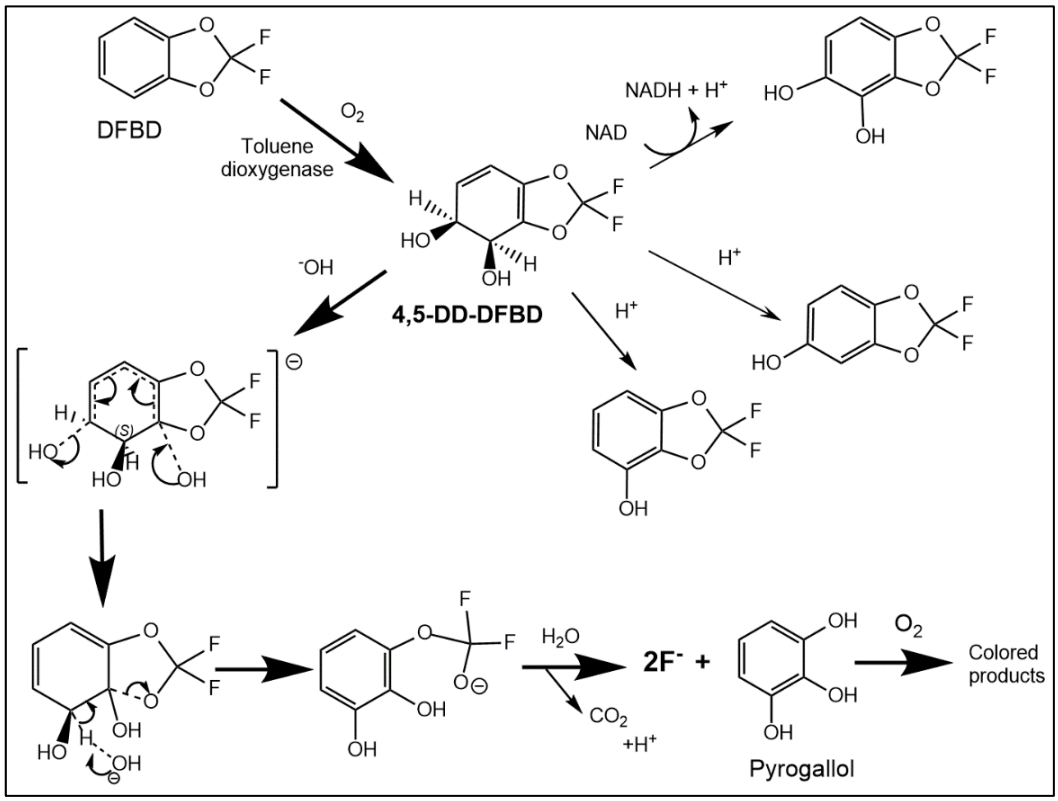

Figure 2.7. Scheme showing 2,2-difluoro-1,3-benzodioxole (DFBD) oxidation by toluene dioxygenase to 4,5-dihyro-dihydroxy-DFBD (4,5-DD-DFBD) and subsequent reactions producing fluoride ion and dark media. The major path is highlighted by darker arrows. The three intermediates between 4,5-DD-DFBD and fluoride plus pyrogallol are expected to have a very short lifetime, cannot be demonstrated directly, and represent a proposed mechanism for fluoride and media darkening. The minor products on the upper right are stable and were demonstrated in this work, as was pyrogallol and the pathway for color formation.

Potential for DFBD defluorination by other aromatic oxygenase-containing bacteria. A question naturally arises as to whether DFBD defluorination by this mechanism is common, since genes encoding the oxygenation of toluene and other

aromatic hydrocarbons are widespread in bacterial genomes (Wackett, 2002, Ferraro, et al., 2005, Jabłońska and Tawfik, 2019). In addition to dioxygenation, many bacteria oxidize toluene via monooxygenases (Jabłońska and Tawfik, 2019). Given the stability of monohydroxy and catecholic DFBD metabolites, we did not expect strains with monooxygenases to defluorinate DFBD. To test this hypothesis, Burkholderia cepacia G4, containing toluene-2-monoxygenase, was grown on glucose and induced with toluene. After 24 h of incubation with DFBD, this strain did not release fluoride or create a dark color in the medium.

Dioxygenases that oxidize multiring substrates were considered to be better candidates to test for DFBD defluorination. Defluorination and darkening of the medium were not observed with *Pseudomonas sp*. strain NCIB 9816 or *Pseudomonas sp*. Strain 9816-11, each of which expresses a naphthalene dioxygenase. Biphenyl dioxygenases that have different amino acid sequences were also tested with two bacteria*, Burkholderia xenovorans* LB400 and *Sphingobium yanoikuyae* B1. After induction with biphenyl and incubation with DFBD for 24 h, no fluoride release or color change was observed with either strain.

Identifying enzymes with greater similarity to the toluene dioxygenase from *P. putida* F1. Toluene dioxygenase is known to be a Rieske oxygenase, a very common class of proteins in aerobic bacteria (Wackett, 2002, Ferraro, et al., 2005, Jabłońska and Tawfik, 2019). The Rieske oxygenases are composed of two protein subunits. The cofactors and the active site are within the larger, or alpha-, subunit. The alpha-subunit contains a Rieske iron sulfur cluster and a mononuclear iron center. Since the alpha-subunit of Rieske dioxygenases determines substrate specificity (Parales, et al., 1998, Parales, et al., 2000), sequence comparisons with this subunit are most germane to the question as to which enzymes and organisms will defluorinate DFBD.

The amino acid sequence of the P. putida F1 toluene dioxygenase alpha-subunit

(WP_012052601) was used to search the Pseudomonas genome database (Goldman, 1965, Alexandrino, et al., 2018) for homologs to the alpha-subunit of toluene dioxygenase on 6 August 2021 using DIAMOND-BLAST. The closer the sequence to the toluene dioxygenase studied here, the more likelihood that the active site would bind and oxygenate DFBD in a manner leading to defluorination (Table 1). This search identified proteins with amino acid sequences that were 100% identical in the following Pseudomonas strains with the locus tags given in the parentheses: *Pseudomonas monteilii* SB3101 (X970_10585), *P. monteilii* SB3078 (X969_10930), *P. putida* YKD221 (TR32_RS03575), *Pseudomonas sp*. strain NBRC 111125 (APH29_RS14695), and *P. putida* UV4/95 (CBP06_RS10555). Published substrate specificity studies with *P. putida* UV4/95 have shown the same substrate spectrum as *P. putida* F1 (Boyd, et al., 2006), consistent with the 100% sequence identity of the dioxygenase alpha-subunits.

Percent identity	Number of sequences	Query sequence coverage
100%	6	100%
>90%	9	100%
>80%	19	>97%
>70%	51	>96%
>60%	177	>96%
>50%	293	>95%

Table 2.1. Homologs of the toluene dioxygenase alpha-subunit (WP_0120552601.1) with high sequence identity over the majority of the sequence length. The sequences searched were from three sources and compiled, the: *Pseudomonas* genome database, RHObase database, and NCBI non-redundant Protein database. Percent identity was determined by pairwise BLAST (Folsom, et al., 1990) and the query sequence coverage refers to the extent over which the two sequences aligned.

Next, we queried the RHObase, or Ring-Hydroxylating Oxygenase database, which focuses specifically on characterized Rieske oxygenases using the term “toluene dioxygenase” on 7 August 2021. This identified several enzymes denoted as toluene dioxygenase or nitrotoluene dioxygenases. One of these, from Pseudomonas putida DOT-

T1E (ADI95397), was 100% identical to the alpha-subunit of toluene dioxygenase from *P. putida* F1.

The large GenBank nonredundant database, with 419,490,021 sequences as of 6 August 2021, was searched to determine the approximate number of homologs and particularly close sequence matches. A BLAST search yielded over 1,200 homologous sequences with an E value lower than e^{250}, indicating they matched extremely well. Of those, 293 showed sequence identity of >50% and 9 showed sequence identity of >90% (Table 1). Closely related sequences are found in *Pseudomonas, Comamonas, Sphingomonas, Paraburkholderia, Nocardioides*, and *Rhodococcus*.

Next, the Rieske dioxygenases in the bacteria that were tested here and found not to release fluoride were analyzed for amino acid sequence relatedness to the *P. putida* F1 toluene dioxygenase. The biphenyl dioxygenase from Sphingobium yanoikuyae B1 is 37% identical in amino acid sequence to toluene dioxygenase via pairwise BLAST alignment. The Pseudomonas sp. strain NCIB 9816 naphthalene dioxygenase is 32% identical to the toluene dioxygenase alpha-subunit. The *Paraburkholderia xenovorans* LB400 biphenyl dioxygenase is 65% identical.

It is not currently known how much a sequence might deviate from 100% identity, and if slightly different, what specific requirements would ensure reactivity with DFBD at the 4,5-position leading to defluorination. Further experimental work is warranted to test other bacteria with closely related Rieske dioxygenases. It is possible that docking and molecular dynamics simulations could also be done to predict enzyme reactivity and regioselectivity with DFBD (Aukema, et al., 2017, Escalante, et al., 2017), but those detailed computational experiments are beyond the scope of the present study. A search of the Protein Data Bank for homologs of toluene dioxygenase yielded four distinct Rieske dioxygenases with X-ray structures and >64% sequence identity. Based on the bioinformatic data presented here and the wide diversity of bacteria known to express Rieske dioxygenases, we suggest that the DFBD moiety in natural environments might be subject to the type of metabolism revealed here with *P. putida* F1.

Conclusions. *Pseudomonas* strains and oxygenases have the potential to catalyze defluorination reactions in unexpected ways as demonstrated here. Previously, *Pseudomonas sp*. strain T-12 expressing toluene dioxygenase was shown to hydroxylate a carbon bearing a fluorine substituent, leading to defluorination by gem elimination (17). In this study, a difluorinated ether was shown to be defluorinated by *P. putida* F1 via a different mechanism but also demonstrated to be dependent upon toluene dioxygenase. Bioinformatic analyses strongly suggest that DFBD and its derivatives will undergo defluorination by dioxygenases found in other known *Pseudomonas* strains and in natural environments.

2.3 Materials and Methods

Bacterial strains, growth, and manipulations. Bacteria, growth substrates, enzymes expressed, and references are compiled in Table 2. Further specific details on growth and manipulations are provided below. *Pseudomonas putida* F1 was grown on Luria-Bertani (LB) plates and then grown overnight on minimal salts basal media (MSB) (Stanier, et al., 1966) with carbon supplied via a vapor bulb containing toluene, as previously described (Gibson, et al., 1968). This 10 mL culture was then added to an additional 25 mL of MSB and the toluene bulb was replaced with a 2,2-difluoro-1,3-benzodioxole bulb. This flask was then held at 30ºC and incubated with shaking at 200 rpm. Aliquots of the culture were taken out at various time points. Samples intended for measuring fluoride release were centrifuged to remove cells and the supernatant removed and placed into a clean tube. For photographs of color change, the media aliquots were taken directly and then stored at -20ºC to photograph simultaneously. *Pseudomonas putida* F39/D was originally streaked onto an LB plate and grown at 28ºC. For liquid cultures, this strain was grown on MSB and 0.2% (w/v) L-arginine. A saturated 10 mL culture of *P. putida* F39/D, grown overnight, was added to 200 mL of MSB and 0.2% (w/v) arginine and allowed to grow to log phase at 30ºC. Once log phase was attained, the culture was induced with toluene for 1 hour.

After induction, the toluene bulb was replaced with a DFBD bulb. After 2 hours of incubation with DFBD, the cells were pelleted, and the supernatant removed.

Table 2.2. Bacterial strains used, growth conditions selected, and known enzymes expressed under the conditions specified.

Bacterial strains	**Growth substrate/Inducer**	**Relevant Enzymes expressed[1]**	**Ref**
Pseudomonas putida F1	L-Arginine	Toluene metabolism enzymes at very low levels	(Gibson, et al., 1968)
Pseudomonas putida F1	Toluene	Toluene pathway and regulatory proteins	(Gibson, et al., 1968)
Pseudomonas putida F39/D	Toluene	All toluene pathway enzymes with mutation in the diol dehydrogenase (TodD)	(Gibson, et al., 1968)
Escherichia coli K12[2]	D-glucose	N/A	
Escherichia coli JM109 (pDTG601a)	IPTG[3]	Toluene dioxygenase	(Zylstra, et al., 1988)
Escherichia coli JM109 (pDTG602)	IPTG[3]	Toluene dioxygenase and diol dehydrogenase	(Zylstra, et al., 1988)
Pseudomonas sp. NCIB9816	Naphthalene	Napthalene dioxygenase pathway	(Davies and Evans, 1964, Yang, et al., 1994)
Pseudomonas sp. NCIB9816-11	Naphthalene	Naphthalene enzymes with diol dehydrogenase mutation	(Davies and Evans, 1964, Yang, et al., 1994)
Burkholderia cepacia G4	Toluene	Toluene-2-monoxygenase pathway	(Folsom, et al., 1990)
Sphingobium yanoikuyae B1	Biphenyl	Biphenyl dioxygenase pathway	(Gibson, 1999)
Paraburkholderia xenovorans LB400	Biphenyl	Biphenyl dioxygenase pathway	(Mondello, 1989)

[1]Based on peer-reviewed references

[2]No aromatic ring oxygenases known to us induced with *E. coli* grown on glucose

[3]IPTG = Isopropyl □-*d*-1-thiogalactopyranoside; added to induce expression of the specified enzyme(s) indicated

E. coli pDTG601a was maintained on LB plates with 100 ug/mL ampicillin at 37ºC. For experimental use, it was grown overnight on LB with ampicillin liquid, cells pelleted, and then the cells were resuspended in MSB and 0.2% (w/v) glucose and 100 ug/mL ampicillin. After growing at 37ºC for two hours, this strain was induced with 1 mM IPTG for 1 hour.

After induction, a DFBD vapor bulb was added to the flask and the culture was left to incubate for a further 2 hours. *E. coli* pDTG602 cells were maintained on LB ampicillin plates at 37ºC. For experimental use, this strain was grown overnight on MSB media with glucose and 100 ug/mL ampicillin. This overnight culture was used to inoculate a culture of 50 mL of MSB, glucose and ampicillin and induced with IPTG for 1 hour. After induction, DFBD was added in vapor form. Aliquots were taken at various time points and left to incubate overnight. *Pseudomonas* sp. NCIB 9816 and 9816-11 were maintained on LB plates at 28ºC. NCIB 9816 was grown to log phase on 100 mL of MSB and naphthalene for induction of naphthalene dioxygenase. Subsequently, the culture was filtered through glass wool to remove naphthalene crystals and a vapor bulb of DFBD was added to the culture. NCIB 9816-11 was grown on MSB media and 15 mM pyruvate. This culture was added to 25 mL of MSB and induced with 0.2% naphthalene. This culture was also filtered through glass wool before adding the DFBD vapor bulb and then the culture was left to incubate for 24 hours. B*urkholderia cepacia* G4 was maintained on LB plates at 28ºC. It was grown in MSB and 0.2% glucose overnight. This culture was added to 25 mL of MSB and induced with toluene for 1 hour. *Sphingobium yanoikuyae* B1 was maintained on LB plates at 28ºC. Overnight, this strain was grown on MSB and biphenyl, which induces the biphenyl dioxygenase. *Paraburkholderia xenovorans* LB400 was maintained on nutrient agar plates at 28ºC. Overnight, this strain was grown on MSB and biphenyl, which induces the biphenyl dioxygenase enzyme.

Chemicals

2,2-difluoro-1,3-benzodioxole (DFBD) was purchased from Matrix Scientific and ^{1}H-NMR indicated 97% purity. 2,2-difluoro-1,3-benzodioxole-4-ol and 2,2-difluoro-1,3-benzodioxole-5-ol were from AstaTech with 95% purity. 1,2,3-benzenetriol was purchased from Mallinckdrodt with a purity of ~95%. Purpurogallin was from Cayman Chemical and had a purity of 95%, as determined by ^{1}H-NMR. N,O-Bis(trimethylsilyl)trifluoro-acetamide was purchased from Fluka Analytical and had a purity of 99%. $CDCl_3$ and CD_3CN were obtained from Cambridge Isotope Laboratories, Inc and had >99% purity. Methyl-*tert*-butyl ether (MTBE) and ethyl acetate (EtOH), solvents used for GC-MS, were

from Sigma-Aldrich, both HPLC grade, >99% pure. Toluene used for specified cell growth and induction was from Fisher Chemical and is 99% purity. Sodium fluoride (NaF) used for fluoride standards was obtained from Aldrich Chemical company, 99% pure. D-glucose, used for growth of *E. coli* recombinant strains was purchased from Sigma Aldrich and 99.5% pure. IPTG was obtained from Gold Bio. *L*-arginine, used for growth of *Pseudomonas* strains, is from Calbiochem. Sodium pyruvate is from Alfa-Aesar with a purity of 99%. Biphenyl was from Spectrum chemical and had a purity of 99%. Naphthalene was from Alfa-Aesar with a purity of 99%.

Nuclear Magnetic Resonance (NMR) experiments

Cell culture supernatants from both *E. coli* pDTG601a and *P. putida* F39/D after incubation with DFBD were extracted with an equal volume of ethyl acetate (EtOAc). In each case, the aqueous layer was drawn off and the organic layer was dried ($MgSO_4$), transferred to a round bottom flask, rotary evaporated. The residue was taken into CD_3CN for initial ^{1}H- and ^{19}F-NMR acquisitions on a Varian INOVA 500 MHz NMR spectrometer. The initial ^{1}H-NMR spectra were too complex to identify signals due to 4,5-dihydro-DFBD-4,5-diol but ^{19}F-NMR (376 Mhz, Fig. 3C and Fig. 6S-1 in CD_3CN) shows a clean AB pattern: 46.65ppm (d, J = 110.8Hz), -49.05 (d, J = 110.8Hz) for the CF_2 fluorine atoms.

Cell culture supernatants from *E. coli* pDTG602 were extracted with MTBE, dried with anhydrous $MgSO_4$ and then rotary evaporated. Subsequently, the CD_3CN solutions were concentrated, then directly dissolved in $CDCl_3$. The product: ^{1}H-NMR (400 MHz, $CDCl_3$): 1,2,3-benzenetriol; 6.68 ppm (*t*, J = 8.0 Hz), 6.48 ppm (*d*, J = 8.2Hz), 5.24 ppm (bs), 5.17 ppm (bs), and DFBD-ols, 6.57 ppm (*d*, J = 8.4Hz), 6.51 ppm (*d*, J = 8.4Hz), and buried OH broad singlets. ^{19}F-NMR (400 MHz, $CDCl_3$) -50.31 ppm (s), CF_2. In the proton NMR, the high field doublet at 6.51 ppm is partly buried in a neighboring peak. Additional significant peaks that do not describe the 4,5-DD-DFBD are shown to be 1,2,3-benzenetriol (Figure 7S and Figure 9S, Appendix A).

Gas chromatography and mass spectrometry (GC-MS) experiments

For GC-MS, cell culture supernatants were extracted with methyl-*tert*-butyl ether (MTBE). Equal volumes of organic and aqueous phases were used. Extraction was done directly in glass GC vials, shaken vigorously and then the organic layer was drawn off and placed in a clean vial. One microliter of derivatizing agent, N,O-Bis(trimethylsilyl)trifluoro-acetamide was added to each extracted sample. Product ion spectra were identified in positive ion mode on a HP7890 gas chromatograph and HP5975 MS detector. GC conditions were as follows: helium gas, 1 mL/min; HP-1ms column (100% dimethylpolysiloxane capillary; 30m x 250 μm x 0.25 μm); starting temperature 50˚C with a ramp of 10˚C/min to 320˚C. Standards run on the GC-MS used the same program specified above. 2,2-Difluoro-1,3-benzodioxole-5-ol and 2,2-difluoro-1,3-benzodioxole-4-ol were prepared by placing a small volume of each into separate GC vials with 500 uL of MTBE. One uL of the derivatizing agent was added to each vial. Pyrogallol (1,2,3-benzenetriol) was prepared similarly, by putting a small solid amount of the compound into 500 uL of MTBE and adding 1 uL of derivatizing agent.

Fluoride Measurements

Fluoride ion measurements were determined using a ISE Ionplus Sure-Flow Orion fluoride probe from ThermoFischer and the Orion Star A214 meter. To perform fluoride measurements, 1 mL of cell culture was pelleted. The supernatant was removed and placed into a 5 mL tube with 1 mL of TISAB (58.5 g/L NaCl, 15 g/L CH_3COOH, 66 g/L CH_3COONa, and 1 g/L 1,2-cyclohexane diaminetetraacetic acid. Calibrations of the probe were made with standard concentrations ranging from 10^{-5} M to 10^{-2} M. Two standards were required for calibration. Standards were made with sodium fluoride in MSB media.

UV-vis spectroscopy

UV-vis absorption scans were performed on a Cary 3500 double beam UV-vis spectrophotometer containing a Xenon flash lamp from Agilent. Measurements of supernatant from an *E. coli* pDTG601a culture was taken after 72 hours of incubation with DFBD. An aliquot was taken from the cell culture and pelleted to remove cells. The

supernatant was removed and placed in a 1.5 mL disposable cuvette. The sample was then measured (300 - 700 nm) in increments of 5 nm. Standard 1,2,3-benzenetriol was prepared to a concentration of 0.1 M in water. To scan this compound, 1 mL of MSB was placed in a 1.5 mL disposable cuvette and 1,2,3-benzenetriol stock solution was added to a final concentration of 0.1 mM. This cuvette of MSB and 0.1 mM pyrogallol was left to sit at room temperature for 72 hours and measured after that.

Bioinformatic methods

BLAST was used to query the NCBI GenBank non-redundant database (Altschul, et al., 1990). DIAMOND-BLAST was used to query the *Pseudomonas* genome database (Buchfink, et al., 2015). The RHObase, or Ring-Hydroxylating Oxygenase database was queried with a word search (Chakraborty, et al., 2014). All hits obtained from the searches were compiled manually. Comparisons with toluene dioxygease and other single enzymes were carried out using pairwise BLAST (Altschul, et al., 1990) on the National Center for Biotechnology Information server.

Supplemental material can be found in **Appendix A**

ACKNOWLEDGEMENTS

We thank Becky Parales for providing the recombinant E. coli strains: E. coli pDTG601a and E. coli pDTG602. We acknowledge Thomas Niehaus for making available the Cary spectrophotometer. We acknowledge Mikael Elias and Amir Shimon for helpful discussion about this project.

This project was funded by MnDRIVE Environment.

L.P.W., K.G.A., and M.D.B. conceived and designed the experiments. M.D.B., K.G.A., and J.E.R. performed the experiments. M.D.B., K.G.A., J.E.R., and L.P.W. analyzed the data. B.P. and T.N. contributed reagents/materials/analysis tools. M.D.B., K.G.A., and L.P.W. wrote the paper. All authors edited and approved the manuscript.

CHAPTER 3

Microwell Fluoride Screen for Chemical, Enzymatic, and Cellular Reactions Reveals Latent Microbial Defluorination Capacity for -CF_3 Groups

Authors: Madison D. Bygd, Kelly G. Aukema, Jack E. Richman, Lawrence P. Wackett

3.1 Introduction

Fluorinated, particularly polyfluorinated, compounds are major pollutants and are widely considered to be poorly, if at all, biodegraded (Ahrens and Bundschuh, 2014, Filho and de Souza, 2020, Lim, 2021). More than one million fluorinated compounds (organic and inorganic) are recorded on PubChem (Kim, et al., 2021). A subset of organofluorine compounds are categorically known as per- and polyfluoroalkyl substances (PFAS), which consist of several thousand compounds introduced into the global market (Wang, et al., 2021). Current understanding of commercially relevant PFAS is on the order of hundreds (Buck, et al., 2021). Further, greater than 20% of newly introduced agricultural chemicals and drugs are fluorinated (Jeschke, 2017, Caron, 2020, Britton, et al., 2021, Ogawa, et al., 2021). By contrast, there are only dozens of known natural product organofluorine compounds (Murphy, et al., 2003, Walker and Chang, 2014). In this context, billions of years of microbial evolution have progressed largely in the absence of fluorinated compounds. Additionally, organofluorine compounds have been introduced commercially

principally because of their chemical inertness (O'Hagan, 2008). For these reasons, some organofluorine compounds are considered recalcitrant due to a lack of or limited biodegradation in the environment (Sima and Jaffé, 2021).

A limited number of bacterial genes and enzymes have been demonstrated to participate in biodefluorination. The most well-studied case of biodefluorination is with a monofluorinated natural product produced by some plants and bacteria, fluoroacetate (Murphy, et al., 2003, Leong, et al., 2017). Fluoroacetate dehalogenase has been studied structurally and mechanistically (Goldman, 1965, Chan, et al., 2011, Miranda-Rojas, et al., 2018). More recently, another structurally determined enzyme, toluene dioxygenase (Tod), was shown to be responsible for the defluorination of a difluorinated ether substrate (Bygd, et al., 2021). In another example, the enzyme benzoyl-CoA reductase was shown to participate in the defluorination of 4-fluorobenzoate (Tiedt, et al., 2016). A limited number of biodegradation studies have also been conducted with mixed and pure cultures of bacteria, including the biodegradation of heavily fluorinated compounds. Recent studies also report the biodegradation of perfluoroalkyl acids (Huang and Jaffé, 2019, Yu, et al., 2020).

Documentation of microbial degradation of fluorinated compounds typically requires monitoring parent compound disappearance and product appearance. Detecting defluorinated organic products often involves extractions, followed by liquid or gas chromatography, and mass spectrometry (Brase, et al., 2021, Fiedler, et al., 2021). With polyfluorinated compounds, these analytical methods can be difficult due to extraction losses, volatility during workup, and external contamination. In addition to the many different organic products expected from the thousands of organofluorine compounds, fluoride anions are a universal co-product of defluorination. This is due to the high electronegativity of fluorine, and fluoride is observed regardless of the mechanism of C-F bond cleavage (Pritchard and Skinner, 1955, O'Hagan and Rzepa, 1997). Fluoride determination as a means of monitoring defluorination reactions is also ideal because natural waters and laboratory buffers typically contain very low levels of fluoride

(Edmunds and Smedley, 2013). This contrasts with chloride, which has a high background and is thus not an ideal indicator for dechlorination (Roessler, et al., 2003).

The value of fluoride anion monitoring has been recognized and has been used in single end-point determinations in batch cultures of microbes tested for biodegradation of C-F compounds. In these studies, the two commonly used methods are ion chromatography and fluoride-specific electrode determination (Ochoa-Herrera, et al., 2009, Huang and Jaffé, 2019, Xie, et al., 2020, Yu, et al., 2020). Each method is done via single-sample, fixed time-point determinations and only a limited number can be carried out per hour. Research on microbial defluorination would accelerate significantly with the introduction of methods to screen multiple organisms, enzymes, and libraries of fluorinated compounds rapidly and combinatorially in small liquid volumes.

Chemists have devised colorimetric and fluorimetric methods for determining and quantifying fluoride but none have been demonstrated for microbiological screening, with the exception of a colorimetric test suitable for petri plate screening of colonies showing fluoroacetate dehalogenase activity (Davis, et al., 2011). That method, using xylenol orange, required an overlay of reagents due to media interferences precluding direct incorporation and it was not demonstrated for liquids. A variety of other approaches have been developed that are only functional in organic solvents, are non-biocompatible, and/or require extensive organic synthesis to make components that are not commercially available (Han, et al., 2007, Hinterholzinger, et al., 2013, Zhao, et al., 2017). As a result, the methods have not been widely adopted for studies of biodefluorination.

In the present work, we systematized a high throughput screening protocol distinct from ion chromatography or fluoride electrode and demonstrated the method's efficacy to rapidly monitor chemical, enzymatic and *in vivo* microorganismal defluorination reactions. The method is based on a previously described fluoride binding reaction and uses all commercially available components (Belcher and West, 1961a, Belcher and West, 1961b, Yamamura, et al., 1962). The method is sensitive; several nanomoles of fluoride is sufficient to bind to a rare earth metal coordination complex to produce a blue chromophore. For the first time here, the method was adapted for biological purposes,

miniaturized, and calibrated in microtiter 96-well plates to determine fluoride concentration visually or via a spectrophotometric plate reader. The method was demonstrated with purified enzyme and cell-based defluorination reactions. Parameters of the microliter screen were determined: sensitivity, accuracy, and interfering substances. The new assay was subsequently used to screen a model microorganism against a library of 63 organofluorine compounds. Surprisingly, 21 compounds, most with multiple fluorine substituents, showed microbially-catalyzed defluorination. One compound containing a $-CF_3$ group underwent significant defluorination and the mechanism of defluorination was demonstrated. Overall, this method can increase the pace of discovering new microbes and enzymes that biodegrade C-F compounds.

3.2 Results

Standard fluoride screen parameters. Failing to find literature on small volume, rapid screening methods for monitoring biodefluorination, we sought here to adapt a method previously used for determining fluoride in liter volumes of drinking water. The method is based on a color change upon fluoride binding to a rare earth metal bound in complex with an alizarin ligand (**Figure 3.1**). Based on previous work (Belcher and West, 1961a, Belcher and West, 1961b), we tested the rare earth metals cerium, lanthanum, neodymium, and praseodymium with standard fluoride concentrations. We found lanthanum best for working in biologically relevant fluids such as buffers and growth media. Additional testing was done to determine optimal pH and concentration of the acetate buffer, as well as reagent ratios. Consistent with one previous report (Belcher and West, 1961b), maintaining a 1:1 ratio of alizarin:lanthanum and the buffer pH in the range 5.0-5.5 was found to be most sensitive for detecting fluoride. However, we determined that increasing the concentration of sodium acetate buffer 3-fold over that used previously (Belcher and West, 1961b) was necessary to counterbalance the buffering capacity of typical enzyme and microbiological media. All subsequent experiments described here use lanthanum as the metal and 84 mM of acetate buffer at pH 5.2 and a 1:1 ratio of alizarin: lanthanum. The

organic solvent, acetone, was also optimized and included routinely, based on previous studies showing acetone enhanced the sensitivity of the assay (Belcher and West, 1961b).

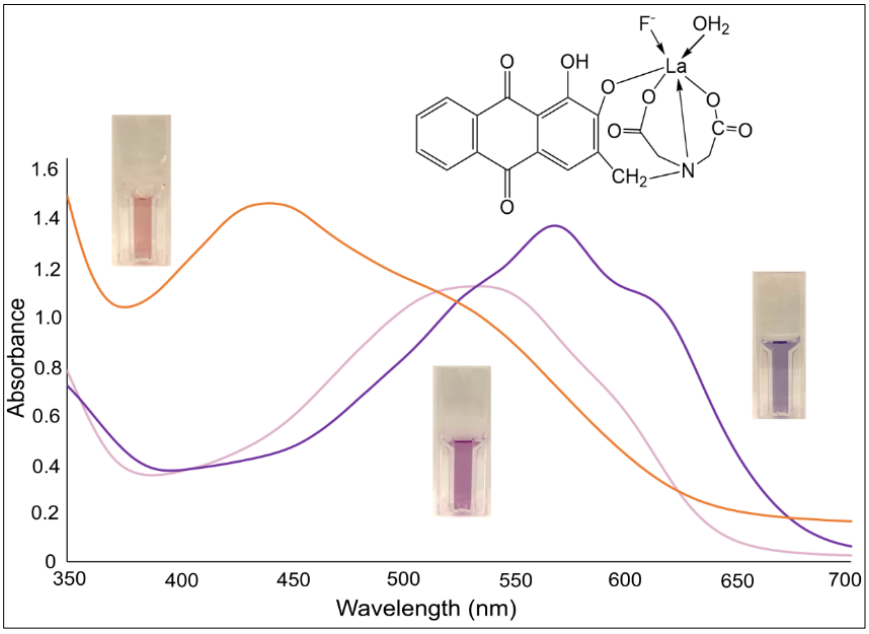

Figure 3.1. UV-vis spectra of the lanthanum-alizarin complex bound to phosphate (orange), water (red), and fluoride (purple). The cuvettes show how the orange, red, and purple species can be differentiated visually. The upper right shows the putative structure of the lanthanum-alizarin complex with bound fluoride as previously reported in several studies (Belcher and West, 1961a, Belcher and West, 1961b, Han, et al., 2007).

The cuvette with red liquid shown in the middle of **Figure 3.1** represents the color of the alizarin-lanthanum-water complex, consistent with previous reports (Belcher and West, 1961a, Belcher and West, 1961b). As fluoride is added to the medium, the absorbance maxima shifts to peak at 565 nm with a strong shoulder at 620 nm. The increase in absorbance at the longer wavelength, 620 nm, is proportional to the amount of fluoride in the range of 10-100 µM (**Figure S1, Appendix B**). Used in shallow well microtiter plates, the method can be monitored visually, or with a plate reader, to detect as little as 4 nmol fluoride in a 200 µl volume.

It was initially curious to us as to why this facile and sensitive method has not been reported to screen biodefluorination previously, but then we found significant interference by typical microbiological and enzymatic reagents. For example, phosphate buffer, often used at millimolar concentrations, outcompetes fluoride to make an orange product (**Figure 3.1**). Subsequently, a series of other buffers and media (Bicine, MOPS, Tris, nutrient broth) also showed significant interference (**Figure S2, Appendix B; Table 3.1**), but HEPES buffer

showed little interference and provided excellent buffering for several microbial media and enzyme buffer. All subsequent experiments were conducted using HEPES as the buffering agent.

Initially, the screen was calibrated with known concentrations of fluoride in HEPES buffer in microtiter well plates. As fluoride was varied, an isosbestic point was observed at 530 nm. So spectrophotometric readings were obtained by dividing the measured 620 nm absorbance by that at the constant 530 nm absorbance. That ratio plotted against fluoride concentration gave an increasing and linear response to fluoride up to 100 µM (**Figure 3.2**) with an $R^2 = 0.96$. The screen was routinely used in in the 10 – 100 µM range, corresponding to 2 – 20 nmol fluoride in the wells. The change in color from red to purple was clearly discernible to the eye and for a spectrophotometric plate reader at and above 4 nmol fluoride in the well. In many experiments, we found visual inspection followed by photography with a simple cell phone camera to serve our purposes well. The high-throughput application of this screen can cover thousands of individual wells daily. Digital photography and available storage systems also allow for image

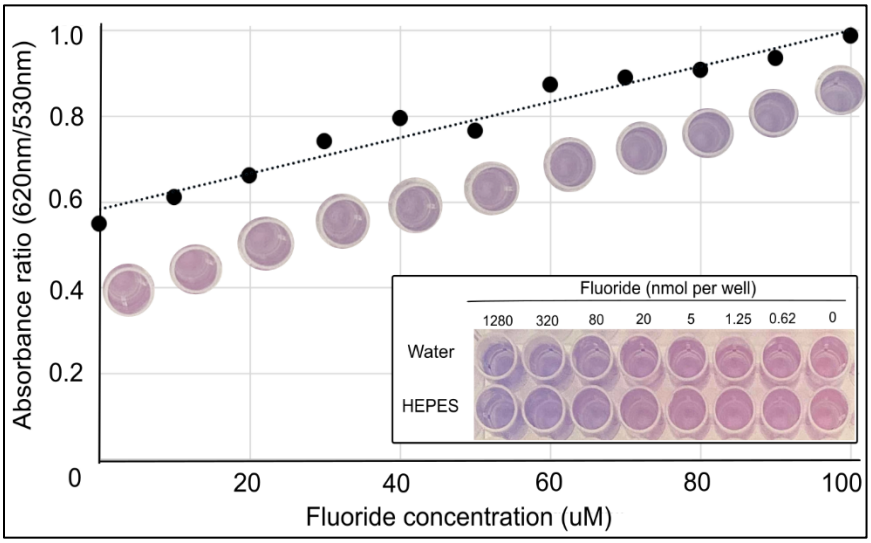

Figure 3.2. Plotted is the ratio of the lambda max of fluoride bound complex (620 nm) over the lambda max of the unbound complex (530 nm). The 530 nm absorbance does not change during the increasing 620 nm absorbance and so the 530 nm absorbance is used as a fixed point to correct for minor baseline fluctuations. This trend of 620 nm/530 nm absorbance is linear from 0 to 100 µM fluoride, which can also be seen by eye in the assay. We define a dark purple well as having a 620/530 ratio >0.7 and a light purple well as having a ratio <0.7. Inset: comparison of fluoride detection in water versus 20 mM HEPES buffer down to a 0.62 nmol concentration. 20 mM HEPES does not inhibit the ability to detect fluoride in comparison to water.

processing that can enhance color for sensitivity, although this was not done routinely here. The method also lends itself to be used in an ultra-high-throughput format if using robotic liquid and plate handling and spectroscopy.

Broad testing for non-interfering and interfering biological reagents. HEPES buffer can be used for the growth of many bacteria and for working with many enzymes *in vitro* (Good, et al., 1966, Taha, et al., 2014) but some studies will require alternative or additive compounds. In that context, a wide variety of bacterial and enzyme media components were tested here and classified as: (i) non-interfering, (ii) moderately interfering, and (iii) strongly interfering as defined in the Methods section (**Table 3.1**). The non-interfering components included organic solvents, buffers, salts, sugars, vitamins, and the general growth medium of casamino acids. These data illustrate that this method can successfully determine fluoride in the presence of components used in a wide variety of microbiological and enzyme-based experiments.

Table 3.1. Interfering and non-interfering buffers and growth media components. Conditions for testing were as described in the Methods section.

Non-interfering	**Moderately Interfering**
25% acetone	0.2 M tris
84 mM acetate buffer	0.25 M bicine
20 mM HEPES	0.2 M MOPS
10% glycerol	2 mM sodium phosphate monobasic
100 mM sodium chloride	2 mM ferric chloride
2 mM sodium bromide	20% ethanol
2 mM sodium sulfate	
2 mM sodium nitrate	
100 µM sodium phosphate monobasic	
47 µM borate (borax)	
10 mM sodium sulfide	
43 µM EDTA	**Strongly Interfering**
2 mM fluorobenzene	500 µM imidazole
0.5% casamino acids	13 g/L nutrient broth
2 mM succinic acid	10 mM sodium phosphate monobasic
2 mM sodium acetate	500 µM mercaptoethanol
20 mM magnesium chloride	0.1% yeast extract
23 mM calcium chloride	1.0% yeast extract
20 mM lithium chloride	37 g/L brain heart infusion
19 mM ammonium chloride	50 µM zinc chloride
20 mM potassium chloride	50 µM cupric chloride
20% DMF	2 mM sodium citrate dihydrate
20% acetonitrile	
2% glucose	
2% arabinose	
2% sucrose	
74 µM thiamine hydrochloride	
0.41 mM nicotinic acid	
2 µM biotin	

Monitoring defluorination reactions *in vitro*. To test the microwell method for monitoring the progress of chemical and enzymatic defluorination, we examined a defluorination reaction that could be catalyzed by either sodium hydroxide or the enzyme TrzN. The *s*-triazine ring is sufficiently activated for nucleophilic aromatic substitution which allows for defluorination of fluoroatrazine to be elicited with sodium hydroxide (pH

11) and heat. The enzyme TrzN has previously been shown to produce hydroxyatrazine from fluoroatrazine (Shapir, et al., 2005). Reaction time course experiments were monitored by the microwell colorimetric method (**Figure 3.3**). This showed that fluoride was increasing over time, as expected for catalytic chemical and enzymatic reactions. Moreover, we found that we could obtain estimates of fluoride at concentrations exceeding the ideal range of color formation by making a series of two-fold dilutions (**Figure S3, Appendix B**). This takes advantage of the ability of this method to easily make 96 determinations at once. The results obtained with the color method were confirmed using a fluoride electrode.

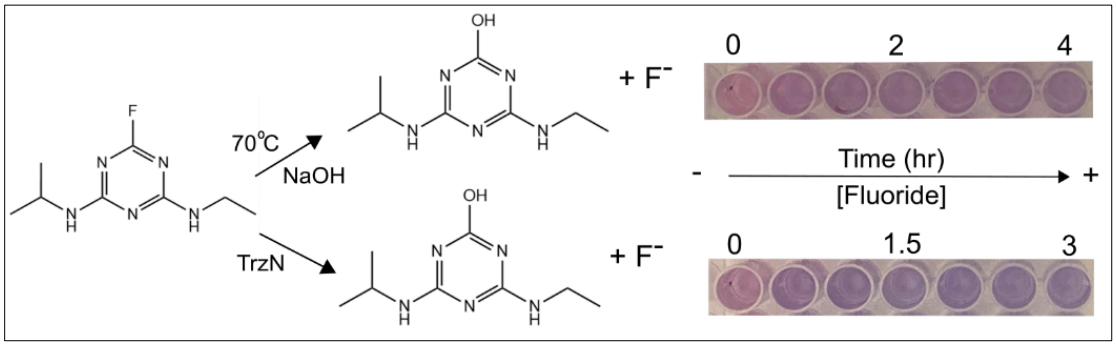

Figure 3.3. Chemical and enzymatic defluorination of fluoroatrazine catalyzed by base or triazine hydrolase (TrzN). The assay wells correspond to fluoride detection over time. Wells shown are a 1:4 dilution of the original sample.

Fluoride release from cells and determination in media. An additional issue addressed here was whether enzyme activity *in vivo* reasonably reflects the activity of the enzyme releasing fluoride internally. TrzN is known to be in found the cytoplasm when recombinantly expressed in *E. coli* (pTrzN) (Seffernick, et al., 2010). To determine if fluoride concentration in the culture supernatant reflects fluoride release by the cytoplasmic enzyme, TrzN was expressed in whole cells of *E. coli*, incubated with fluoroatrazine *in vivo*, and fluoride was measured by fluoride electrode. The media concentration of fluoride was 36 μM. An additional sample was taken at the same time, but the cells were lysed using heat, and the fluoride concentration was detected to be 40 μM. This indicated that 90% of the fluoride released by TrzN could be detected in the media alone. That observation supported the idea that fluoride was not bound to cells in the cell pellet, and there is no need to lyse cells to release the fluoride. Avoiding cell lysis allows the assay to

be high throughput and mitigates against potential interferences by cytoplasmic cellular compounds. Consistent with these findings, *E. coli* is known to produce a highly active fluoride export protein to protect itself from fluoride, a toxic anion to bacteria (Baker, et al., 2012, Ji, et al., 2014). *Pseudomonas* strains are also known to readily export fluoride into media during biodegradation (Misiak, et al., 2011) and following external exposure (Calero, et al., 2020). These data here and published literature together suggest that fluoride determination in microbiological media will serve to detect fluoride produced by cytoplasmic enzymes.

Screening for discovery of new defluorination reactions. It had been known that the TrzN enzyme would defluorinate fluoroatrazine, providing a good test of the method, but the major incentive for devising a microwell screening method was to expand the known constellation of microbial defluorination reactions. In that context, we screened a library of fluorinated compounds with *Pseudomonas putida* F1, a model bacterium recently reported to catalyze a novel defluorination reaction with 2,2-difluoro-1,3-benzodioxole (DFBD) (Bygd, et al., 2021). All results from the color screening in 200 µl were compared to fluoride electrode measurements.

Table 3.2. Types and number of fluorinated compounds tested, with the corresponding positive hits of fluoride release after incubation with *P. putida* F1 and an example of compound containing a given number of fluorine atoms.

# of F^- atoms	# of tested compounds	# of positives	Example compound
1	22	6	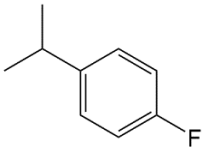 4-Fluorocumene
2	21	9	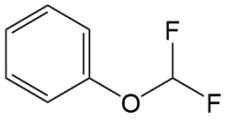 (Difluoromethoxy)benzene
3	11	4	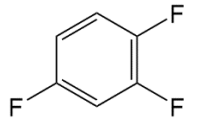 1,2,4-Trifluorobenzene
4	4	2	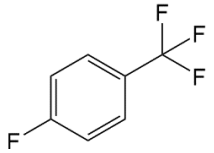 4-Fluorobenzotrifluoride
5	2	0	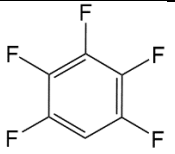 Pentafluorobenzene
>5	3	0	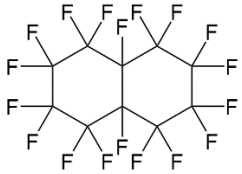 Perfluorodecalin
Total	**63**	**21**	

The screen was run with toluene-grown whole cell suspensions of *P. putida* F1 incubated with 63 different fluorinated compounds in 96 deep well plates. Growth on toluene is known to induce enzymes of the Tod pathway for the oxidation of aromatic hydrocarbons. In the screening, more than 60% of the fluorinated compounds were polyfluorinated and a remarkable 33%, or 21 compounds, showed evidence of defluorination (**Table 3.2**; **Figure S4, Appendix B**). All reported compounds were chemically stable and did not undergo defluorination in the absence of microbial cells. A sample of the culture in each well was subsequently tested by fluoride electrode (**Figure 5S, Appendix B**). A side-by-side comparison was made to determine the sensitivity and selectivity of the color screen (**Table 3.3; Figure S6, Appendix B**).

Table 3.3. Summarized results after 2 mM fluorinated chemical incubation with *P. putida* F1. Cell supernatant was tested in the color screen and measured with the fluoride electrode to confirm each positive or negative result. The cutoff for fluoride detection with the electrode was set at 30 μM, as this value was deemed to be the reliable limit of detection in the colorimetric method. If the sample in the color assay was "+" or "++" (see Screen Development Section in Methods) and the probe reading as above 30 μM, it was considered a true positive. If the well was not purple but more than 30 μM was detected with the fluoride electrode, it was considered a false negative. If the color screen indicated purple but the probe read less than 30 μM, then it was considered a false positive.

Compound	Color Screen (+/-)	Electrode >30 µM (+/-)	Result
2-fluorotoluene	+	+	True +
3-fluorotoluene	++	+	True +
4-fluorotoluene	+	+	True +
4-fluorobenzotrifluoride	++	+	True +
α,α,α-trifluorotoluene	++	+	True +
2,5-difluorotoluene	++	+	True +
3,5-difluorotoluene	++	+	True +
2,3-difluorotoluene	+	+	True +
2,4-difluorotoluene	+	+	True +
2,4,5-trifluorotoluene	++	+	True +
1,2-difluorobenzene	++	+	True +
1,3-difluorobenzene	++	+	True +
1,2,3-trifluorobenzene	++	+	True +
1,2,4-trifluorobenzene	++	+	True +
1,3,5-trifluorobenzene	-	+	False -
1,2,3,4-tetrafluorobenzene	-	+	False -
1,2,3,5-tetrafluorobenzene	+	-	False +
1,2,4,5-tetrafluorobenzene	+	+	True +
(difluoromethoxy)benzene	++	+	True +
phenyl trifluoromethyl sulfide	+	-	False +
4-(difluoromethoxy)benzoic acid	++	+	True +
4-fluoro acetophenone	++	+	True +
2-fluoro-4-(propanyl)benzoic acid	+	+	True +
4-fluorocumene	+	+	True +
4-(difluoromethoxy)aniline	+	+	True +

All compounds showing a strong color reaction were positive in releasing fluoride as determined by the fluoride electrode, a 100% selectivity by this measure. Two remaining weaker positive (lighter purple) proved to be negative in the fluoride electrode test. Two compounds positive in the fluoride electrode test were negative by visual inspection of the color screen. The few false positives and negatives were with compounds showing marginal or no defluorination. In total the method proved to be very reliable in giving true positives when fluoride release was greater than 15 nmoles per microtiter well. This makes the rapid method described here reasonable for screening a directed evolution, or other large cell library, in which using the fluoride electrode would be too cumbersome. In the present study, we decided to follow up with the strongest positive to determine the mechanism of defluorination, as that was not immediately obvious.

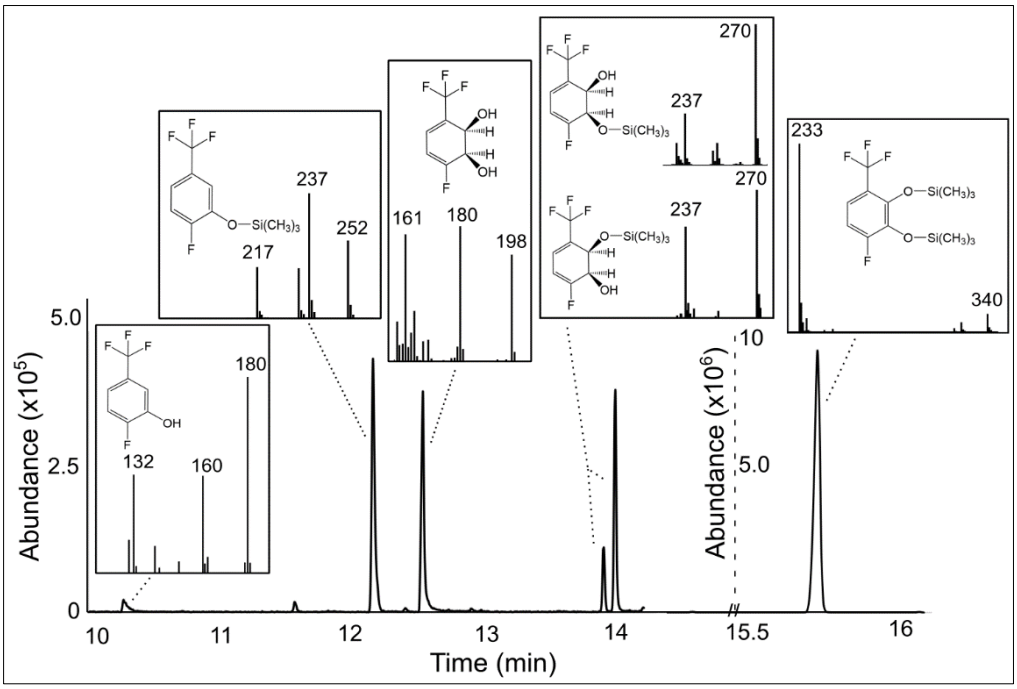

Figure 3.4. Gas-chromatogram and mass spectra showing the initial fluorinated products from the oxidation of 4-fluorobenzotrifluoride by *P. putida* F1 and following a short-time derivatization with bis-trimethylsilane. Both derivatized and underivatized products are shown. The GC abundance for products eluting after 15.5 minutes is 20-fold higher, indicating that the derivatized catechol of 4-fluorobenzotrifluoride is the major product. The key masses of the MS are highlighted. Full MS data are available in the Supplemental Information (**Figure S8, Appendix B**). ^{19}F- and ^{1}H-NMR data are provided in the Methods section.

Unexpected insights on defluorination. To our knowledge, 4-fluorobenzotrifluoride biodefluorination had not been studied previously and substantial fluoride release was observed here despite the known resistance of -CF_3 groups to biodegradation. CF_3 groups are often substituted for CH_3 in drugs and agricultural chemicals to inhibit biodegradation (Goldman, 1965, Murphy, et al., 2003, O'Hagan, 2008, Chan, et al., 2011, Walker and Chang, 2014, Jeschke, 2017, Leong, et al., 2017, Romero, 2019, Caron, 2020, Britton, et al., 2021, Ogawa, et al., 2021, Sima and Jaffé, 2021). Moreover, toluene dioxygenase is known to oxidize the 2,3-carbon atoms between 1,4-substituents on an aromatic ring, making it unlikely to be directly attacking the fluorinated carbon *para* to the CF_3 group (Gibson, et al., 1974, Boyd, et al., 2007). In that context, we sought here to further confirm defluorination and elucidate the mechanism by which defluorination occurs.

P. putida F1 wild-type and *P. putida* F39/D, a mutant strain lacking an active dihydrodiol dehydrogenase (Gibson, et al., 1973), were each incubated separately with 4-fluorobenzotrifluoride via a vapor bulb. The wild type gave 1.7 mM fluoride and the mutant 0.7 mM fluoride in overnight cultures. To better understand those observations, we first purified the transformation product from *P. putida* F39/D cultures. The major product was a *cis*-2,3-dihydrodiol, identified by ^{1}H-NMR and ^{19}F-NMR as presented in the Methods and **Figure S7 (Appendix B)**. The four fluorine atoms remained in this product. The ^{1}H-NMR was compared to the *cis*-2,3-dihydrodiol produced by toluene dioxygenase in *Pseudomonas putida* UV4 in (Boyd, et al., 2007), which confirmed the major product to be 4-fluorobenzotrifluoride-2,3-dihydrodiol (i.e, 1,2-dihydroxy-3-trifluoromethyl-6-fluorocyclohexa-3,5-diene). Next, we extracted transformation products from the wild-type culture and used bis-trimethylsilane as a derivatizing reagent. GC-MS revealed a range of products (**Figure 3.4**). We observed the 4-fluorobenzotrifluoride-2,3-dihydrodiol, underivatized and partially derivatized, a phenol and the major product was identified as 4-fluoro-(trifluoromethyl)catechol (i.e, 3-trifluoromethyl-6-fluoro-1,2-benzenediol). These are the stable products that still contain fluorine. Note in **Figure 3.4** that the scale is

20-fold higher for the catechol, which we estimate to represent >90% of the recovered products.

P. putida F39/D also produced phenolic products, with either the hydroxyl *ortho*- or *meta*- to the trifluoromethyl group, consistent with many studies showing that *cis*-dihydrodiols can readily undergo dehydration (Jerina, et al., 1976, Williams, et al., 1990, Bygd, et al., 2021) (**Figure 3.5**). Further experiments were conducted with synthetic standards of each phenol. The *meta*-phenol (**III**) was quite stable in growth medium and buffers at different pH values. The *ortho*-phenol (**IV**) is not stable and readily released fluoride into growth medium or buffer solutions. This explains fluoride release by *P. putida* F39/D. Extraction of the media and subsequent, GC-MS, ^{1}H-NMR and ^{19}F-NMR spectroscopy identified 4-fluorosalicylate (**VII, Figure S9, Appendix B**). This compound, **VII** in **Figure 3.5**, was shown experimentally to be derived from spontaneous defluorination of the *ortho*-phenol (**IV**). Defluorination of the *ortho*-phenol was rapid in the growth medium and accelerated at pH values above the pKa value of 7.0 (**Figure 3.5**). This is consistent with the defluorination being driven by the deprotonation of the phenolic hydroxyl group with the intermediate formation of a difluoro quinone methide. This is shown by the middle-bracketed compound in **Figure 3.5**. Base-catalyzed difluoro quinone methide formation has been demonstrated with 2-(trifluoromethyl)phenol (Reinscheid, et al., 2006) and the additional fluorine substituent on the ring, in the compound studied here, lowers the pKa. Groups that lower the hydroxyl pKa will increase the rate of defluorination, as reported in

numerous studies with other (trifluoromethyl)phenols (Jones, 1947, Reinscheid, et al., 2006).

Additional experiments done with *E.coli* pDTG 602, a recombinant strain that only expresses toluene dioxygenase (TDO) and dihydrodiol dehydrogenase (TodD) and

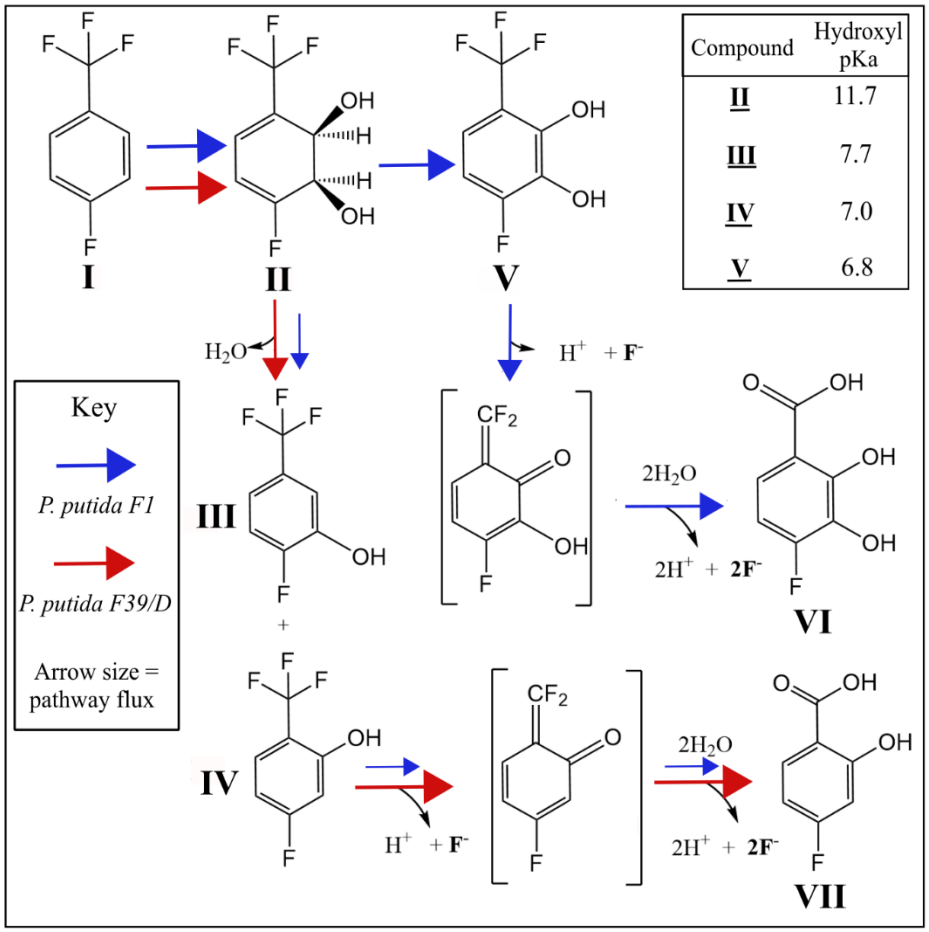

Figure 3.5. Schematic showing the oxygenation and defluorination of 4-fluorobenzotrifluoride. Arrows show pathway differences between *P. putida* F1 and *P. putida* F39/D with the size of the arrows illustrating the relative magnitude of the products. In the top row, the product II and V are formed by toluene dioxygenase and *cis*-dihydrodiol dehydrogenase, respectively. Compounds III and IV derive from spontaneous dehydration of compound II. Compounds VI and VII arise from V and IV, respectively via the relatively low pKa phenolic groups undergoing deprotonation and fluoride elimination to form the quinone methide intermediates shown in brackets, following established chemistry (51, 55). The pKas of the hydroxyl groups are indicated in the inset at the upper right, predicted using SciFinder (54). The pKas for dihydroxy compounds are for the hydroxyl group *ortho*- to the trifluoromethyl group.

accumulates catechols (Zylstra and Gibson, 1989), was grown and incubated with 4-fluorobenzotrifluoride. After incubation, 4-fluoro-(trifluoromethyl)catechol (**V**) was extracted and identified by GC-MS (**Figure 3.4)** and via ^{1}H-NMR and ^{19}F-NMR (**Figure S10, Appendix B**). Compound **V** is predicted to have the lowest pKa of 6.8 (Gabrielson, 2018) and was thus expected to undergo fluoride elimination readily. The defluorination of 4-fluoro-(trifluoromethyl)catechol is proposed to proceed via the quinone methide shown in the brackets, followed by hydrolysis to give complete defluorination. The quinone methide intermediate has been discussed previously by (Kiel and Engesser, 2015) with 3-trifluoromethyl catechol. In our experiments, the defluorination is predicted to be even more facile due to the additional fluorine substituent. This explains the greater amount of fluoride observed with wild-type *P. putida* F1 than with the mutant *P. putida* F39/D. Millimolar levels of fluoride release were detected in many experiments. However, stoichiometric calculations were not possible because 4-fluorobenzotrifluoride is highly volatile, additions cannot be controlled, and the substrate was by necessity added via a vapor bulb.

The 4-fluorosalicylate, or 4-fluoro-2,3-dihydroxy benzoic acid (**VI**) did not undergo further metabolism that we could discern. The ring cleavage product is reported to absorb strongly in the visible region, 375 nm, with an extinction coefficient of 31,600 $cm^{-1}M^{-1}$ (Marín, et al., 2012). There was no evidence for this product or its further metabolism to trifluoroacetic acid. Moreover, we observed a similar product profile as with *P. putida* F1 when we used *E. coli* (pDTG602) that lacks enzymes to transform the catechols. Previous studies with trifluoromethylbenzoates (Engesser, et al., 1988) and other electron withdrawing substituents (Groce, et al., 2004) have also observed no or very low activity of ring cleavage dioxygenases with the respective substrates. Other studies have observed ring cleavage with trifluoromethyl catechols (Engesser, et al., 1988, Engesser, et al., 1990), suggesting that catechol 2,3-dioxygenases may show variation in their reactivity. It is also possible that the extra fluorine substituent *para* to the trifluoromethyl group negates ring cleavage. Regardless of the explanation, it is the block of further metabolism and

accumulation of the trifluoromethyl catechol and *ortho*-phenol that leads to extensive defluorination.

3.3 Discussion

Numerous colorimetric methods are known to determine fluoride in organic solvents and pure water, but this study overcame interferences in an aqueous method to apply rapid, microwell determinations for studying microbiological defluorination reactions *in vitro* and *in vivo*.

Currently, there is an increasing interest in determining inorganic and organic fluorine in many different types of samples (Han, et al., 2021). Thousands of organofluorine compounds have been developed and they are becoming more heavily regulated (Hogue, 2021), so new analytical methodologies are needed (Fiedler, et al., 2021, Menger, et al., 2021). There is also a need for determining inorganic fluorine, principally fluoride, in natural waters and in municipal drinking waters where fluoride is added for cavity prevention (Tolkou, et al., 2021). To meet that need, several analytical methods for determining fluoride in water were developed. The most pervasive of the methods was based on color formation from fluoride binding to an alizarin dye complexed with a rare earth metal: cerium, lanthanum, or praseodymium (Belcher and West, 1961b). They subsequently used cerium as the fluoride binding metal (Belcher and West, 1961a). Variations of the method have been used to determine fluoride after extractions from silicate rocks (Bloxam, 1968, West, et al., 1970).

More recently, there has been increased interest to determine fluoride relevant to biological systems and processes. Fluoride is toxic to microorganisms and many strains use a fluoride-sensitive riboswitch to sense the anion and induce a resistance response (Baker, et al., 2012). A fluoride riboswitch has been adapted subsequently to detect fluoride intracellularly (Nelson, et al., 2015) and extracellularly (Thavarajah, et al., 2020, Ma, et

al., 2021). The latter built on the natural regulatory property of the fluoride riboswitch, in these cases engineered to give a readout of fluoride from the transcriptional product.

Another analytical need is monitoring the biodegradation of fluorinated compounds. Many so-called PFAS compounds and their potential metabolites are determined daily by academic, industry and government scientists using expensive extraction, chromatography, and mass spectrometry methods. However, fluoride determination is relatively inexpensive and can be applied to any of the thousands of fluorinated organic compounds under study. In laboratory microbiology experiments, there is a need for determining fluoride in solid and/or liquid media, or in buffers for resting cells or enzyme reactions. In the present study, we developed a more versatile method that could be used directly with certain media and buffers. Building on past work using a sensitive metal-based fluoride binding assay (Belcher and West, 1961a, Belcher and West, 1961b), we determined: (i) the metal showing most reproducibility for our purposes was lanthanum, (ii) the signal formed within minutes and was stable in certain buffer solutions, and (iii) a range of buffers, media and biological additives did not interfere with fluoride determination.

We chose to test the microtiter well method developed here by screening *Pseudomonas putida* F1 against a library of 63 fluorinated aromatic compounds and comparing the results to measurements made in larger volumes using a fluoride electrode. *P. putida* F1 was chosen because it previously showed significant rates of defluorination with 2,2-difluoro-1,3-benzodioxole (Bygd, et al., 2021), catalyzed by toluene dioxygenase, and this organism is known to express other aromatic-metabolizing enzymes (Gibson and Parales, 2000, Kasahara, et al., 2012). As such, it was considered likely to show defluorination with multiple substrates. The library choice also reflects that a significant number of fluorinated aromatic compounds can be purchased commercially and economically. The combination of organism and substrates provided for multiple opportunities to see what could interfere with the screen and for a reasonable numerical test of sensitivity and selectivity of the method.

Following the significant extent of defluorination of these compounds here, a deeper investigation served to better understand the environmental fate of trifluoromethylphenyl

compounds. While oxidative defluorination has been demonstrated previously (Renganathan, 1989, Wang and Liu, 2020, Xie, et al., 2020), the mechanism of defluorination of 4-fluorobenzotrifluoride was not immediately obvious. Moreover, the trifluoromethylphenyl moiety has become common in drugs and agricultural chemicals with the goal of increasing effective lifetime by inhibiting microbial degradation (Jeschke, 2017, Manfrin, et al., 2020). 4-Fluorobenzotrifluoride underwent only partial transformation via the toluene biodegradative (Tod) pathway, and this was the key to the high extent of defluorination observed. Indeed, it was determined here that the metabolic weakness of the trifluoromethyl group derives from the strongly electron-withdrawing propensity of the three fluorine substituents to drive the formation of a *gem*-difluorovinyl (difluoromethide) functionality via the metabolic incorporation of electron-donating groups *ortho*- or *para*- to the trifluoromethyl moiety (**Figure 3.5**). This has been described previously for the hydroxylation of α α, α,-trifluorotoluene (benzotrifluoride) (Kiel and Engesser, 2015). 4-Fluorobenzotrifluoride is predicted to defluorinate faster than benzotrifluoride due to the lower pKa of the phenol group for the former compound, and this was indicated here via the color screening method.

In conclusion, the development of a rapid screening method has facilitated multiple discoveries for new defluorination reactions, including a cryptic ability to degrade trifluoromethylphenyl groups, a very significant functionality in new pharmaceutical and agricultural chemicals. Rapid screening by visual inspection or machine will allow for greater discovery in, and the engineering of, new defluorination biochemistry.

3. 4 Materials and Methods

Chemicals. Alizarin-3-methyliminodiacetic acid was purchased from Cayman Chemical. Lanthanum (III) nitrate hexahydrate, Cerium (III) nitrate hexahydrate, Neodymium (III) nitrate hexahydrate, and Praseodymium (III) nitrate hexahydrate were from Sigma-Aldrich at 99.99% pure. Sodium acetate used for the buffer was from J.T. Baker and 99% pure.

Glacial acetic acid was from Fisher Scientific. Acetone from Fisher Scientific and ethyl acetate and methyl-*tert*-butyl-ether (MTBE) from Sigma-Aldrich were HPLC grade and > 99% purity. Fluoroatrazine was synthesized (Nikolaeva, et al., 1990) and ^{1}H-NMR analysis indicated a purity of ~90%. 4-fluorobenzotrifluoride was purchased from Oakwood Chemical. GC-MS and NMR data show ~98% purity of this compound. Standard 5-fluoro-2-(trifluoromethyl)phenol and 2-fluoro-5-(trifluoromethyl)phenol were both purchased from Sigma-Aldrich, ~97% purity. L-arginine used for growth was from Calbiochem. IPTG was obtained from Gold Bio. Toluene used for specified cell growth and induction was from Fisher Chemical and 99% purity. N,O-Bis(trimethylsilyl)trifluoroacetamide was purchased from Fluka Analytical and had a purity of 99%. $CDCl_3$ and CD_3CN were obtained from Cambridge Isotope Laboratories, Inc., both 99% purity.

Screen development. The method was developed by testing different alizarin-3-methyliminodiacetic acid complexone (alizarin) concentrations, different rare earth metals (lanthanum (III) nitrate hexahydrate, neodymium (III) nitrate hexahydrate, praseodymium (III) nitrate hexahydrate, and cerium (III) nitrate hexahydrate), and varying acetate buffer pH and concentrations. The acetate buffer was prepared as done in (Belcher and West, 1961b) using sodium acetate and glacial acetic acid. Stock solutions of alizarin and metals were each prepared in water to concentrations of 500 μM. Individual stock solutions were kept in the dark and found to be stable for at least 6 months. For use in the assay, alizarin and acetate buffer were mixed first, then the metal was added. This solution was then added to samples containing fluoride, followed with the addition of the organic solvent, acetone. The complexone solution of alizarin, metal and acetate buffer was made fresh before each experiment and was stable for up to 2 hours.

First, each metal was tested with varying concentrations of fluoride to evaluate sensitivity. It was determined that lanthanum (III) was best for our applications. Concentration and pH were also tested. To determine ideal pH of the reaction, the pH of the acetate buffer was modified using hydrochloric acid or sodium hydroxide. pH values of 2.8, 3.3, 4.5, 5.0, 5.5, and 6.0 were all tested. The pH range of 5-5.5 was found to be the most sensitive for detecting fluoride in the screen. To test concentrations, reagents were combined in varying

ratios of lanthanum to alizarin (1:1, 2:1, 1:2, and 2x and 3x the concentration previously used (Belcher and West, 1961b) and reacted with a given concentration of fluoride in a 96-well plate for 5-10 minutes at room temperature. At which point, wells of the plate were read using a Molecular Devices SpectraMax 384plus plate reader. Samples were scanned from 350 nm to 700 nm. Optimal sensitivity was determined by a linear absorbance pattern at a 620 nm.

Ideal final concentrations of each compound were found to be 50 μM alizarin-3-methyliminodiacetic acid, 50 μM lanthanum, 84 mM acetate buffer (three times the concentration used by (Belcher and West, 1961b), and 25% acetone (v/v). Higher concentrations of fluoride were visually detected after 5 minutes. However, low concentrations of fluoride were allowed to react for 30-60 minutes before visual detection. The reaction color is stable for up to 3 hours.

Serial dilutions to observe interferences to screen sensitivity were performed as follows: a known concentration of fluoride was added to the first well in a series. The following wells would be diluted with either the media of interest or water. Half of the volume would be taken from the initial well and then diluted subsequently 1:2 into the other wells. Screen components were combined and added to each well at concentrations described above.

In visual determination of fluoride release in the color screen, qualitative observations could be made. High fluoride release was a dark purple well, designated with "++." Low fluoride release was a light purple well, designated with "+." The dark and light colors were defined quantitatively using the absorbance at 620 nm divided by the absorbance at 530 nm from standards. Wells defined as having darker color (designated ++) have a 620/530 ratio above 0.7. Wells with lighter purple color (designed +) showed a 620/530 value <0.7 (**Figure 3.2**). Red wells, or no fluoride release showed values <0.6. Interferences were identified in wells that were an altered color or intensity, such as dark brown, grey, yellow, or light pink (**Figure S2, Appendix B**) and do not have a specified ratio value. The results were found to correlate with fluoride determinations made with a fluoride specific electrode as shown in the Results section.

UV-visible spectroscopy. Samples were placed in a quartz cuvette and measurements were collected on a Cary 3500 double-beam UV-vis spectrometer containing a Xenon flash lamp from Agilent. Absorbance as a function of wavelength was recorded from 350 nm to 700 nm. Samples were tested at pH 5.2 and used with the optimum reagent concentrations as described above. The Results section shows the samples: 1) deionized (DI) water; 2) 2 mM sodium fluoride in DI water; and 3) 2 mM sodium fluoride in mineral salts basal medium (MSB), that contains 30 mM phosphate.

Interfering and non-interfering substances. The fluoride screen has been made amenable to microbiological experiments here by determining buffers and media that show non-interference with color development. Buffer, media, and other components in normal aqueous solution were tested at concentrations given in **Table 3.1** of the results section. To each solution, 2 mM fluoride was added and then the standard screen conditions were used as described in an earlier section. No interference was defined as matching the color intensity of the control and having no alterations to color. Moderate interference was defined as a slightly lighter purple (difference in intensity) sample with no drastic color change. Strong interference is described as a sample with an obviously different color (i.e, red, orange, brown) or intensity (i.e, transparent). The presence of a moderately interfering compound may reduce the sensitivity of the screen for lower concentrations of fluoride, while a strong interfering compound would make it virtually impossible to detect the presence of fluoride, even at high fluoride concentrations.

Bacterial strains and growth conditions. *Pseudomonas putida* F1 was maintained on Luria-Bertani (LB) plates, and the strain was grown in liquid on minimal salts basal medium (MSB) (Stanier, et al., 1966) and toluene in a vapor bulb as previously described (Gibson, et al., 1968) at 28˚C. *Pseudomonas putida* F39/D was also maintained on LB plates and grown on MSB and 0.2% (w/v) arginine at 28˚C. *Escherichia coli* pDTG 602 was grown on LB ampicillin (100 µg/mL) as described previously (Bygd, et al., 2021).

Kinetic assay for fluoroatrazine defluorination. TrzN enzyme was expressed and purified with small variations to a previously described protocol (Shapir, et al., 2005). One liter of *Eschericia coli* pAG TrzN was grown and induced as in Shapir et al (Shapir, et al.,

2006). After growth, the cells were centrifuged, resuspended in buffer and passed through a chilled French press cell at 140 Mpa to lyse the cells. The cell crude extract was centrifuged at 16,000 rpm for one hour. The centrifuged extract was filtered through a 0.45 μm filter. A 5 mL nickel column was used to purify the His-tagged TzN (Shapir, et al., 2005) protein from lysate. The column was washed with water and 20 mM Tris with 10% glycerol (buffer A). The sample was then placed on the column with an additional 3 ml of buffer A. Protein was eluted from the column using a second buffer containing 20 mM Tris, 500 mM imidazole and 10% glycerol (buffer B). Fractions containing purified TrzN were then buffer exchanged using 30 kDa Amicon Ultra-15 cellulose centrifugal filters into 20 mM HEPES buffer containing 10% glycerol. Buffer was exchanged until imidazole concentration was less than 60 μM. It was important that the concentration of Tris and imidazole be reduced since they were observed to interfere with the color screen.

The color screen was used to follow the course of fluoride release from fluoroatrazine in separate reactions catalyzed by NaOH and heat or TrzN enzyme. For the base catalyzed reaction, fluoroatrazine was added to make 2 mM in 50 mL water adjusted to pH 11 with NaOH and at 70˚C. Aliquots were taken in microtiter plates at fixed time points for up to 4 hours and immediately frozen. At the conclusion of the time course the aliquots were thawed and assayed by the standard alizarin-La reaction mixture. Enzymatic defluorination was carried out with 250 nM TrzN and 2 mM of fluoroatrazine in 20 mM HEPES (pH 7.0). The reaction was sampled and assayed as described above for the base and heat-catalyzed defluorination mixture. Note that fluoroatrazine is not soluble in water/buffer at a 2 mM concentration. The excess solid material was left to float on top of the buffer and solubility increased as the reaction proceeded.

Rapid micro-well screening of defluorination catalyzed by *Pseudomonas putida* F1. *P. putida* F1 was grown in a 150 mL culture in MSB medium with a vapor bulb containing toluene to an OD_{600} of 0.4. The cells were pelleted, resuspended in 75 mL of 20 mM HEPES, and 1 mL aliquots were transferred into individual wells of a 96 deep-well plate. A 40 mM chemical stock in 20 mM HEPES was added in 100 uL aliquots to each well. Although many of the fluorinated chemicals are not soluble at 40 mM in HEPES, each

stock solution was vortexed and mixed thoroughly before use in each assay. Many studies use substrates above the solubility limit in *P. putida* F1 experiments, and the organism continually metabolizes the chemicals as they dissolve. The plate was incubated overnight at 28˚C, on an Eppendorf Thermomixer R plate shaker at 400 rpm. Prior to fluoride determination with the color screen, the cells were pelleted in the deep well plate using a swinging bucket rotor at 1000 rpm for 20 min. Supernatant solutions (100 µL) were transferred to a flat bottom 96-well plate and screened as described above in the screen development section.

Fluoride detection with fluoride electrode. Using 1 mL of sample supernatant, an ion-plus SureFlow Fluoride electrode from Thermo Scientific (Coon Rapids, Minnesota) was used as in (Bygd, et al., 2021).

Generation and analysis of intermediates and products from tetrafluorinated compounds. Biological transformation of 4-fluorobenzotrifluoride was conducted with *Pseudomonas putida* F39/D. The strain was grown overnight on MSB and 0.2% arginine (w/v) and was used to inoculate cultures grown in MSB containing 0.2% arginine (w/v), and toluene in a vapor bulb. The cultures were grown to early log phase at 28˚C and then the toluene was replaced with 4-fluorobenzotrifluoride and incubated for an additional 2 hours. Subsequently, the cells were pelleted, and 1 mL of cleared medium was frozen for later GC analysis. The remaining supernatant was extracted in a separatory funnel with equal volumes of ethyl acetate. The extract was dried with anhydrous magnesium sulfate and rotary evaporated under vacuum. Once dry, the crystallized sample was dissolved in deuterated chloroform. ^{1}H and ^{19}F-NMR were both performed as described below. The ^{19}F-NMR showed the dihydrodiol product from 4-fluorobenzotrifluoride only. The ^{1}H-NMR showed largely the dihydrodiol product from 4-fluorobenzotrifluoride with some contaminating toluene dihydrodiol. Both of those ^{1}H-NMR have been described previously so they were readily distinguishable (Boyd, et al., 2007).

Biological transformation of 4-fluorobenzotrifluoride was also conducted with *Escherichia coli* pDTG 602, which was grown to mid-log phase on LB with ampicillin (100 µg/mL) at 37˚C. Subsequently, the cells were pelleted and resuspended in MSB (at OD_{600} 0.65) and

0.2% glucose and supplemented with 1 mM IPTG for induction (Zylstra and Gibson, 1989). After 1 hour at 30˚C, a vapor bulb containing 4-fluorobenzotrifluoride was added and the culture and incubated an additional 2 hours. After 2 hours, the medium appeared purple and was centrifuged at 10,000 rpm for 10 minutes. The cell-free supernatant was extracted and handled as described above for *P. putida* F39/D.

An abiotic transformation was conducted by adding 8 mM 5-fluoro-2-(trifluoromethyl)phenol to MSB (pH 9.3) with shaking at 200 rpm at 28˚C overnight. Fluoride was measured using a fluoride electrode. Strong acid was added to adjust the pH of the media to pH 1.9. The sample was extracted in a separatory funnel with equal volumes of ethyl acetate and dissolved in deuterated chloroform, as described above. The sample was poorly soluble in chloroform so it was filtered through cotton. A small amount of the product remaining on the cotton filter was then placed in fresh $CDCl_3$ and used for NMR, using trimethylsilane (TMS) as a reference for ^{1}H-NMR.

Analytical methods. Gas-chromatography and mass spectrometry (GC-MS) was conducted as in (Bygd, et al., 2021) except that the GC oven temperature started at 40˚C, instead of 50˚C. Standard solutions of 5-fluoro-2-(trifluoromethyl)phenol and 2-fluoro-5-(trifluoromethyl)phenol were prepared in methyl-*t*-butyl ether (MTBE). One microliter of derivatizing agent, N,O-bis(trimethylsilyl) trifluoroacetamide, was added to each extracted sample or standard. Product ion spectra were identified in positive ion mode on an HP6890 gas chromatograph with an HP5973 MS detector.

Nuclear Magnetic Resonance (NMR)_was performed using a Varian INOVA 400-MHz NMR spectrometer. For both ^{1}H-NMR and ^{19}F-NMR, deuterated chloroform ($CDCl_3$) was the solvent. Trimethylsilane (TMS) and trichlorofluoromethane (F11) served as reference for ^{1}H-NMR and ^{19}F-NMR, respectively. Extracts from bacterial or abiotic incubations were obtained as described previously.

The product extracted from incubation of *P. putida* F39/D with 4-fluorobenzotrifluoride was analyzed: ^{1}H-NMR (400MHz, $CDCl_3$), 4-fluorobenzotrifluoride-2,3-dihydrodiol; 4.53 ppm (apparent t, J = 5.5 Hz and 6.0 Hz), 4.62 ppm (d, J = 6.44 Hz), 5.65 ppm (dd, J =

6.6 Hz and 9.2 Hz) 6.55 ppm (m), ^{19}F-NMR (400 MHz, $CDCl_3$), -66.04 ppm (s), -109.33 ppm (m) (**Figure S7, Appendix B**).

The products extracted from the 5-fluoro-2-(trifluoromethyl)phenol incubation in MSB media were analyzed: ^{1}H-NMR (400MHz, $CDCl_3$), 4-fluorosalicylate; 1.25 ppm (s), 6.7 ppm (apparent dt, J = 2.5 Hz and 3.3 Hz), 7.95 ppm (dd, J = 6.4 Hz and 8.8 Hz), 10.65 ppm (d, J = 1.6 Hz), ^{19}F-NMR (400 MHz, $CDCl_3$), 4-fluorosalicylate; -99.58 ppm (m), 5-fluoro-2-(trifluoromethyl)phenol; -67.71 ppm (s) (**Figure S9, Appendix B**).

The products extracted from incubation of *E. coli* pDTG 602 with 4-fluorobenzotrifluoride were analyzed: ^{1}H-NMR (400MHz, $CDCl_3$), 4-fluoro-(trifluoromethyl)catechol; 6.75 ppm (apparent t, J = 9.0 Hz and 9.6 Hz), 7.09 ppm (dd, J = 6.0 Hz and 9.0 Hz), and additional minor product was identified as 4-fluorobenzotrifluoride-2,3-dihydrodiol, as seen in spectra described in the ^{1}H-NMR above. Additional minor peaks in this spectrum were not identified. ^{19}F-NMR (400 MHz, $CDCl_3$), 4-fluoro-(trifluoromethyl)catechol; -61.91 ppm (s), -132.83 ppm (bs), a second minor product in this spectra was identified as 4-fluorobenzotrifluoride-2,3-dihydrodiol, as described in the ^{19}F-NMR above (**Figure S10, Appendix B**).

Supplemental material can be found in **Appendix B**

ACKNOWLEDGEMENTS

We thank Becky Parales for providing the recombinant E. coli strain pDTG602. We thank Thomas Niehaus for making available the Cary spectrophotometer.

This project was partly funded by the MnDRIVE Industry and the Environment programand a grant from ExxonMobil Environmental and Property Solutions Company.

We have no conflicts of interest to declare.

L.P.W., K.G.A., and M.D.B. conceived and designed the experiments. M.D.B., K.G.A., and J.E.R. performed the experiments. M.D.B., K.G.A., J.E.R., and L.P.W. analyzed the data. M.D.B., K.G.A., and L.P.W. wrote the paper. All authors edited and approved the manuscript.

CHAPTER 4

Mircowell Fluoride Screen of *E. coli* ASKA Library Reveals Undocumented Defluorination of Sodium Fluorophosphate

4.1 Introduction

After the development of the color assay and understanding what causes many interferences with fluoride determination, the next step was to implement the assay into higher-throughput experiments. In using the assay with fluorinated chemicals and with *P. putida* F1, we saw minimal interferences and got highly accurate and conclusive results, detecting many defluorination reactions. Next, we proposed using the assay for a larger screen in search of defluorinating enzymes.

There are many ways to perform screening experiments. In the previous chapter we used a chemical library with one strain of bacteria. Additional screens can be done with enzyme libraries, gene knock out libraries, overexpression libraries or enrichment cultures/consortia (Davis, et al., 2011, Yu, et al., 2020). The goal was to find a new enzyme, or number of enzymes that could degrade fluorinated chemicals, so we decided to start with an over-expression library. This method provides a good starting point in which to find a functional enzyme that can defluorinate PFCs, rather than choosing an enzyme and trying to formulate defluorination activity with mutagenesis.

An over-expression library is the use of one bacterium that has each gene over-expressed on an inducible plasmid. Alternatively, a knock-out library is the mutation of each non-

essential gene in a strain to make it non-functional. Since this would not lead us to finding new defluorination mechanisms, we chose the former. The library used for these experiments is the ASKA *E. coli* library, strain K12 W1130 (Kitagawa, et al., 2005, Barrick, et al., 2020). The plasmid present in the strain is pCA24N, a high copy number plasmid which has the T5-lac promoter, inducible by IPTG. Each of the proteins on the plasmid are also histidine tagged, which allows for convenient protein purification if needed. In these experiments, we chose to test the strain library with eight fluorinated chemicals and used the color assay described in the previous chapter to screen for defluorination activity.

4.2 Results

Induction and reduction of interference in the ASKA library. The *E. coli* ASKA strains contain a T5-lac promoter, which is traditionally used by growing the cells in rich media and inducing with IPTG at a specific cell density. However, due to the volume of cells used in screening a library, matching a specific cell density across thousands of strains is challenging. To accommodate this aspect, we adapted an autoinduction media, ZYM-5052 (Studier, 2005), in which the carbon sources are provided in strategic quantities. The cells are then able to fully consume the carbon sources in a specific order with the use of lactose last, which induces the T5-lac promoter such that protein expression from the T5-lac promoter begins. Autoinduction media greatly reduced the total time needed for screening and the cells were induced successfully.

Early in experimentation, protein gels were run to test induction. It was observed that 18 hours of growth and induction on ZYM autoinduction media was not sufficient to express high levels of protein. Instead, the cells were incubated for 24 hours, which greatly improved protein expression levels.

After the cells were grown, a 20 mM HEPES and 50 mM sodium chloride solution (pH 7.0) was used to resuspend the cells. It was observed in early trials of screening that an

aspect of the transfer from rich media to minimal buffer resulted in an unspecified interference with the assay. The limit of detection for fluoride was greatly improved by implementing a wash step with buffer before administering the fluorinated chemical to the cells. The wash step involved the use HEPES and sodium chloride to resuspend the cells after the first harvest to eliminate the interfering component and acclimate the cells to a new buffer. Then a second pellet and resuspension were done for incubation with the chemical of interest.

Screening fluorinated compounds with the overexpression library. In total, eight compounds were tested with the ASKA library (**Table 4.1**). Of the compounds, one positive hit was identified. This positive was with sodium fluorophosphate in plate D, well C12 (**Figure 4.1**). To confirm this positive hit, and narrow down which strain catalyzed the defluorination, each individual strain from plate D well C12 was grown from the freezer on autoinduction media. In total, there were 4 known strains in well C12 of the combination plate D. These strains included the overexpression of phosphatidyl glycerophosphatase B, a putative oxidoreductase, cell division topological specificity factor, and a cold shock like protein (Altschul, et al., 1990, Barrick, et al., 2020). After incubation of each individual strain with sodium fluorophosphate, it was shown that the defluorination was initiated by the *E. coli* strain expressing the enzyme phosphatidylglycerophosphatase, or pbpB.

Table 4.1. Compounds screened for defluorination with the ASKA library

Compounds Tested with ASKA Library	Compound Structure
2-trifluoromethyl phenol	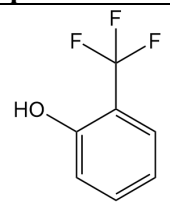
4-trifluoromethyl phenol	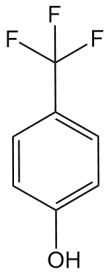
2-trifluoromethyl aniline	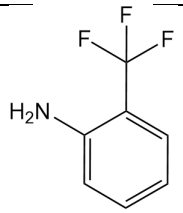
Sodium fluorophosphate	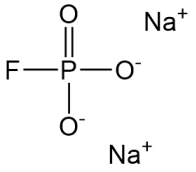
Phenyl sulfur pentafluoride	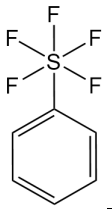
2-fluorocyclopropanearboxylic acid	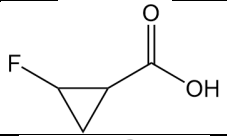
1- fluorocyclopropanearboxylic acid	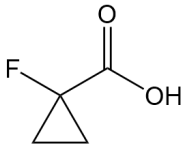
Fluoroacetonitrile	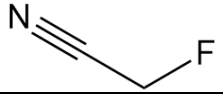

The strain expressing PgpB released 1.2 mM fluoride during a 2 hour incubation with 2 mM sodium fluorophosphate. This was comparable to a known defluorination reaction of sodium fluorophosphate by *E. coli* expressing alkaline phosphatase (Fernley and Walker, 1967), phoA, which released the same amount of fluoride under the same conditions.

Other chemicals tested with the ASKA library include fluoroacetonitrile, 1-fluorocyclopropanecarboxylic acid, 2-fluorocyclopropanecarboxylic acid, 4-trifluoromethyl phenol, 2-trifluoromethyl phenol, 2-trifluoromethyl aniline, and phenyl sulfur pentafluoride (**Table 4.1**). None of these compounds showed fluoride release during the specified incubation time with the cells (See methods section, Chemical incubation and color screen).

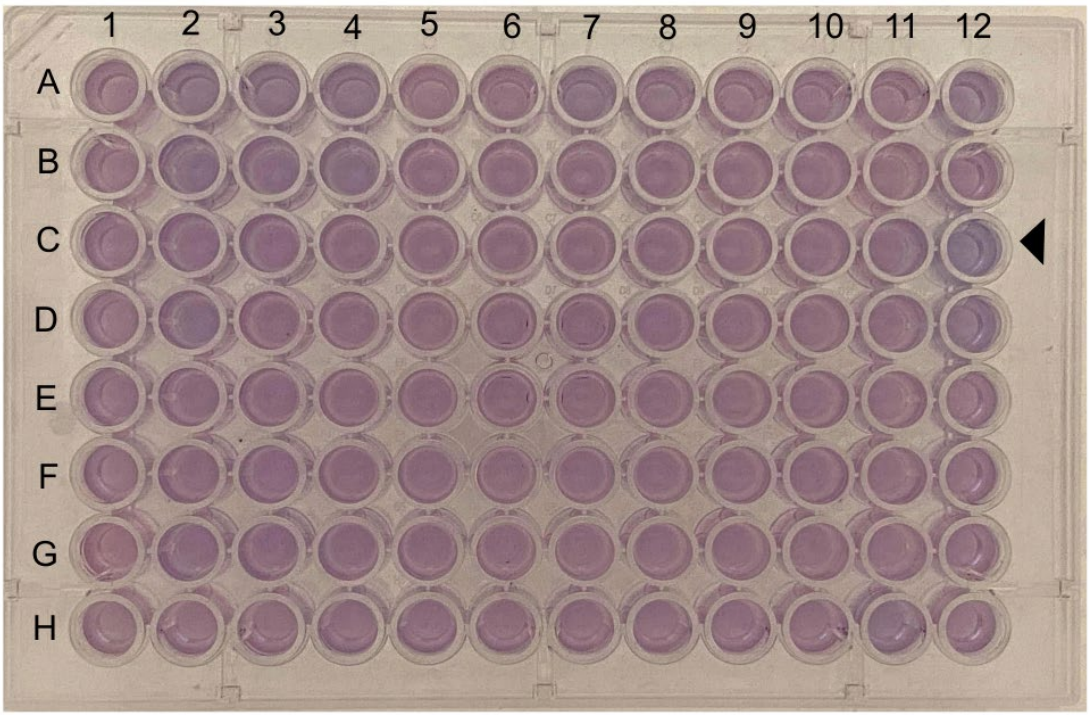

Figure 4.1. Positive hit of sodium fluorophosphate defluorination in well C12 of plate D (black arrow) of *E. coli* ASKA library. Plate D contains strains 11-15.

4.3 Discussion

The use of a high-throughput fluoride detection method is essential to furthering research with polyfluorinated chemicals. Compatibility with microbiological media and solvents is

important to implement rapid fluoride detection from biological based sources. This colorimetric method can be adapted for many uses, including screening enzyme libraries, chemical libraries, or over-expression libraries like the one outlined in this chapter.

The benefits of performing a screen in this manner is the ability to test almost 5,000 different gene products of a bacterium in a quick and accurate manner. Thousands of samples can be condensed down to a very workable format such that this assay can easily be applied. The small volumes retain sensitivity to low concentrations of fluoride, providing an efficient and effective tool.

Although the benefits of this method outweigh the negatives, its limitations must be taken into consideration when using in new applications. Interferences must be evaluated and the effect of the new application on color formation should be investigated before drawing conclusions. Some interferences may prevent full detection of fluoride release. For example, different enzymes, membrane components, or cells could affect the media or other aspects of the screen very differently. This can influence detection or lead to false positives or negatives.

Additional limitations specific to these experiments include the possibility of the fluorinated chemicals not successfully getting into the cytoplasm due to polarity or size, strains out-competing each other during growth in the combination plates, or cross-contamination between wells of the plate. These are important aspects of this study to evaluate regarding accuracy of detecting defluorination reactions. One well containing 5 strains could have different levels of growth for each strain. For example, some may grow slower due to the overproduction of a disadvantageous enzyme. It may also be unsurprising to find cross contamination between wells. The use of small-volume 96-well plates can lead to artifactual results, due to problems such as cell suspensions splashing from well to well.

Overall, using the color assay for detection of defluorination reactions in the *E. coli* ASKA library was a very useful method. To perform the same experiments with other fluoride detection methods such as HPLC, the fluoride electrode or xylenol orange would

take significantly more time and resources (Davis, et al., 2011). The number of chemicals and strains we were able to screen in weeks with the color assay could take months to years to do with other methods.

4.4 Materials and Methods

***Escherichia coli* ASKA Library.** The library was provided to our lab by a collaborator, Amir Shimon, who had replicated and combined strains of the library. The library was built and maintained in 96 well plates, each well containing one strain. To reduce the number of plates to a manageable number for screening, the cells were grown on Luria Bertani (LB) broth and chloramphenicol (25 ug/mL), replicated, and combined in sets. The final number of combination plates was 10. All plates are stored at -80˚C.

Chemicals. Fluoroacetonitrile is from Aldrich Chemical Company with a purity of 99%. 1-fluorocyclopropanecarboxylic acid is from Ambeed with a purity of 97%, 2-fluorocyclopropanecarboxylic acid 98% pure from AmBeed, 4-trifluoromethyl phenol is 98% pure from AmBeed, 2-trifluoromethyl phenol is from Aldrich chemical with a purity of 97%, 2-trifluoromethyl aniline is 99% pure from Sigma-Aldrich, and phenyl sulfur pentafluoride is 98% pure from AstaTech. Sodium fluorophosphate is from Alfa Aesar. Tryptone is from research products international. Yeast extract is from EMD Millipore Corporation. Sodium phosphate dibasic has a purity of 98.5% from Sigma-Aldrich. Potassium phosphate monobasic is from Sigma-Aldrich with a purity of 99%. Magnesium sulfate is from J.T. Baker. Ammonium chloride is from Sigma-Aldrich with a purity of 99.5%. 2-[4-(2-hydroxyethyl)-1-piperazinyl] ethanesulfonic acid (HEPES) is from TCI with a purity of 99%. Sodium chloride is from Fisher BioReagents. Glycerol is from Macron fine chemicals. Glucose is from Sigma with a purity of 99.5%. Lactose monohydrate is from JT Baker. Chloramphenicol is from Sigma with a purity of >98%.

Autoinduction media and growing the cells. An autoinduction media was chosen in which the cells could grow and then be induced by the specific carbon sources present.

This autoinduction media was adapted from (Studier, 2005) and contained 1% tryptone, 0.5% yeast extract, 25 mM sodium phosphate dibasic, 25 mM potassium phosphate dibasic, 50 mM ammonium chloride, and 2 mM magnesium sulfate heptahydrate, 0.2x trace metals and 1x 5052 carbon source. Separate stock solution of the carbon sources and trace metals were made, and filter sterilized before use. 50x 5052 carbon source contained 25% glycerol, 2.5% glucose, and 10% lactose. Trace metals were made to 1000x as in (Studier, 2005). The media was made and sterilized, excluding the carbon sources and antibiotic. Right before use, 1x carbon was added, as well as chloramphenicol to a final concentration of 25 μg/mL.

Once all components of the media were combined, 96 deep well plates (square wells with 2 mL capacity and semi-rounded bottom) were used to grow the cells. Using a Dispensette® from BRANDtech, (Essex, CT), each well of the plate was filled with 1 mL of media. A 96 well pinning tool, stored in 70% ethanol, was used to inoculate the media plates with the frozen stocks of the combined ASKA strains. Each inoculated plate was then covered with a 96 well silicone seal or a clear crystallography seal and placed in a 37˚C incubator, shaking at 200 rpm to grow for 24 hours.

Chemical incubation and color screen. Since phosphate, yeast extract and other components of the autoinduction media are known to interfere with detecting fluoride in the color assay (see chapter 3), the cells were washed and resuspended in 20 mM HEPES and 50 mM NaCl. After the overnight incubation, each plate was pelleted at 1700 rpm for 15 minutes. The media was dumped off the top of the cell pellet and 20 mM HEPES and 50 mM NaCl buffer was added to each well. Buffer was added using the Dispensette® set at a 1 mL volume. Each plate of cells was washed once in this manner and then pelleted again, as described above. After centrifugation the buffer was dumped off the top of the pellets and the cells were resuspended again in 20 mM HEPES, 50 mM NaCl and 2 mM fluorinated chemical of interest. The plates were re-sealed with the silicone or crystallography seals and left to incubate at the appropriate temperature for a specified amount of time (**Table 4.2**).

Chemical	Incubation Temperature (℃)	Incubation Time (h)
2-trifluoromethyl phenol	28	4
4-trifluoromethyl phenol	28	4
2-trifluoromethyl aniline	28	4
Sodium fluorophosphate	37	2
Phenyl sulfur pentafluoride	37	24
2-fluorocyclopropanearboxylic acid	37	24
1-fluorocyclopropanearboxylic acid	37	24
Fluoroacetonitrile	37	24

Table 4.2. The chemicals screened with the ASKA library with the corresponding incubation time and temperature.

After the incubation period, the plates were again pelleted in pairs. 100 µL of the supernatant was taken from each well of the plate and transferred to a standard clear flatbottom 96 well plate (300 µL capacity). A bulk solution of color assay reagents (alizarin, lanthanum and acetate buffer) was prepared to the concentration specified in Chapter 3. 52 µL of the prepared reagents were then added to each well of the plate containing supernatant. Lastly, 50 µL of 100% acetone was added and the covered plate was left to incubate at room temperature for one hour. After incubation, the plates were monitored for positive hits, which are defined in chapter 3.

Analyzing positive hits. Positive hits were followed up on to confirm true fluoride release. The 96-well plate map of the strains (Barrick, et al., 2020) was referenced to determine which strains are present in each specific well. The documented number of strains was then selected from the individual ASKA plate freezer stocks and grown individually on the autoinduction media in 5 mL volumes. After overnight growth the strains were then pelleted, washed as described above and resuspended with 20 mM HEPES and 50 mM NaCl and 2 mM substrate. After incubation with the chemical the samples were measured for fluoride release with a Thermo Scientific Orion 9609BNWP sure-flow fluoride electrode (Bygd, et al., 2021).

CHAPTER 5

Conclusion

Polyfluorinated chemicals are a large group of fluorinated carbon compounds found in many industrial, household, and chemical applications (Mueller and Yingling, 2020, Wu, et al., 2020). There is a wide variety of these chemicals, including aromatic and aliphatic compounds containing varying numbers of fluorine atoms. One major class of these compounds are well known as PFAS compounds, but other types of polyfluorinated compounds are just as prominent in industry. We see examples of these chemicals in the two larger studies reported here, 2,2-difluoro-1,3-benzodioxole and 4-fluorobenzotrifluoride, both of which have been used in agricultural applications (Müller, et al., 2007, Thomas and Hand, 2012, Walker and Chang, 2014, Alexandrino, et al., 2020).

In the research reported in this thesis, we see two novel defluorination reactions initiated by the toluene dioxygenase in *Pseudomonas putida* F1. This enzyme initiates the degradation and defluorination of these chemicals by dioxygenating the aromatic ring, which leads to downstream reactions and the loss of fluorine. The importance of documenting these defluorination reactions and new methods for initiating defluorination is to better understand how these compounds may be degraded in natural environments. Their use in pharmaceuticals or fungicides creates relevant applications in which knowledge of these reactions can be used for bioremediation. Applying these discoveries for remediation provides an eco-friendly, scalable, and cost-effective solution to widespread and problematic pollution.

The color screen developed for better detection of fluoride in microbiological media and enzyme buffers will also provide immense opportunity for future application in defluorination research. Previously documented assays are often not compatible with

aqueous microbiological media and are therefore less useful than the one described in Chapters 3 and 4 (Belcher and West, 1961a, Belcher and West, 1961b, Davis, et al., 2011). The color assay developed here was modified for detecting fluoride from a biological source and interferences were determined so they can be avoided in future experiments. This assay also proved to be a very accurate method for detecting fluoride and can be used with small volumes for hundreds or thousands of samples. Other methods, such as a fluoride electrode, can be used but are more instrument intensive, not amenable to high-throughput, and require larger sample volumes.

Overall, great progress has been made in better understanding and revealing new biological defluorination mechanisms. This research will be highly beneficial in future research for screening and detection, as well as predicting novel defluorination reactions.

References

Abrash, H.I., Shih, D., Elias, W., and Malekmehr, F. (1989) A kinetic study of the air oxidation of pyrogallol and purpurogallin, *Int J Chem Kinet* **21**: 465-476.

Ahrens, L., and Bundschuh, M. (2014) Fate and effects of poly- and perfluoroalkyl substances in the aquatic environment: a review, *Environ Toxicol Chem* **33**: 1921-1929.

Aigueperse, J., Mollard, P., Devillers, D., Chemla, M., Faron, R., Romano, R., and Pierre Cuer, J. (2000) Fluorine Compounds, Inorganic. Ullmann's Encyclopedia of Industrial Chemistry.

Alexandrino, D., Mucha, A.P., Almeida, M.R., and Carvalho, M.F. (2020) Microbial degradation of two highly persistent fluorinated fungicides - epoxiconazole and fludioxonil, *J Hazard Mater* **394**.

Alexandrino, D.A.M., Ribeiro, I., Pinto, L.M., Cambra, R., Oliveira, R.S., Pereira, F., and Carvalho, M.F. (2018) Biodegradation of mono-, di- and trifluoroacetate by microbial cultures with different origins, *N Biotechnol* **43**: 23-29.

Altschul, S., Gish, W., Miller, W., Myers, E., and Lipman, D. (1990) Basic local alignment search tool, *J Mol Biol* **215**: 403-410.

Andrews, D., and Naidenko, O. (2020) Population-Wide Exposure to Per- and Polyfluoroalkyl Substances from Drinking Water in the United States, *Environ Sci Technol* **7**: 931-936.

ATSDR (2017) The Family Tree of Per- and Polyfluoroalkyl Substances (PFAS) for Environmental Health Professionals. Agency for Toxic Substances and Disease Registry Division of Community Health Investigations. 1-2.

Aukema, K.G., Escalante, D.E., Maltby, M.M., Bera, A.K., Aksan, A., and Wackett, L.P. (2017) In silico identification of bioremediation potential: carbamazepine and other recalcitrant personal care products, *Environ Sci Technol* **51**: 880-888.

Baker, J.L., Sudarsan, N., Weinberg, Z., Roth, A., Stockbridge, R.B., and Breaker, R.R. (2012) Widespread genetic switches and toxicity resistance proteins for fluoride, *Science* **335**: 233-235.

Barrick, J., Leonard, S., Barnhart, C., and Dalton, S. (2020) Keio and ASKA collections.

Belcher, R., and West, T. (1961b) A Comparative Study of Some Lanthanon Chelates of Alizarin Complexan as Reagents for Fluoride, *Talanta* **8**: 863-870.

Belcher, R., and West, T. (1961a) A study of the cerium(iii)-alizarin complexan-fluoride reaction, *Talanta* **8**: 853-862.

Belkouteb, N., Franke, V., McCleaf, P., Köhler, S., and Ahrens, L. (2020) Removal of per- and polyfluoroalkyl substances (PFASs) in a full-scale drinking water treatment plant: Long-term

performance of granular activated carbon (GAC) and influence of flow-rate, *Water Res* **182**: 115913.

Biegel, L.B., Hurtt, M.E., Frame, S.R., O'Connor, J.C., and Cook, J.C. (2001) Mechanisms of extrahepatic tumor induction by peroxisome proliferators in male CD rats, *Toxicol Sci* **60**: 44-55.

Bloxam, T. (1968) A rapid method for the determination of fluoride in silicate rocks, *Chem Geology* **3**: 89-94.

Bondar, V.S., Boersma, M.G., Golovlev, E.L., Vervoort, J., Van Berkel, W.J., Finkelstein, Z.I., et al. (1998) 19F NMR study on the biodegradation of fluorophenols by various *Rhodococcus* species, *Biodegradation* **9**: 475-486.

Boyd, D., Sharma, N., Coen, G., Gray, P., Malone, J., and Gawronski, J. (2007) Enzyme-catalysed synthesis and absolute configuration assignments of c*is*-dihydrodiol metabolites from 1,4-disubstituted benzenes, *Chemistry* **13**: 5804-5811.

Boyd, D.R., Sharma, N.D., Bowers, N.I., Dalton, H., Garrett, M.D., Harrison, J.S., and Sheldrake, G.N. (2006) Dioxygenase-catalysed oxidation of disubstituted benzene substrates: benzylic monohydroxylation versus aryl cis-dihydroxylation and the meta effect, *Org Biomol Chem* **4**: 3343-3349.

Brase, R.A., Mullin, E.J., and Spink, D.C. (2021) Legacy and Emerging Per- and Polyfluoroalkyl Substances: Analytical Techniques, Environmental Fate, and Health Effects, *Int J Mol Sci* **22**.

Britton, R., Gouverneur, V., Lin, J., Meanwell, M., Ni, C., Pupo, G., et al. (2021) Contemporary synthetic strategies in organofluorine chemistry, *Nature Rev Meth Primers* **1**: 1-22.

Brusseau, M.L., Anderson, R.H., and Guo, B. (2020) PFAS concentrations in soils: Background levels versus contaminated sites, *Sci Total Environ* **740**: 140017.

Buchfink, B., Xie, C., and Huson, D.H. (2015) Fast and sensitive protein alignment using DIAMOND, *Nat Methods* **12**: 59-60.

Buck, R.C., Korzeniowski, S.H., Laganis, E., and Adamsky, F. (2021) Identification and classification of commercially relevant per - and poly - fluoroalkyl substances (PFAS), *Integr Environ Assess Manag* **17**: 1045-1055.

Bui, V.P., Hansen, T.V., Stenstrøm, Y., Hudlicky, T., and Ribbons, D.W. (2001) A study of substrate specificity of toluene dioxygenase in processing aromatic compounds containing benzylic and/or remote chiral centers, *New J Chem* **25**: 116-124.

Burkhardt, J.B., Burns, N., Mobley, D., Pressman, J.G., Magnuson, M.L., and Speth, T.F. (2022) Modeling PFAS Removal Using Granular Activated Carbon for Full-Scale System Design, *J Environ Eng (New York)* **148**: 1-11.

Bygd, M., Aukema, K., Richman, J., and Wackett, L. (2021) Unexpected mechanism of 2,2-difluoro-1,3-benzodioxole defluorination by P*seudomonas putida* F1, *mBio* **12**: e3001-3021.

Calero, P., Volke, D.C., Lowe, P.T., Gotfredsen, C.H., O'Hagan, D., and Nikel, P.I. (2020) A fluoride-responsive genetic circuit enables in vivo biofluorination in engineered Pseudomonas putida, *Nat Commun* **11**: 5045.

Caron, S. (2020) Where does the fluorine come from? A review on the challenges associated with the synthesis of organofluorine compounds, *Organ Proc Res Develop* **24**: 470-480.

Chakraborty, J., Jana, T., Saha, S., and Dutta, T. (2014) Ring-Hydroxylating Oxygenase database: a database of bacterial aromatic ring-hydroxylating oxygenases in the management of bioremediation and biocatalysis of aromatic compounds, *Environ Microbiol Rep* **6**: 519-523.

Chan, P.W., Yakunin, A.F., Edwards, E.A., and Pai, E.F. (2011) Mapping the reaction coordinates of enzymatic defluorination, *J Am Chem Soc* **133**: 7461-7468.

Che, S., Jin, B., Liu, Z., Yu, Y., Liu, J., and Men, Y. (2021) Structure-specific aerobic defluorination of short-chain fluorinated carboxylic acids by activated sludge communities, *Environ Sci Technol Lett* **8**: 668-674.

Crawford, N., Fenton, S., Strynar, M., Hines, E., Pritchard, D., and Steiner, A. (2017) Effects of perfluorinated chemicals on thyroid function, markers of ovarian reserve, and natural fertility, *Reprod Toxicol* **69**: 53-59.

Dalvi, V.H., and Rossky, P.J. (2010) Molecular origins of fluorocarbon hydrophobicity, *Proc Natl Acad Sci U S A* **107**: 13603-13607.

Davies, J.I., and Evans, W.C. (1964) Oxidative metabolism of naphthalene by soil *pseudomonads*. The ring-fission mechanism, *Biochem J* **91**: 251-261.

Davis, C.K., Denman, S.E., Sly, L.I., and McSweeney, C.S. (2011) Development of a colorimetric colony-screening assay for detection of defluorination by micro-organisms, *Lett Appl Microbiol* **53**: 417-423.

Edelbach, B., and Jones, W. (1997) Mechanism of carbon- fluorine bond activation by (C5Me5) Rh (PMe3) H2 *Journal of the American Chemistry Society* **119**: 7734-7742.

Edmunds, W., and Smedley, P. (2013) Fluoride in natural waters, *Essentials of Medical Geology*: 311-336.

Engesser, K.H., Cain, R.B., and Knackmuss, H.J. (1988) Bacterial metabolism of side chain fluorinated aromatics: cometabolism of 3-trifluoromethyl(TFM)-benzoate by *Pseudomonas putida (arvilla)* mt-2 and *Rhodococcus rubropertinctus* N657, *Arch Microbiol* **149**: 188-197.

Engesser, K.H., Rubio, M.A., and Knackmuss, H.J. (1990) Bacterial metabolism of side-chain-fluorinated aromatics: unproductive meta-cleavage of 3-trifluoromethylcatechol, *Appl Microbiol Biotechnol* **32**: 600-608.

Engesser, K.H., Rubio, M.A., and Ribbons, D.W. (1988) Bacterial metabolism of side chain fluorinated aromatics: cometabolism of 4-trifluoromethyl(TFM)-benzoate by 4-isopropylbenzoate grown *Pseudomonas putida* JT strains, *Arch Microbiol* **149**: 198-206.

EPA (2016.2) Drinking Water Health Advisory for Perfluorooctane Sulfonate (PFOS). Agency, E.P. (ed). 1-88.

EPA (2016.1) Drinking Water Health Advisory for Perfluorooctanoic Acid (PFOA). Agency, E.P. (ed). 1-103.

EPA (2022) Our Current Understanding of the Human Health and Environmental Risks of PFAS. epa.gov/pfas: Environmental Protection Agency.

Escalante, D.E., Aukema, K.G., Wackett, L.P., and Aksan, A. (2017) Simulation of the bottleneck controlling access into a Rieske active site: predicting substrates of naphthalene 1,2-dioxygenase, *J Chem Inf Model* **57**: 550-561.

Evans, S., Andrews, D., Stoiber, T., and Naidenko, O. (2020) PFAS Contamination of Drinking Water Far More Prevalent Than Previously Reported. ewg.org/research: Environmental Working Group.

Fernley, H.N., and Walker, P.G. (1967) Studies on alkaline phosphatase. Inhibition by phosphate derivatives and the substrate specificity, *Biochem J* **104**: 1011-1018.

Ferraro, D.J., Gakhar, L., and Ramaswamy, S. (2005) Rieske business: structure-function of Rieske non-heme oxygenases, *Biochem Biophys Res Commun* **338**: 175-190.

Ferreira, M.I., Iida, T., Hasan, S.A., Nakamura, K., Fraaije, M.W., Janssen, D.B., and Kudo, T. (2009) Analysis of two gene clusters involved in the degradation of 4-fluorophenol by *Arthrobacter sp*. strain IF1, *Appl Environ Microbiol* **75**: 7767-7773.

Fiedler, H., Kennedy, T., and Henry, B. (2021) A critical review of a recommended analytical and classification approach for organic fluorinated compounds with an emphasis on per - and polyfluoroalkyl substances, *Int Environ Assess Manage* **17**: 331-351.

Filho, A.H.D.S., and de Souza, G.L.C. (2020) Examining the degradation of environmentally-daunting per- and poly-fluoroalkyl substances from a fundamental chemical perspective, *Phys Chem Chem Phys* **22**: 17659-17667.

Finette, B.A., and Gibson, D.T. (1988) Initial studies on the regulation of toluene degradation by *Pseudomonas putida* F1, *Biocatal Biotransformation* **2**: 29-37.

Folsom, B.R., Chapman, P.J., and Pritchard, P.H. (1990) Phenol and trichloroethylene degradation by *Pseudomonas cepacia* G4: kinetics and interactions between substrates, *Appl Environ Microbiol* **56**: 1279-1285.

Fox, B.G., Borneman, J.G., Wackett, L.P., and Lipscomb, J.D. (1990) Haloalkene oxidation by the soluble methane monooxygenase from *Methylosinus trichosporium* OB3b: mechanistic and environmental implications, *Biochemistry* **29**: 6419-6427.

Furukawa K, Hirose J, Suyama A, Zaiki T, and S, H. (1993) Gene Components Responsible for Discrete Substrate Specificity in the Metabolism of Biphenyl (bph Operon) and Toluene (tod Operon), *Journal of Bacteriology* **175**: 5224-5232.

Gabrielson, S. (2018) SciFinder, *J Medl Library Assoc: JMLA* **106**: 588.

Gibson, D., Koch, J., and Kallio, R. (1968) Oxidative degradation of aromatic hydrocarbons by microorganisms. I. Enzymic formation of catechol from benzene, *Biochemistry* **7**: 2653-2662.

Gibson, D.T. (1999) *Beijerinckia sp* strain B1: a strain by any other name, *J Ind Microbiol Biotechnol* **23**: 284-293.

Gibson, D.T., Gschwendt, B., Yeh, W.K., and Kobal, V.M. (1973) Initial reactions in the oxidation of ethylbenzene by *Pseudomonas putida*, *Biochemistry* **12**: 1520-1528.

Gibson, D.T., Koch, J.R., Schuld, C.L., and Kallio, R.E. (1968) Oxidative degradation of aromatic hydrocarbons by microorganisms. II metabolism of halogenated aromatic hydrocarbons, *Biochemistry* **7**: 3795-3802.

Gibson, D.T., Mahadevan, V., and Davey, J.F. (1974) Bacterial metabolism of para- and meta-xylene: oxidation of the aromatic ring, *J Bacteriol* **119**: 930-936.

Gibson, D.T., and Parales, R.E. (2000) Aromatic hydrocarbon dioxygenases in environmental biotechnology, *Curr Opin Biotechnol* **11**: 236-243.

Goldman, P. (1965) The enzymatic cleavage of the carbon-fluorine bond in fluoroacetate, *J Biol Chem* **240**: 3434-3438.

Goldman, P., and Milne, G.W. (1966) Carbon-fluorine bond cleavage. II. Studies on the mechanism of the defluorination of fluoroacetate, *J Biol Chem* **241**: 5557-5559.

Good, N., Winget, G., Winter, W., Connolly, T., Izawa, S., and Singh, R. (1966) Hydrogen ion buffers for biological research, *Biochemistry* **5**: 467-477.

Greenhalgh, R., and Riley, J.P. (1961) The determination of fluorides in natural waters, with particular reference to sea water, *Anal Chim Acta* **25**: 179-188.

Groce, S.L., Miller-Rodeberg, M.A., and Lipscomb, J.D. (2004) Single-turnover kinetics of homoprotocatechuate 2,3-dioxygenase, *Biochemistry* **43**: 15141-15153.

Göckener, B., Weber, T., Rüdel, H., Bücking, M., and Kolossa-Gehring, M. (2020) Human Biomonitoring of Per- and Polyfluoroalkyl Substances in German Blood Plasma Samples from 1982 to 2019, *Environment International* **145**.

Han, F., Bao, Y., Yang, Z., Fyles, T., Zhao, J., Peng, X., et al. (2007) Simple bisthiocarbonohydrazones as sensitive, selective, colorimetric, and switch - on fluorescent chemosensors for fluoride anions, *Chemistry- A European J* **13**: 2880-2892.

Han, J., Kiss, L., Mei, H., Remete, A.M., Ponikvar-Svet, M., Sedgwick, D.M., et al. (2021) Chemical Aspects of Human and Environmental Overload with Fluorine, *Chem Rev* **121**: 4678-4742.

Harper, D.B., and O'Hagan, D. (1994) The fluorinated natural products, *Nat Prod Rep* **11**: 123-133.

Hassner, A., and Namboothiri, I. (2012) SAEGUSA Enone Synthesis to SZARVASY-SCHOPF Carbomethoxylation. In: *Organic Synthesis Based on Name Reactions*. 415-476.

Herken, O. (2021) Updated: New EPA strategy on PFAS could aid in response to crisis in La Crosse. In: *La Crosse Tribune*. lacrossetribune.com.

Hinterholzinger, F.M., Rühle, B., Wuttke, S., Karaghiosoff, K., and Bein, T. (2013) Highly sensitive and selective fluoride detection in water through fluorophore release from a metal-organic framework, *Sci Rep* **3**: 2562.

Hogue, C. (2021) PFAS targeted in legislation passed by US House of Representatives. Chemical & Engineering News.

Huag, L.S., Huber, S., Becher, G., and Thomsen, C. (2011) Characterization of human exposure pathways to perfluorinated compounds- Comparing exposure estimates with biomarkers of exposure, *Environ Int* **37**: 687-693.

Huang, S., and Jaffé, P.R. (2019) Defluorination of perfluorooctanoic acid (PFOA) and perfluorooctane sulfonate (PFOS) by *Acidimicrobium sp.* strain A6, *Environ Sci Technol* **53**: 11410-11419.

Jabłońska, J., and Tawfik, D.S. (2019) The number and type of oxygen-utilizing enzymes indicates aerobic vs. anaerobic phenotype, *Free Radic Biol Med* **140**: 84-92.

Jerina, D.M., Selander, H., Yagi, H., Wells, M.C., Davey, J.F., Mahadevan, V., and Gibson, D.T. (1976) Dihydrodiols from anthracene and phenanthrene, *J Am Chem Soc* **98**: 5988-5996.

Jeschke, P. (2017) Latest generation of halogen - containing pesticides, *Pest Manage Sci* **73**: 1053-1066.

Ji, C., Stockbridge, R.B., and Miller, C. (2014) Bacterial fluoride resistance, Fluc channels, and the weak acid accumulation effect, *J Gen Physiol* **144**: 257-261.

Jones, R. (1947) Ortho and Para Substituted Derivatives of Benzotrifluoride, *J Am Chem Soc* **69**: 2346-2350.

Kasahara, Y., Morimoto, H., Kuwano, M., and Kadoya, R. (2012) Genome-wide analytical approaches using semi-quantitative expression proteomics for aromatic hydrocarbon metabolism in *Pseudomonas putida* F1, *J Microbiol Methods* **91**: 434-442.

Key, B.D., Howell, R.D., and Criddle, C.S. (1997) Critical review fluorinated organics in the biosphere, *Environ Sci Technol* **31**: 2445-2454.

Kiel, M., and Engesser, K.H. (2015) The biodegradation vs. biotransformation of fluorosubstituted aromatics, *Appl Microbiol Biotechnol* **99**: 7433-7464.

Kim, S., Chen, J., Cheng, T., Gindulyte, A., He, J., He, S., et al. (2021) PubChem in 2021: new data content and improved web interfaces, *Nucleic Acids Res* **49**: D1388-D1395.

Kitagawa, M., Ara, T., Arifuzzaman, M., Ioka-Nakamichi, T., Inamoto, E., Toyonaga, H., and Mori, H. (2005) Complete set of ORF clones of Escherichia coli ASKA library (a complete set of E. coli K-12 ORF archive): unique resources for biological research, *DNA Res* **12**: 291-299.

Leahy, J.G., and Olsen, R.H. (2006) Kinetics of toluene degradation by toluene-oxidizing bacteria as a function of oxygen concentration, and the effect of nitrate, ***FEMS*** *Microbiol Ecol* **23**: 23-30.

Leong, L.E.X., Khan, S., Davis, C.K., Denman, S.E., and McSweeney, C.S. (2017) Fluoroacetate in plants - a review of its distribution, toxicity to livestock and microbial detoxification, *J Anim Sci Biotechnol* **8**: 55.

Lim, X. (2021) Can Microbes Save Us from PFAS?, *ACS Cent Sci* **7**: 3-6.

Lindstrom, A., Strynar, M., and Libelo, E. (2011) Polyfluorinated compounds: Past, present, and future, *Environ Sci Technol* **45**: 7954-7961.

Liu, X., and Mullin, M. (2019) Inadvertent Polychlorinated Biphenyls (PCBs) in Consumer Products. In: *ISEE and ISIAQ Joint Conference*. Kaunas, Europe, Lithuania: United States Environmental Protection Agency.

Liu, Z., Bentel, M.J., Yu, Y., Ren, C., Gao, J., Pulikkal, V.F., et al. (2021) Near-quantitative defluorination of perfluorinated and fluorotelomer carboxylates and sulfonates with integrated oxidation and reduction, *Environ Sci Technol* **55**: 7052-7062.

Ma, Y., Mou, Q., Yan, P., Yang, Z., Xiong, Y., Yan, D., et al. (2021) A highly sensitive and selective fluoride sensor based on a riboswitch-regulated transcription coupled with CRISPR-Cas13a tandem reaction, *Chem Sci* **12**: 11740-11747.

Manfrin, A., Hänggli, A., van den Wildenberg, J., and McNeill, K. (2020) Substituent Effects on the Direct Photolysis of Benzotrifluoride Derivatives, *Environ Sci Technol* **54**: 11109-11117.

Marín, M., Plumeier, I., and Pieper, D. (2012) Degradation of 2,3-dihydroxybenzoate by a novel meta-cleavage pathway, *J Bacteriol* **194**: 3851-3860.

McCleaf, P., Englund, S., Östlund, A., Lindegren, K., Wiberg, K., and Ahrens, L. (2017) Removal efficiency of multiple poly- and perfluoroalkyl substances (PFASs) in drinking water using granular activated carbon (GAC) and anion exchange (AE) column tests, *Water Res* **120**: 77-87.

Menger, R., Funk, E., Henry, C., and Borch, T. (2021) Sensors for detecting per-and polyfluoroalkyl substances (PFAS): A critical review of development challenges, current sensors, and commercialization obstacles, *Chem Eng J*.

Miranda-Rojas, S., Fernández, I., Kaestner, J., Toro Labbé, A., and Mendizábal Emaldía, F. (2018) Unraveling the nature of the catalytic power of fluoroacetate dehalogenase, *Chem Cat Chem* **10**: 1052-1063.

Misiak, K., Casey, E., and Murphy, C.D. (2011) Factors influencing 4-fluorobenzoate degradation in biofilm cultures of *Pseudomonas knackmussii* B13, *Water Res* **45**: 3512-3520.

Mondello, F.J. (1989) Cloning and expression in *Escherichia coli* of *Pseudomonas* strain LB400 genes encoding polychlorinated biphenyl degradation, *J Bacteriol* **171**: 1725-1732.

Mueller, R., and Yingling, V. (2020) History and Use of Per- and Polyfluoroalkyl Substances (PFAS). Interstate Technology Regulatory Council.

Mueller, R., and Yingling, V. (2018) Remediation Technologies and Methods for Per- and Polyfluoroalkyl Substances (PFAS). Interstate Technology Regulatory Council.

Murphy, C.D. (2016) Microbial degradation of fluorinated drugs: biochemical pathways, impacts on the environment and potential applications, *Appl Microbiol Biotechnol* **100**: 2617-2627.

Murphy, C.D., Schaffrath, C., and O'Hagan, D. (2003) Fluorinated natural products: the biosynthesis of fluoroacetate and 4-fluorothreonine in *Streptomyces cattleya*, *Chemosphere* **52**: 455-461.

Müller, K., Faeh, C., and Diederich, F. (2007) Fluorine in pharmaceuticals: looking beyond intuition, *Science* **317**: 1881-1886.

Nagata, Y., Nariya, T., Ohtomo, R., Fukuda, M., Yano, K., and Takagi, M. (1993) Cloning and sequencing of a dehalogenase gene encoding an enzyme with hydrolase activity involved in the degradation of gamma-hexachlorocyclohexane in *Pseudomonas paucimobilis*, *J Bacteriol* **175**: 6403-6410.

Nelson, J.W., Plummer, M.S., Blount, K.F., Ames, T.D., and Breaker, R.R. (2015) Small molecule fluoride toxicity agonists, *Chem Biol* **22**: 527-534.

Newton, J.J., Brooke, A.J., Duhamel, B., Pulfer, J.M., Britton, R., and Friesen, C.M. (2020) Fluorodesulfurization of thionobenzodioxoles with silver(I) fluoride, *J Org Chem* **85**: 13298-13305.

Nikolaeva, S., Kolbin, A., Sapozhnikov, Y., Valitov, R., and Ivanov, V. (1990) Synthesis of fluoro-substituted symmetrical dialkylaminotriazines under interphase-catalysis conditions, *Chem Heterocycl Compd* **26**: 1142-1144.

O'Hagan, D. (2008) Understanding organofluorine chemistry. An introduction to the C-F bond, *Chem Soc Rev* **37**: 308-319.

Ochoa-Herrera, V., Banihani, Q., León, G., Khatri, C., Field, J.A., and Sierra-Alvarez, R. (2009) Toxicity of fluoride to microorganisms in biological wastewater treatment systems, *Water Res* **43**: 3177-3186.

Ogawa, Y., Tokunaga, E., Kobayashi, O., Hirai, K., and Shibata, N. (2021) Current Contributions of Organofluorine Compounds to the Agrochemical Industry, *iScience* **23**: 101467.

Osawa, R., and Walsh, T. (1995) Detection of bacterial gallate decarboxylation by visual color discrimination, *J Gen Appl Microbiol* **41**: 165-170.

O'Hagan, D., and Rzepa, H. (1997) Some influences of fluorine in bioorganic chemistry, *Chem Comm* **7**: 645-652.

Pan, Y., Shi, Y., Wang, J., Cai, Y., and Wu, Y. (2010) Concentrations of perfluorinated compounds in human blood from twelve cities in China, *Environ Toxicol Chem* **29**: 2695-2701.

Panieri, E., Baralic, K., Djukic-Cosic, D., Buha Djordjevic, A., and Saso, L. (2022) PFAS Molecules: A Major Concern for the Human Health and the Environment, *Toxics* **10**: 44.

Parales, J., Parales, R., Resnik, S., and Gibson, D. (1998) Enzyme specificity of 2-nitrotoluene 2,3-dioxygenase from P*seudomonas sp.* strain JS42 is determined by the C-terminal region of the alpha subunit of the oxygenase component, *J Bacteriol* **180**: 1194-1199.

Parales, R.E., Lee, K., Resnick, S.M., Jiang, H., Lessner, D.J., and Gibson, D.T. (2000) Substrate specificity of naphthalene dioxygenase: effect of specific amino acids at the active site of the enzyme, *J Bacteriol* **182**: 1641-1649.

Pritchard, H., and Skinner, H. (1955) The concept of electronegativity, *Chem Rev* **55**: 745-786.

Ramasarma, T., Rao, A.V.S., Devi, M.M., Omkumar, R.V., Bhagyashree, K.S., and Bhat, S.V. (2015) New insights of superoxide dismutase inhibition of pyrogallol autoxidation, *Mol Cell Biochem* **400**: 277-285.

Reardon, K.F., Mosteller, D.C., and Bull Rogers, J.D. (2000) Biodegradation kinetics of benzene, toluene, and phenol as single and mixed substrates for *Pseudomonas putida* F1, *Biotechnol Bioeng* **69**: 385-400.

Reinscheid, U., Vervoort, J., and Zuilhof, H. (2006) Mild hydrolysis of 2-trifluoromethylphenol: Kinetics, mechanism and environmental relevance, *Chemosphere* **65**: 318-323.

Renganathan, V. (1989) Possible involvement of toluene-2,3-dioxygenase in defluorination of 3-fluoro-substituted benzenes by toluene-degrading *Pseudomonas sp.* Strain T-12, *Appl Environ Microbiol* **55**: 330-334.

Roessler, M., Sewald, X., and Müller, V. (2003) Chloride dependence of growth in bacteria, *FEMS Microbiol Lett* **225**: 161-165.

Romero, A.H. (2019) Role of Trifluoromethyl Substitution in Design of Antimalarial Quinolones: a Comprehensive Review, *Top Curr Chem (Cham)* **377**: 9.

Ross, R. (2019) What are PFAS? LiveScience.

Sanger, F. (1945) The Free Amino Groups of Insulin, *Biochem J* **39**: 507-515.

Seffernick, J.L., Reynolds, E., Fedorov, A.A., Fedorov, E., Almo, S.C., Sadowsky, M.J., and Wackett, L.P. (2010) X-ray structure and mutational analysis of the atrazine Chlorohydrolase TrzN, *J Biol Chem* **285**: 30606-30614.

Seong, H., Kwon, S., Dong-Cheol, S., Kim, J., and Jang, Y. (2019) Enzymatic defluorination of fluorinated compounds. *Appl Biol Chem*. 62.

Shapir, N., Pedersen, C., Gil, O., Strong, L., Seffernick, J., Sadowsky, M.J., and Wackett, L.P. (2006) TrzN from Arthrobacter aurescens TC1 Is a zinc amidohydrolase, *J Bacteriol* **188**: 5859-5864.

Shapir, N., Rosendahl, C., Johnson, G., Andreina, M., Sadowsky, M.J., and Wackett, L.P. (2005) Substrate specificity and colorimetric assay for recombinant TrzN derived from Arthrobacter aurescens TC1, *Appl Environ Microbiol* **71**: 2214-2220.

Sima, M.W., and Jaffé, P.R. (2021) A critical review of modeling Poly- and Perfluoroalkyl Substances (PFAS) in the soil-water environment, *Sci Total Environ* **757**: 143793.

Smart, B. (2001) Fluorine substituent effects (on bioactivity), *J Fluor Chem* **109**: 3-11.

Stanier, R.Y., Palleroni, N.J., and Doudoroff, M. (1966) The aerobic *pseudomonads*: a taxonomic study, *J Gen Microbiol* **43**: 159-271.

Stigaard Kjeldsen, L., and Bonefeld-Jørgensen, C. (2013) Perfluorinated compounds affect the function of sex hormone receptors, *Environ Sci Pollut Res* **20**: 8031-8044.

Storlie, J. (2021) City's PFAS Investigation Around the La Crosse Regional Airport. cityoflacrosse.org: City of La Crosse.

Strotmann, U.J., Pentenga, M., and Janssen, D.B. (1990) Degradation of 2-chloroethanol by wild type and mutants of *Pseudomonas putida* US2, *Arch Microbiol* **154**: 294-300.

Studier, F.W. (2005) Protein production by auto-induction in high density shaking cultures, *Protein Expr Purif* **41**: 207-234.

Sunderland, E.M., Hu, X.C., Dassuncao, C., Tokranov, A.K., Wagner, C.C., and Allen, J.G. (2019) A review of the pathways of human exposure to poly- and perfluoroalkyl substances (PFASs) and present understanding of health effects, *J Expo Sci Environ Epidemiol* **29**: 131-147.

Taha, M., E Silva, F.A., Quental, M.V., Ventura, S.P., Freire, M.G., and Coutinho, J.A. (2014) Good's buffers as a basis for developing self-buffering and biocompatible ionic liquids for biological research, *Green Chem* **16**: 3149-3159.

Thavarajah, W., Silverman, A.D., Verosloff, M.S., Kelley-Loughnane, N., Jewett, M.C., and Lucks, J.B. (2020) Point-of-Use Detection of Environmental Fluoride, *ACS Synth Biol* **9**: 10-18.

Thomas, K.A., and Hand, L.H. (2012) Assessing the metabolic potential of phototrophic communities in surface water environments: fludioxonil as a model compound, *Environ Toxicol Chem* **31**: 2138-2146.

Tiedt, O., Mergelsberg, M., Boll, K., Müller, M., Adrian, L., Jehmlich, N., et al. (2016) ATP-Dependent C-F Bond Cleavage Allows the Complete Degradation of 4-Fluoroaromatics without Oxygen, *mBio* **7**.

Tolkou, A., Manousi, N., Zachariadis, G., Katsoyiannis, I., and Deliyanni, E. (2021) Recently developed adsorbing materials for fluoride removal from water and fluoride analytical determination techniques: A review, *Sustainability* **13**: 7061.

Wackett, L. (2021) Why is the biodegradation of polyfluorinated compounds so rare?, *mSphere* **6**: e00721-00721.

Wackett, L.P. (2002) Mechanism and applications of Rieske non-heme iron dioxygenases, *Enzyme and Microbial Technology* **31**: 577-587.

Wackett, L.P. (2021) Nothing lasts forever: understanding microbial biodegradation of polyfluorinated compounds and perfluorinated alkyl substances, *Microb Biotechnol* **15**: 773-792.

Wackett, L.P., Kwart, L.D., and Gibson, D.T. (1988) Benzylic monooxygenation catalyzed by toluene dioxygenase from *Pseudomonas putida*, *Biochemistry* **27**: 1360-1367.

Wackett, L.P., and Robinson, S.L. (2020) The ever-expanding limits of enzyme catalysis and biodegradation: polyaromatic, polychlorinated, polyfluorinated, and polymeric compounds, *Biochem J* **477**: 2875-2891.

Walker, M.C., and Chang, M.C. (2014) Natural and engineered biosynthesis of fluorinated natural products, *Chem Soc Rev* **43**: 6527-6536.

Wang, Y., and Liu, A. (2020) Carbon-fluorine bond cleavage mediated by metalloenzymes, *Chem Soc Rev* **49**: 4906-4925.

Wang, Z., Buser, A.M., Cousins, I.T., Demattio, S., Drost, W., Johansson, O., et al. (2021) A New OECD Definition for Per- and Polyfluoroalkyl Substances, *Environ Sci Technol* **55**: 15575-15578.

Weelink, S., Eekert, M., and Stams, A. (2010) Degradation of BTEX by anaerobic bacteria: physiology and application, *Reviews in Environmental Science and BioTechnology* **9**: 359-385.

West, P.W., Lyles, G.R., and Miller, J.L. (1970) Spectrophotometric determination of atmospheric fluorides, *Environ Sci Technol* **4**: 1150.

Williams, M.G., Olson, P.E., Tautvydas, K.J., Bitner, R.M., Mader, R.A., and Wackett, L.P. (1990) The application of toluene dioxygenase in the synthesis of acetylene-terminated resins, *Appl Microbiol Biotechnol* **34**: 316-321.

Winsor, G.L., Griffiths, E.J., Lo, R., Dhillon, B.K., Shay, J.A., and Brinkman, F.S. (2016) Enhanced annotations and features for comparing thousands of *Pseudomonas* genomes in the *Pseudomonas* genome database, *Nucleic Acids Res* **44**: D646-653.

Winsor, G.L., Van Rossum, T., Lo, R., Khaira, B., Whiteside, M.D., Hancock, R.E., and Brinkman, F.S. (2009) *Pseudomonas* Genome Database: facilitating user-friendly, comprehensive comparisons of microbial genomes, *Nucleic Acids Res* **37**: D483-488.

Wu, Y., Romanak, K., Bruton, T., Blum, A., and Venier, M. (2020) Per- and polyfluoroalkyl substances in paired dust and carpets from childcare centers, *Chemosphere* **251**: 126771.

Xie, Y., Chen, G., May, A.L., Yan, J., Brown, L.P., Powers, J.B., et al. (2020) *Pseudomonas sp*. strain 273 degrades fluorinated alkanes, *Environ Sci Technol* **54**: 14994-15003.

Yamamura, S., Wade, M., and Sikes, J. (1962) Direct Spectrophotometric Fluoride Determination, *Analytical Chemistry* **34**: 1308-1312.

Yang, Y., Chen, R.F., and Shiaris, M.P. (1994) Metabolism of naphthalene, fluorene, and phenanthrene: preliminary characterization of a cloned gene cluster from Pseudomonas putida NCIB 9816, *J Bacteriol* **176**: 2158-2164.

Yoshida, H., and Yamada, H. (1985) Microbial production of pyrogallol through decarboxylation of gallic acid, *Agric Biol Chem* **49**: 659-663.

Yu, Y., Zhang, K., Li, Z., Ren, C., Chen, J., Lin, Y.H., et al. (2020) Microbial cleavage of C-F bonds in two C6 per- and polyfluorinated compounds via reductive defluorination, *Environ Sci Technol* **54**: 14393-14402.

Zhao, Y., Li, Y., Long, Y., Zhou, Z., Tang, Z., Deng, K., and Zhang, S. (2017) Highly selective fluorescence turn-on determination of fluoride ions via chromogenic aggregation of a silyloxy-functionalized salicylaldehyde azine, *Tet lett* **58**: 1351-1355.

Zheng, G., Schreder, E., Dempsey, J.C., Uding, N., Chu, V., Andres, G., et al. (2021) Per- and polyfluoroalkyl substances (PFAS) in breast milk- and trends for current-use PFAS, *Environ Sci Technol*.

Zylstra, G.J., and Gibson, D.T. (1989) Toluene degradation by Pseudomonas putida F1. Nucleotide sequence of the todC1C2BADE genes and their expression in Escherichia coli, *J Biol Chem* **264**: 14940-14946.

Zylstra, G.J., Mccombie, W.R., Gibson, D.T., and Finette, B.A. (1988) Toluene degradation by *Pseudomonas putida* F1: genetic organization of the tod operon, *J Appl Environ Microbiol* **54**: 1498-1503.

Appendix A: Chapter 2 Supplement

Figure 1S. Cultures of PpF1 grown and induced with toluene, then moved to the respective carbon sources. From left to right: PpF1 with vapor bulb containing DFBD, PpF1 with vapor bulb containing toluene, PpF1 with no carbon source.

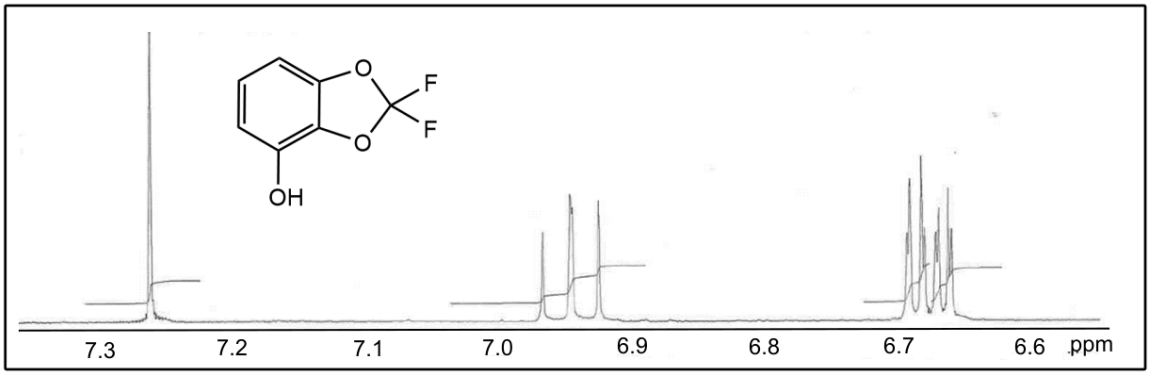

Figure 2S. ^{1}H-NMR of the DFBD-4-OL standard.

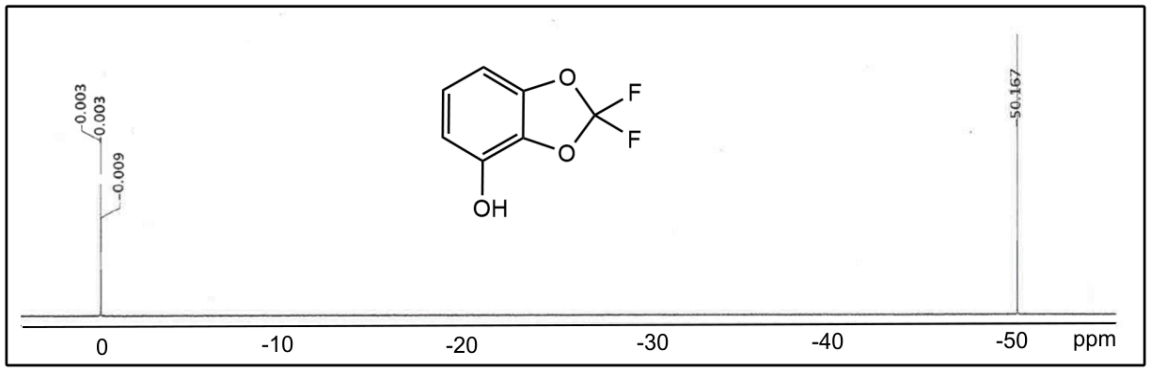

Figure 3S ^{19}F-NMR of the DFBD-4-OL standard.

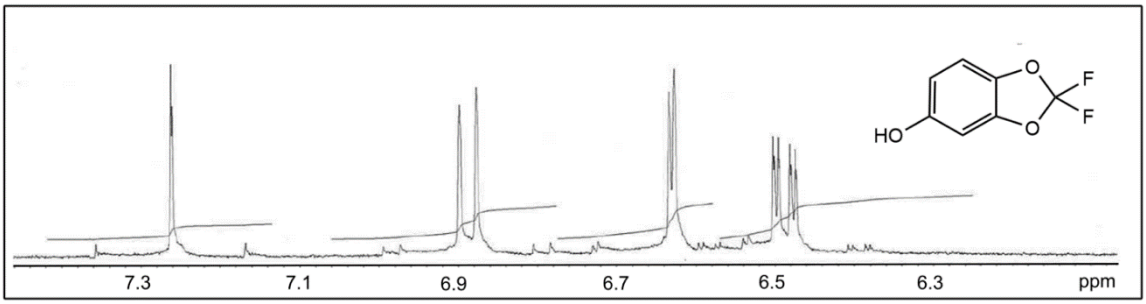

Figure 4S. ^{1}H-NMR of the DFBD-5-ol standard.

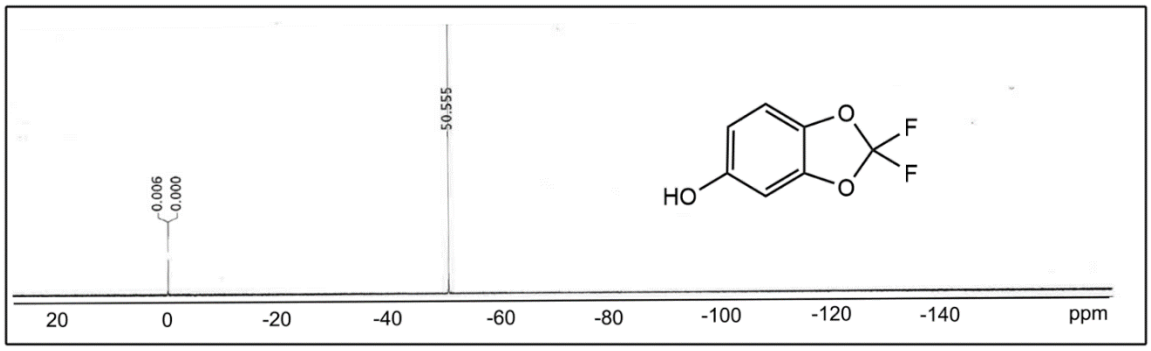

Figure 5S. ^{19}F-NMR of the DFBD-5-OL standard.

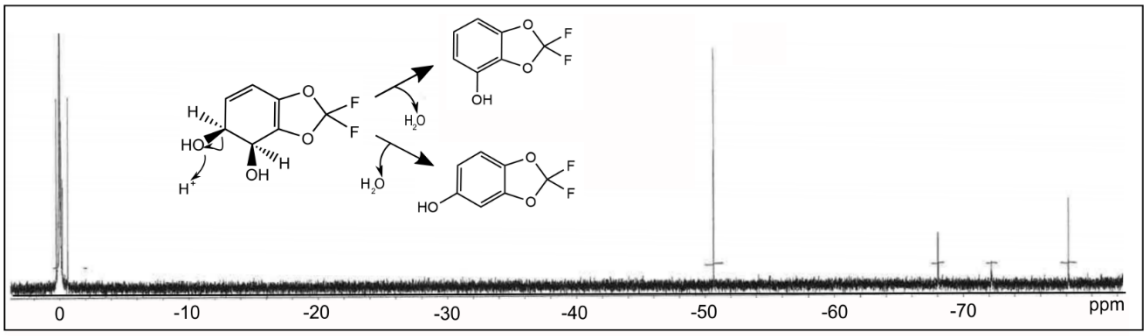

Figure 6S. ^{19}F-NMR of the chloroform (acid) treated acetonitrile sample, previously containing the cis-diol. Reaction showing the predicted dehydration of the diol in the presence of acid. Smaller peaks are predicted to be free fluoride ion.

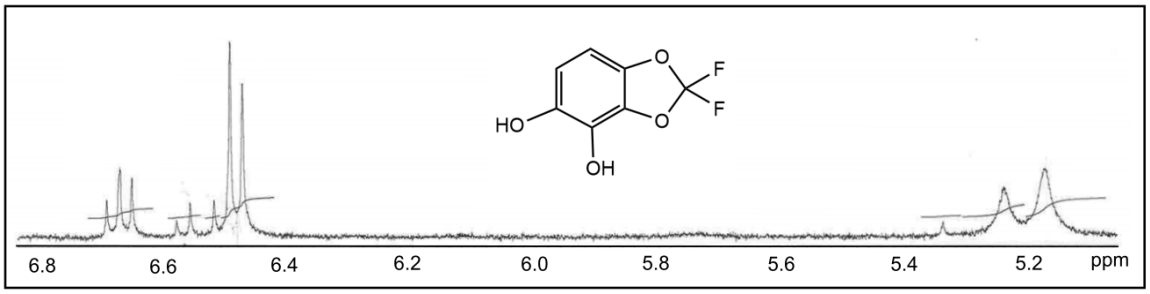

Figure 7S. ^{1}H-NMR of the *E.coli* pDTG602 supernatant extract containing 4,5-dihydroxy-DFBD and 1,2,3-benzenetriol.

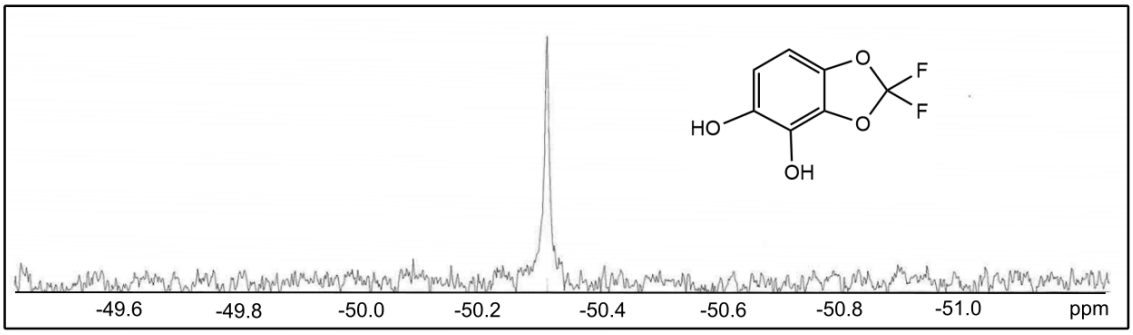

Figure 8S. ^{19}F-NMR of the the *E.coli* pDTG602 supernatant extract containing 4,5-dihydroxy-DFBD. Fluorine singlet illustrating rearomatized compound with identical fluorines.

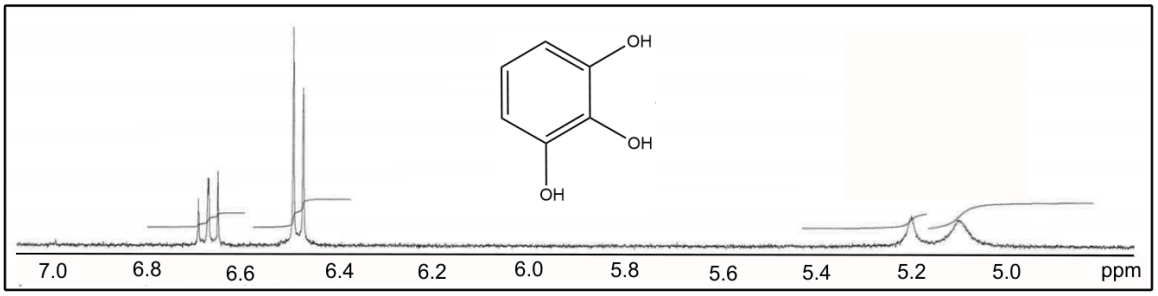

Figure 9S. ^{1}H-NMR of standard 1,2,3-benzenetriol.

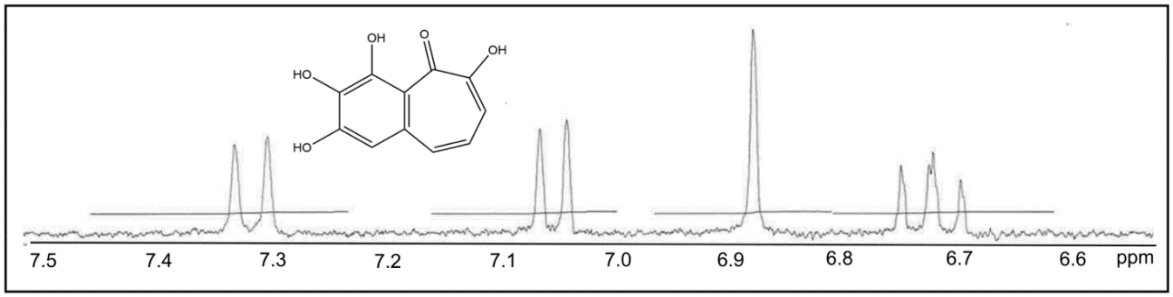

Figure 10S. [1]H-NMR of standard purpurogallin.

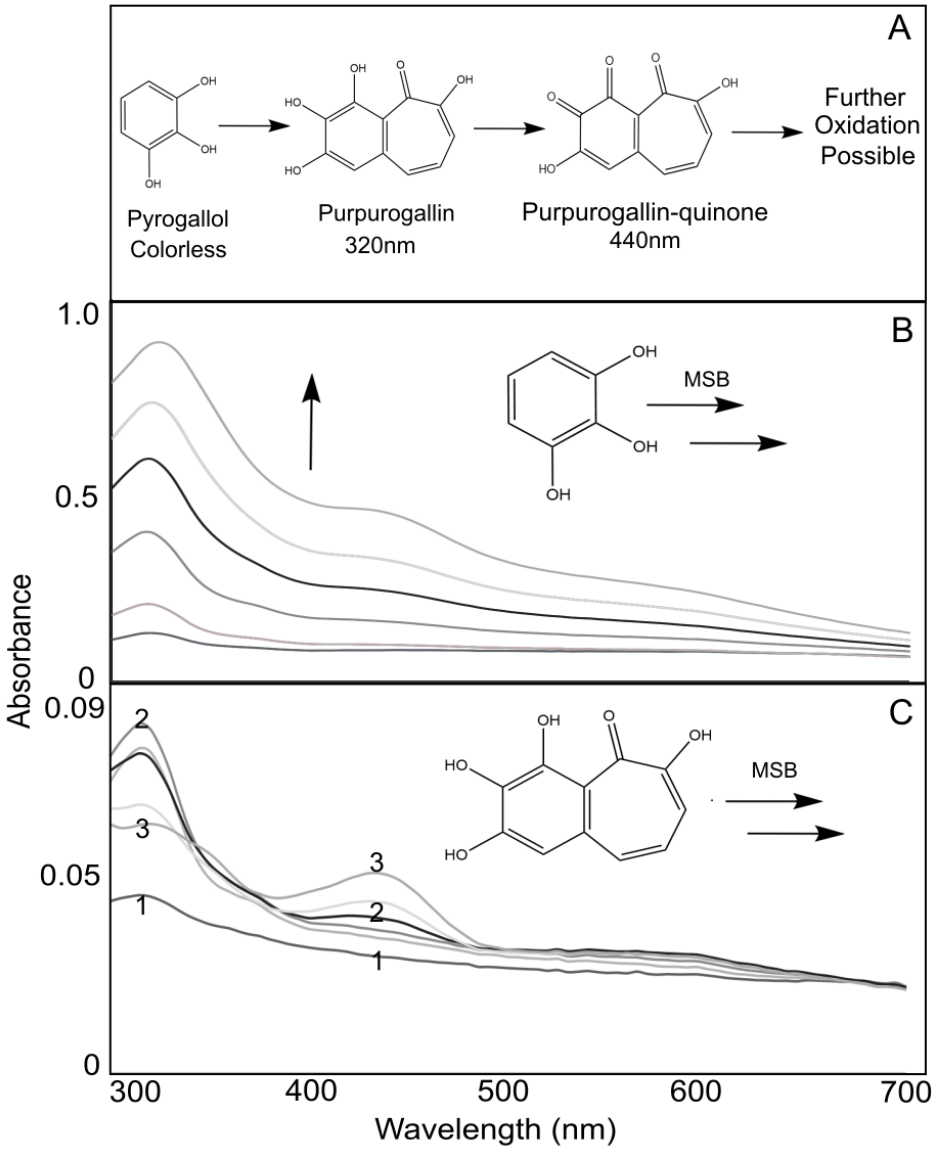

Figure 11S. UV-Vis absorbance measurements taken from 300-700nm at 5 nm intervals. A) time course of pyrogallol (0.1 mM) oxidation in MSB media over 2.5 hours. Absorbance increases at 320nm and 440nm. B) Time course of purpurogallin (0.02mM) oxidation in MSB media over 1.2 hours. As the purpurogallin dissolved, an immediate increase was seen at 320 nm. Then, the 320nm decreased and the absorbance at 440 nm increased.

Appendix B: Chapter 3 Supplement

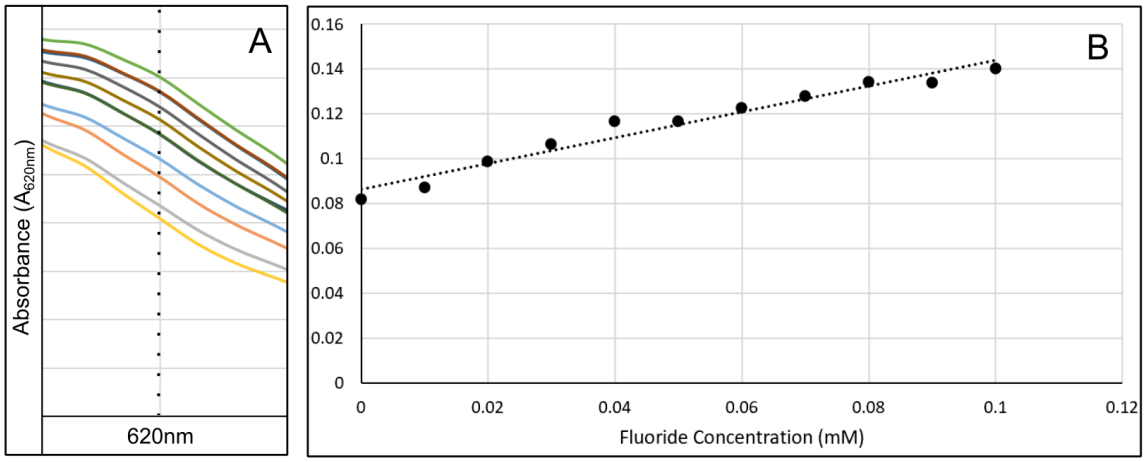

Figure S1. A) Wavelength scan of samples from 0-100 µM fluoride in the alizarin-lanthanum complex over 620nm. This wavelength provided the best linear sample separation, as seen in panel B.

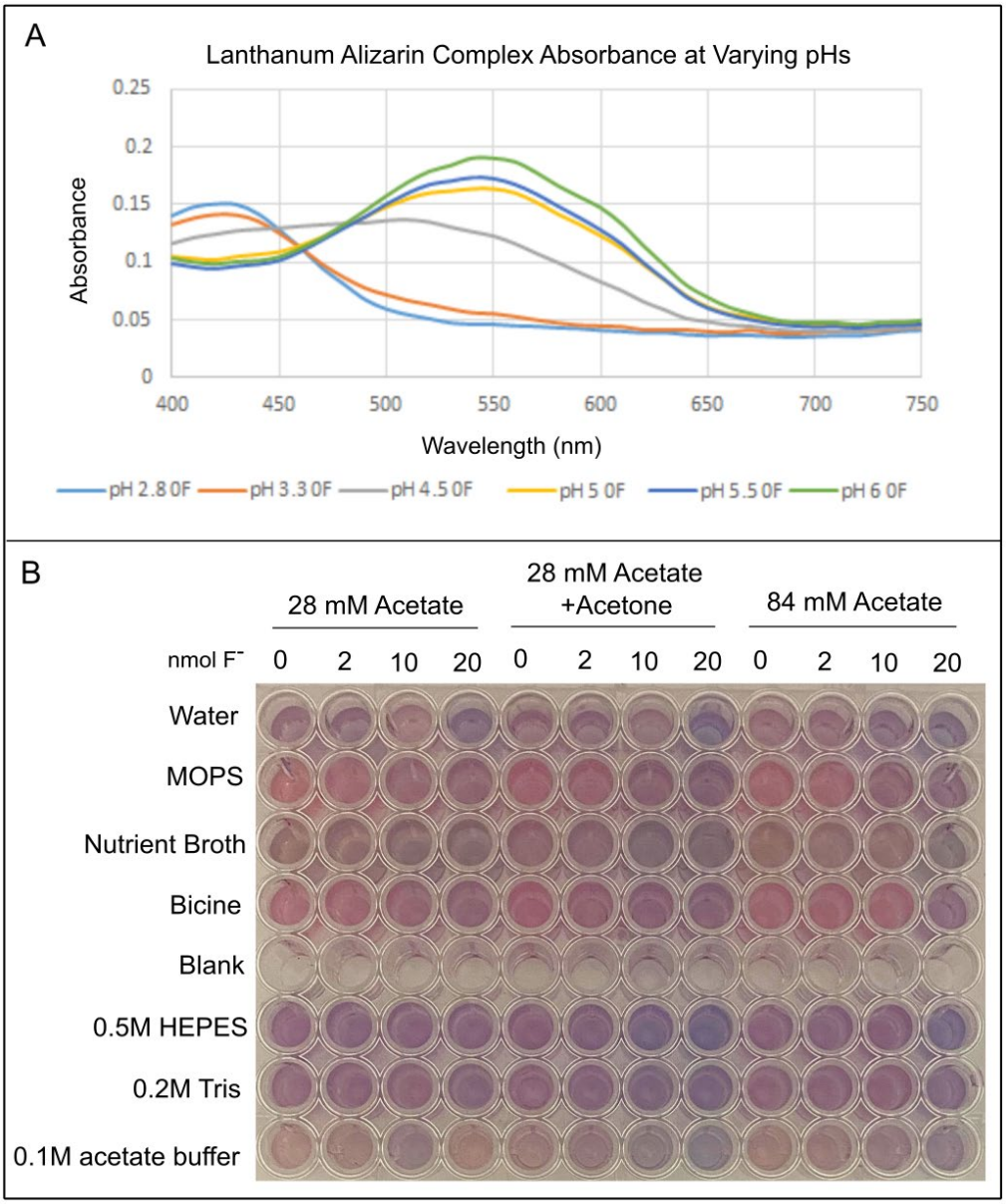

Figure S2. Optimization of conditions for maximizing sensitivity and minimizing interferences for the color assay. A) Spectrophotometric measurements of the difference in Lanthanum-Alizarin absorbance at varying pH's. The samples shown contain no fluoride but illustrate that a higher pH (>5) is necessary for proper complex formation (see main Figure 1). Additional tests (not shown) indicate pH 5.0-5.5 was the most sensitive for detecting fluoride. As previously reported, the sensitivity of the assay with lanthanum was not improved by replacing the metal with cerium, praseodymium or neodymium (35, 36). Spectrophotometric tests were done with the four different rare earth metals with acetone and fluoride (not shown) and indicated comparable absorbance values at 620 nm. Because of previous use and reliability at low fluoride concentrations, lanthanum was used for the remainder of this study. B) Microtiter plate testing various types of media and concentrations of buffer with or without acetone. Level of interference was compared to the well containing only water.

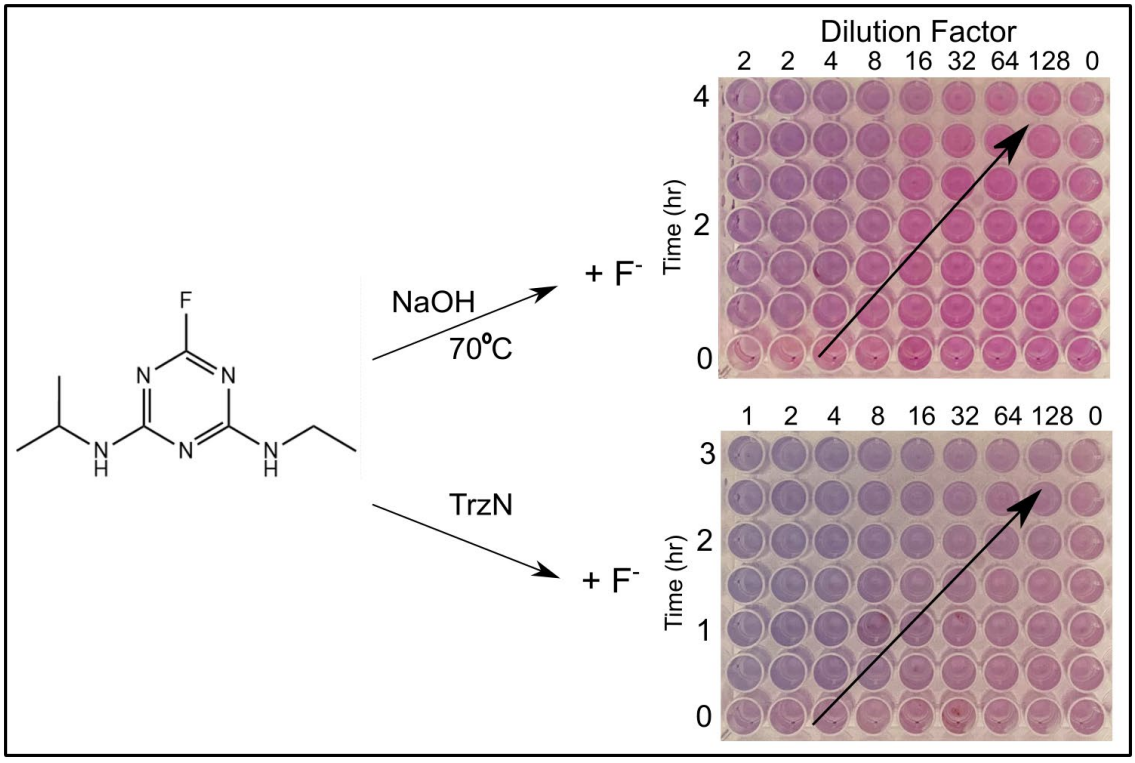

Figure S3. Plated serial dilution over time from chemical (top) and enzymatic (lower) reactions starting with fluoroatrazine and measuring defluorination using the color assay and dilutions to estimate fluoride concentrations increasing over time. Samples were taken from each individual reaction over time and diluted to demonstrate concentration. Purple wells at higher dilutions indicates a higher concentration of fluoride in the sample. The chemical reaction was done in water at pH 11 while the enzymatic reaction was done in 20 mM HEPES buffer (pH 7.3) at 37˚C. There were no interferences with the assay in either reaction.

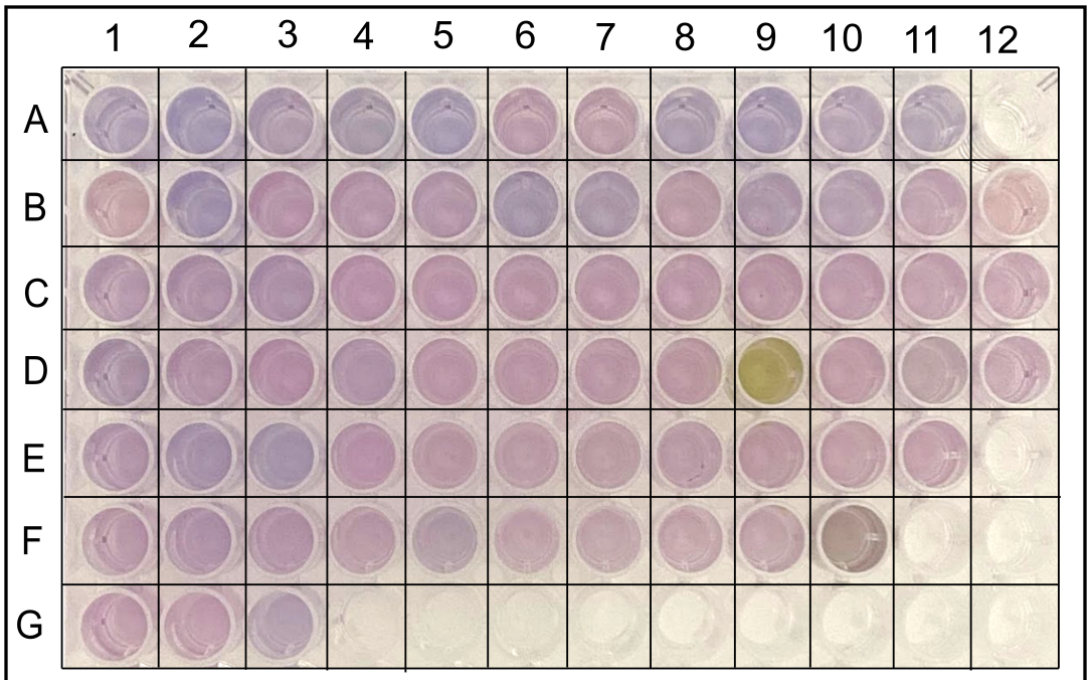

A1	2-fluorotoluene	C1	1,2,3,4-tetrafluorobenzene	E1	4-fluorophenyl acetic acid
A2	3-fluorotoluene	C2	1,2,3,5-tetrafluorobenzene	E2	4-(difluoromethoxy)benzoic acid
A3	4-fluorotoluene	C3	1,2,4,5-tetrafluorobenzene	E3	4-fluoro acetophenone
A4	4-fluorobenzotrifluoride	C4	pentafluorobenzene	E4	4-fluoro-1-methylphenyl acetic acid
A5	ααα-trifluorotoluene	C5	hexafluorobenzene	E5	4-fluorobenzonitrile
A6	5-chloro-2-fluorotoluene	C6	chloropentafluorobenzene	E6	fluoroacetonitrile
A7	2,6-difluorotoluene	C7	perfluorodecalin	E7	3-fluorophenyl hydrazine hydrochloride
A8	2,5-difluorotoluene	C8	3-fluoro-o-xylene	E8	3-fluorouracil
A9	3,5-difluorotoluene	C9	4-fluoro-o-xylene	E9	2,2-difluoro-5-nitro-1,3-benzodioxole
A10	2,3-difluorotoluene	C10	2-fluoro-m-xylene	E10	2,2-difluoro-1,3-benzodioxole-carboxylic acid
A11	2,4-difluorotoluene	C11	4-fluoro-m-xylene	E11	heptafluorobutyramide
B1	2,3,4-trifluorotoluene	C12	5-fluoro-m-xylene	F1	1-(1-bromoethyl)-4-fluorobenzene
B2	2,4,5-trifluorotoluene	D1	(difluoromethoxy)benzene	F2	2-fluoro-4-(propanyl)benzoic acid
B3	2,3,6-trifluorotoluene	D2	(trifluoromethoxy)benzene	F3	4-fluorocumene
B4	2,4,6-trifluorotoluene	D3	4-(trifluoromethoxy)benzene	F4	1-(1-chloroethyl)-4-fluorobenzene
B5	fluorobenzene	D4	phenyl trifluoromethyl sulfide	F5	4-(difluoromethoxy)aniline
B6	1,2-difluorobenzene	D5	1-difluoromethoxy-4-iodobenzene	F6	3-(difluoromethoxy)aniline
B7	1,3-difluorobenzene	D6	4-(difluoromethoxy)bromobenzene	F7	2,4-difluorophenol
B8	1,4-difluorobenzene	D7	1-nitro-4-(trifluoromethoxy)benzene	F8	2,5-difluorophenol
B9	1,2,3-trifluorobenzene	D8	4-(difluoromethoxy)nitrobenzene	F9	2,6-diflluorophenol
B10	1,2,4-trifluorobenzene	D9	1-fluoro-2,4-dinitrobenzene	F10	3-fluorocatechol
B11	1,3,5-trifluorobenzene	D10	2-(difluoromethoxy)nitrobenzene	G1	No compound
B12	2-fluoro-p-xylene	D11	2,4-(dinitrotrifluoromethoxy)benzene	G2	toluene
		D12	3-fluoro-4-methyl acetophenone	G3	2,2-difluoro-1,3-benzodioxole

Figure S4. Representative fluorinated compound screening plate with *Pseudomonas putida* F1. Positive hits for fluoride release are highlighted yellow in the key. Compounds that interfered with the assay by creating an alternative color are highlighted red in the key.

Compound	Electrode calculated concetration (mM)
2-fluorotoluene	0.058
3-fluorotoluene	0.155
4-fluorotoluene	0.034
4-fluorobenzotrifluoride	0.287
aaa-trifluorotoluene	0.638
5-chloro-2-fluorotoluene	0.010
2,6-difluorotoluene	0.008
2,5-difluorotoluene	0.087
3,5-difluorotoluene	0.127
2,3-difluorotoluene	0.088
2,4-difluorotoluene	0.191
2,3,4-trifluorotoluene	0.058
2,4,5-trifluorotoluene	0.119
2,3,6-trifluorotoluene	0.007
2,4,6-trifluorotoluene	0.013
fluorobenzene	0.022
1,2-difluorobenzene	0.123
1,3-difluorobenzene	0.115
1,4-difluorobenzene	0.009
1,2,3-trifluorobenzene	0.061
1,2,4-trifluorobenzene	0.090
1,3,5-trifluorobenzene	0.049
2-fluoro-p-xylene	0.061
1,2,3,4-tetrafluorobenzene	0.032
1,2,3,5-tetrafluorobenzene	0.023
1,2,4,5-tetrafluorobenzene	0.044
pentafluorobenzene	0.005
hexafluorobenzene	0.004
chloropentafluorobenzene	0.007
perfluorodecalin	0.005
3-fluoro-o-xylene	0.005
4-fluoro-o-xylene	0.005
2-fluoro-m-xylene	0.006
4-fluoro-m-xylene	0.009
5-fluoro-m-xylene	0.005

Compound (cont.)	Electrode calculated concetration (mM) (cont.)
(difluoromethoxy)benzene	0.037
(trifluoromethoxy)benzene	0.015
4-(trifluoromethoxy)fluorobenzene	0.009
phenyl trifluoromethyl sulfide	0.029
1-difluoromethoxy-4-iodobenzene	0.006
4-(difluoromethoxy)bromobenzene	0.007
1-nitro-4-(trifluoromethoxy)benzene	0.008
4-(difluoromethoxy)nitrobenzene	0.007
1-fluoro-2,4-dinitrobenzene	0.576
2-(difluoromethoxy)nitrobenzene	0.006
2,4-dinitro(trifluoromethoxy)benzene	0.087
3-fluoro-4-methyl acetophenone	0.002
4-fluorophenylaceticacid	0.019
4-(difluoromethoxy) benzoic acid	0.047
4-fluoro acetophenone	0.083
4-fluoro- 1-methylphenyl acetic acid	0.006
4-fluorobenzonitrile	0.020
fluoroacetonitrile	0.017
3-fluorophenyl hydrazine hydrochloride	0.018
3-fluorouracil	0.008
2,2-difluoro-5-nitro-1,3-benzodioxole	0.013
2,2-difluoro-1,3-benzodioxole-carboxylic acid	0.007
heptafluorobutyramide	0.003
1-(1-bromoethyl)-4-fluorobenzene	0.011
2-fluoro-4-(propanyl)benzoic acid	0.034
4-fluorocumene	0.083
1-(1-chloroethyl)-4-fluorobenzene	0.007
4-(difluoromethoxy)aniline	0.035
3-(difluoromethoxy)aniline	0.027
2,4-difluorophenol	0.027
2,5-difluorophenol	0.017
2,6-diflluorophenol	0.018
3-fluorocatechol	0.286
No compound	0.003
Toluene	0.002
2,2-difluoro-1,3-benzodioxole	0.162

Figure S5. Tested fluorinated compounds and controls with the calculated free fluoride ion concentration after each chemical was incubated with *P.putida* F1. Fluoride ion measurements were taken using the fluoride electrode and a standard curve was used to calculate concentration based on millivolt readings. The structures of compounds with common names are shown below for clarity.

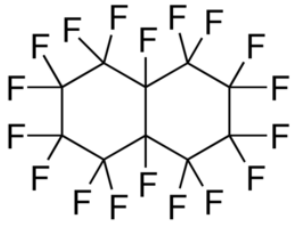

Perfluorodecalin

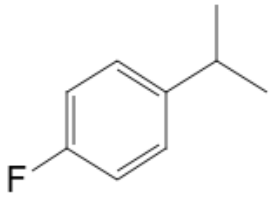

4-Fluorocumene

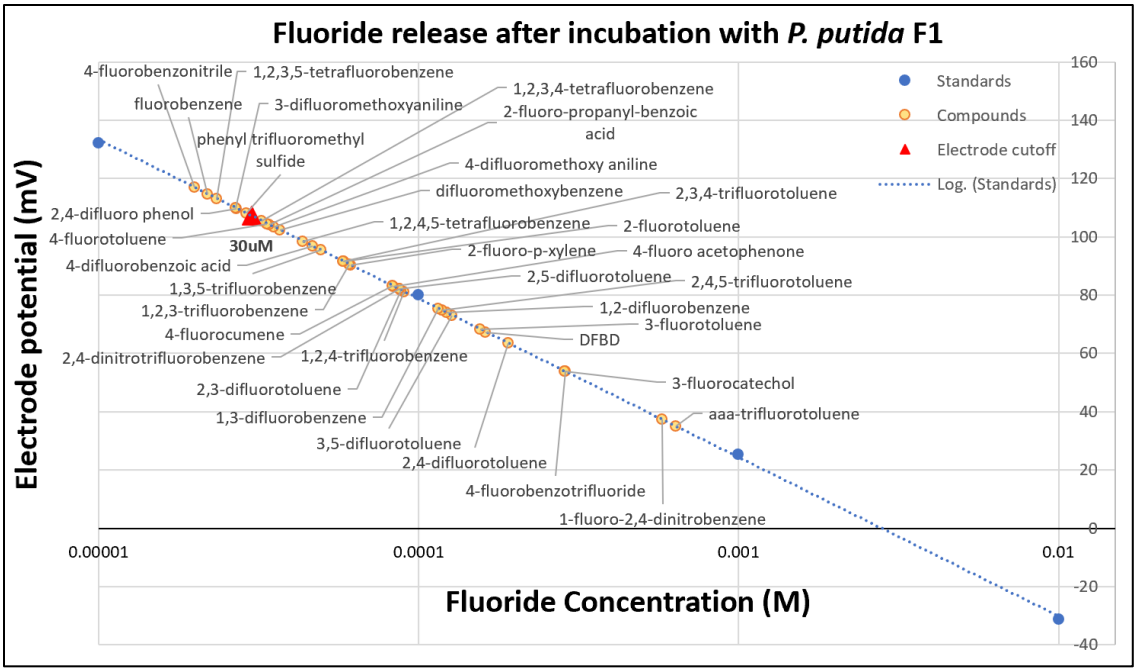

Figure S6. The electrode reading (mV) of supernatant after *P. putida* F1 incubation with each fluorinated chemical plotted against the concentration of fluoride. A standard curve (blue) was created using known concentrations of fluoride (sodium fluoride in 20mM HEPES) and their corresponding electrode readings to calculate the experimental values of fluoride (yellow) released from incubation. The red triangle in the plot indicates the cutoff in which samples were deemed positive hits (>30 µM) or negative hits (<30 µM). The 30 µM point was determined by the approximate visual detection limit of fluoride in the color assay.

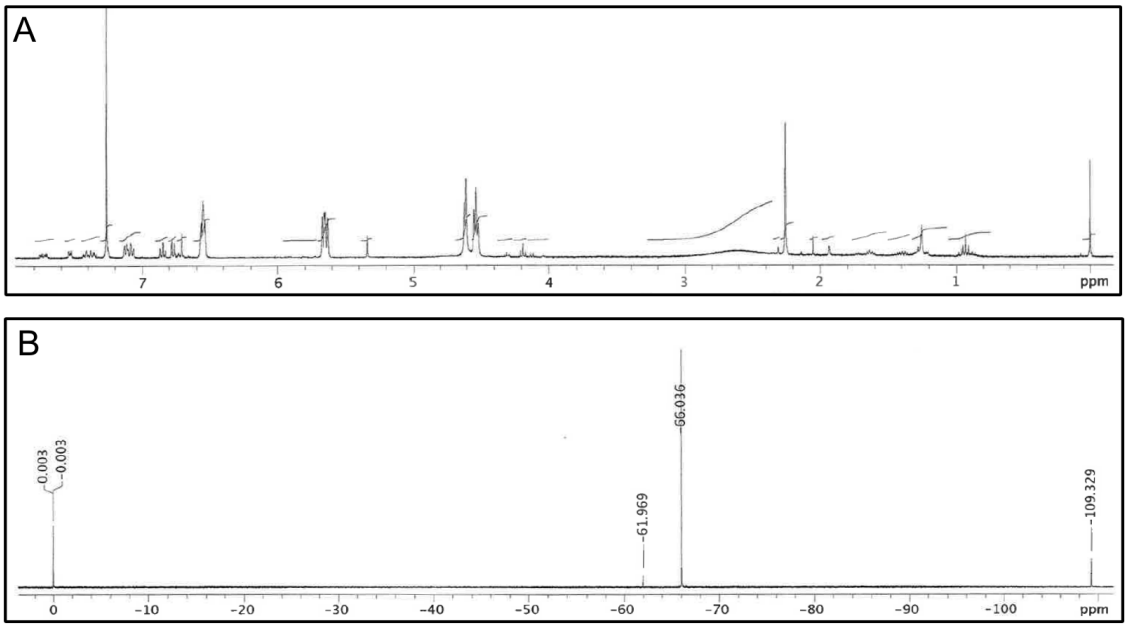

Figure S7. A) ^{1}H-NMR of the products from the extracted supernatant after incubation of *P. putida* F39/D with 4-fluorobenzotrifluoride. B) ^{19}F-NMR of the same extracted supernatant. The major product in these NMR was identified as 4-fluorobenzotrifluoride-2,3-dihydrodiol (i.e, 1,2-dihydroxy-3-trifluoromethyl-6-fluorocyclohexa-3,5-diene). See main text methods for chemical shifts.

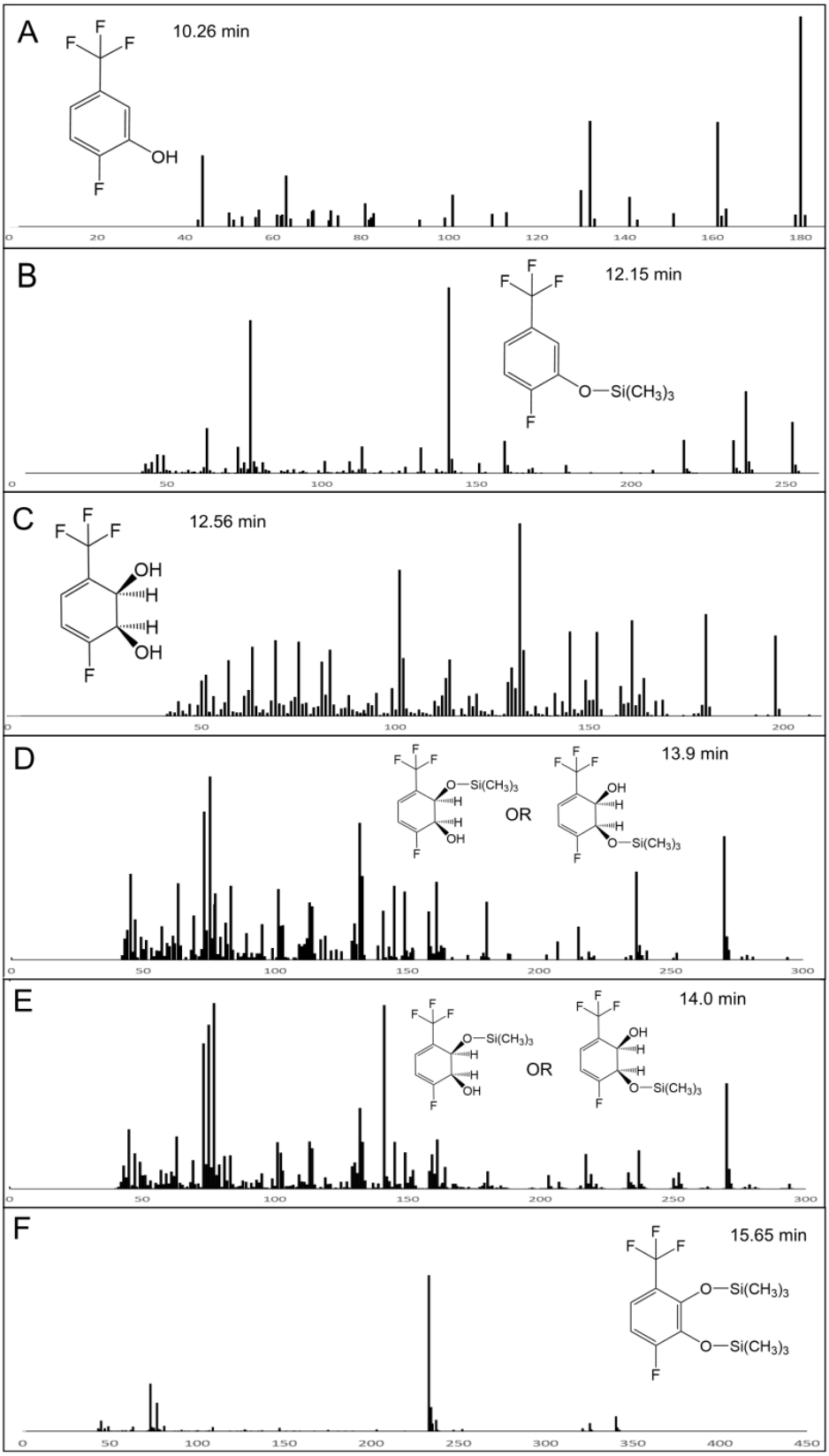

Figure S8. Full mass spectra for the designated peaks in main text figure 4. Fragmentation pattern labeled with corresponding structure and retention time.

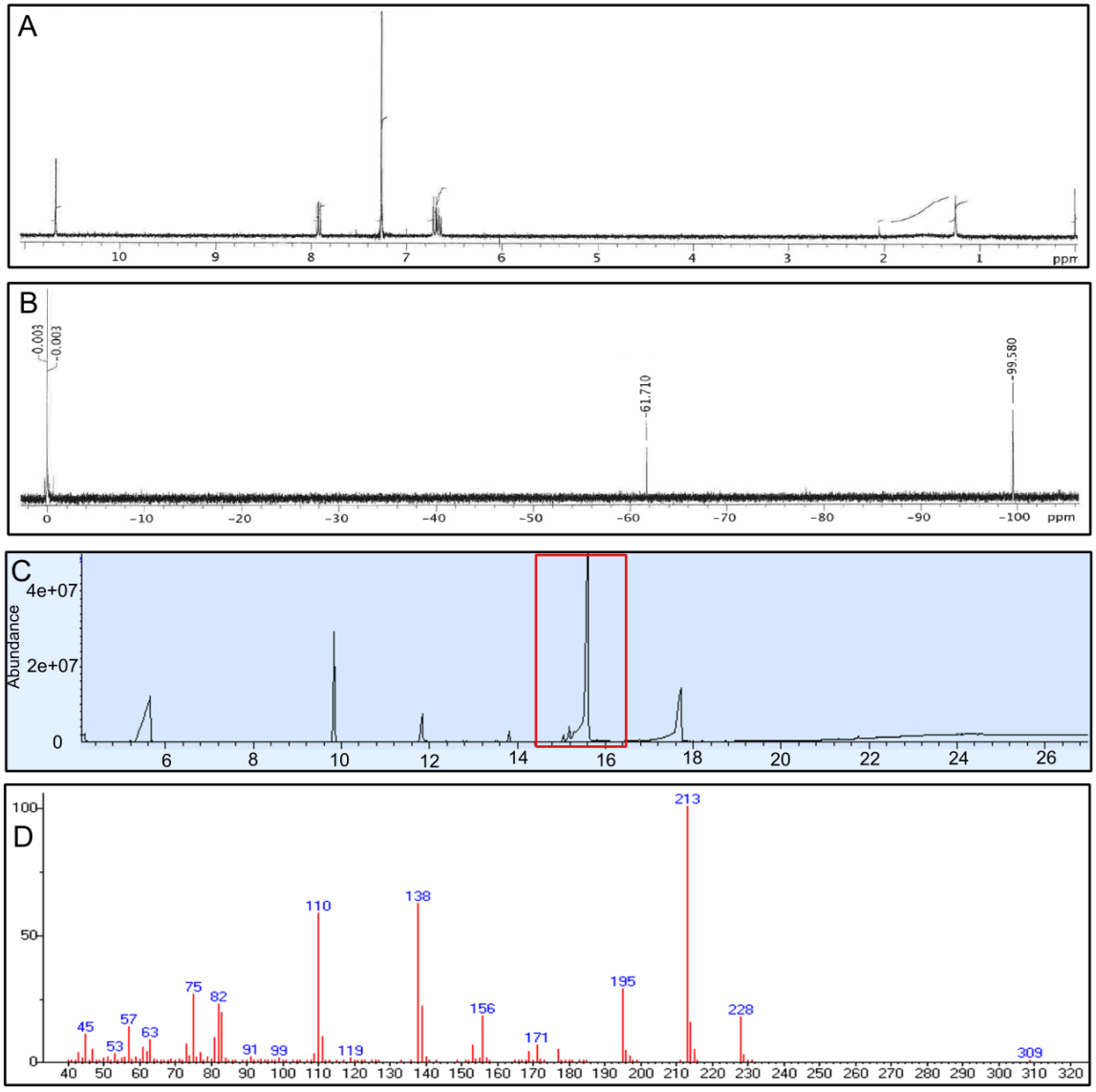

Figure S9. A) ^{1}H-NMR of the products from the extracted media after incubation of 5-fluoro-2-(trifluoromethyl)phenol in MSB overnight. B) ^{19}F-NMR of the same extracted sample. The major product in these NMR was identified as 4-fluorosalicylate. C) GC chromatograph of the extracted product from the spontaneous degradation of 5-fluoro-2-(trifluoromethyl)phenol in MSB. The boxed peak at 15.6 minutes is the most abundant product. D) The relative mass spectra fragmentation pattern of the major peak indicated in panel C shown and the compound was identified to be 4-fluorosalicylate (i.e, 4-fluoro-2-hydroxybenzoic acid).

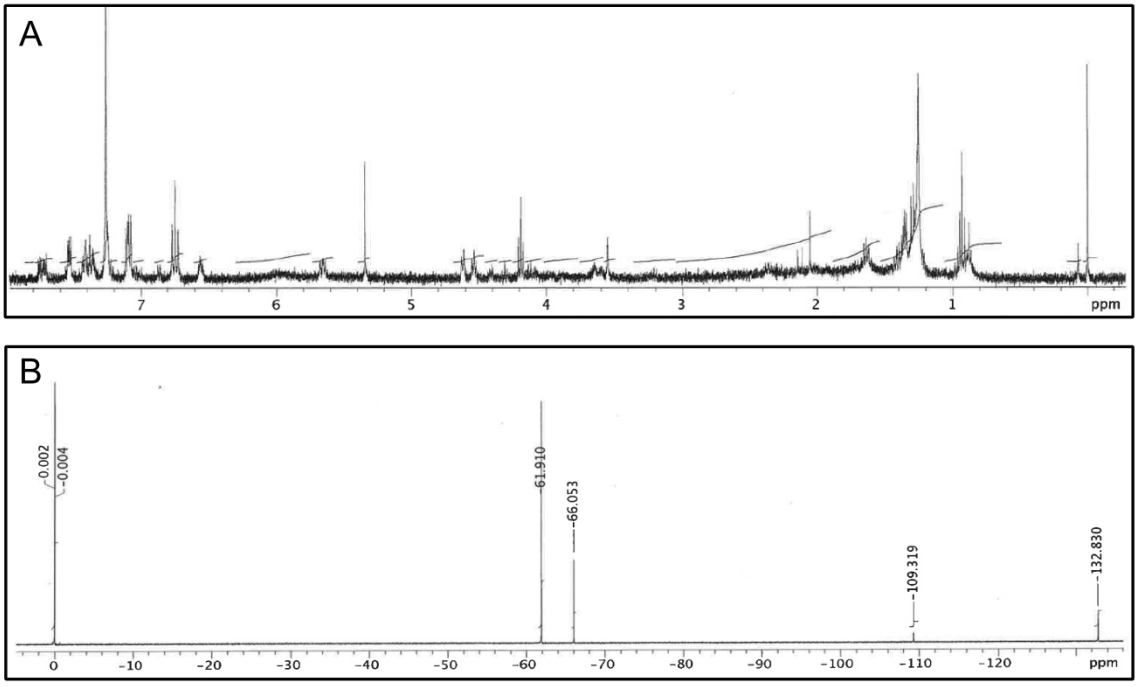

Figure S10. A) ^{1}H-NMR of the products from the extracted material from the culture supernatant after incubation of *E.coli* pDTG 602 with 4-fluorobenzotrifluoride. B) ^{19}F-NMR of the same extracted material. The major product in these NMR was identified as 4-fluoro-(trifluoromethyl)catechol (i.e, 3-trifluoromethyl-6-fluoro-1,2-benzenediol). See main text methods for chemical shifts.